RESEARCH & REVIEWS IN SCIENCE AND MATHEMATICS

EDITOR
PROF. DR. HASAN AKGÜL

gece kitaplığı

İmtiyaz Sahibi / Publisher • Yaşar Hız

Genel Yayın Yönetmeni / Editor in Chief • Eda Altunel

Kapak & İç Tasarım / Cover & Interior Design • Gece Kitaplığı

Editör / Editor • Prof. Dr. Hasan Akgül

Birinci Basım / First Edition • © Şubat 2021

ISBN • 978-625-7342-80-3

Gece Kitaplığı / Gece Publishing

Türkiye Adres / Turkey Address: Kızılay Mah. Fevzi Çakmak 1. Sokak Ümit Apt. No: 22/A Çankaya / Ankara / TR

Telefon / Phone: +90 312 384 80 40

web: www.gecekitapligi.com

e-mail: gecekitapligi@gmail.com

Baskı & Cilt / Printing & Volume

Sertifika / Certificate No: 47083

Research & Reviews in Science and Mathematics

Editors

PROF. DR. HASAN AKGÜL

gece kitaplığı

CONTENTS

Chapter 1

REVIEW OF COUMARIN-CONTAINING ANTICANCER AGENTS SYNTHESIZED IN RECENT YEARS

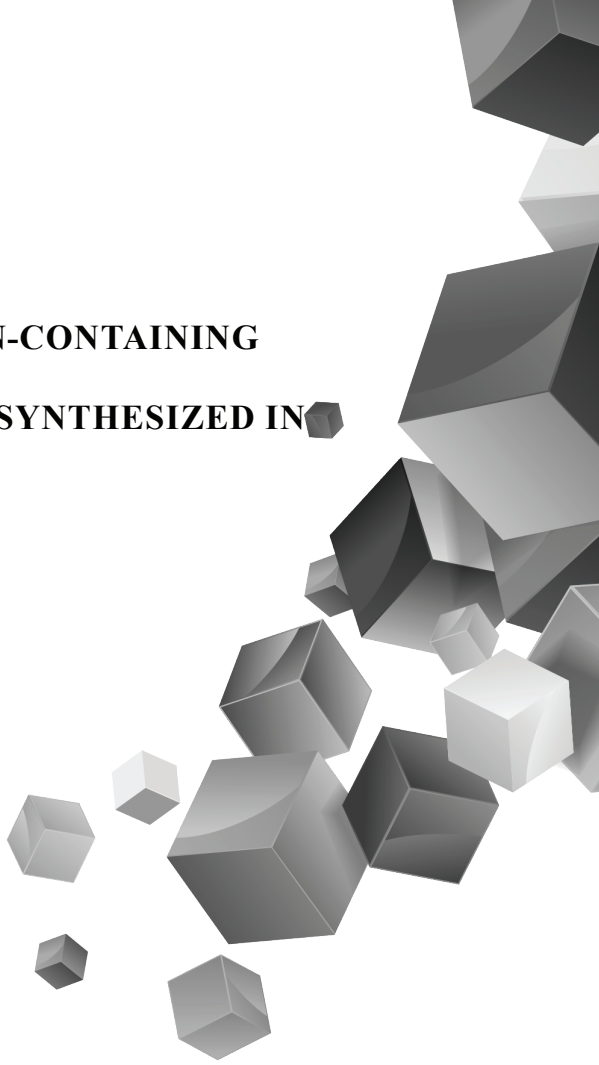

Hülya ÇELİK ONAR[1]

1 Hülya ÇELİK ONAR, Istanbul University-Cerrahpaşa, Engineering Faculty, Chemistry Department, Organic Chemistry Devision Avcılar/ İstanbul /Turkey

Cancer, the uncontrolled growth of abnormal cells called cancer cells, malignant cells or tumor cells anywhere in the body, is the second most common cause of death worldwide, killing more than 8 million people each year. The most common types of cancer that cause death are lung, stomach, liver, colon and breast cancer. With an estimated 13.1 million deaths (an increase of about 70%) in 2030, cancer deaths are projected to continue to rise worldwide.

Many natural and synthetic compounds have been used in cancer treatment for years. Coumarin compounds are also one of the compounds used (Borges et al., 2013). Psoralen (or 7H-furo [3,2-g]chromen-7-one) is a furanocoumarin that exhibits anti-arthritic, antimicrobial and anti-inflammatory effects (Asif, 2015). On the other hand, esculetin the IUPAC name of which is 6,7-dihydroxy-2H-chromen-2-one has been reported to protect single-cell DNA from oxidative attack (Aneko et al., 2007). Esculetin is propitious to regulate vasoconstriction by diminishing the release of nitric oxide (Liang et al., 2017), it overcomes the Sp1 transcription factor (Liang et al., 2017) and binds with β-catenin proteins resulting in the inhibition of β-catenin–Tcf signaling pathway of gastrointestinal tumorigenesis (Lee et al., 2013) and it also inhibits melanin biosynthesis (Sollai et al., 2008). New coumarin compounds are added to the literature every year as anticancer agents. Coumarins are heterocyclic compounds belonging to the class of benzopyrone and the breakdown of them results in the formation of active metabolites with therapeutic activity, such molecules are called as pro-drugs (Stefanachi et al., 2018). Therefore they have a lot of bioactive properties such as anticoagulant, antibacterial, anti-inflammatory, antioxidant, antitumor, antiviral, and enzyme inhibition. Higher doses of coumarin are found to be hepatotoxic (Iwata et al., 2016). However they reduce the risk of cancer and other neuronal and cardiovascular ailments. These effects are due to their free radical scavenging effects. Coumarins such as umbelliferone, esculetin and quercetin show antioxidant properties and protect the cellular DNA from oxidative damage. The dicumarol shows anticoagulant properties by inhibiting the action of vitamin K, whereas angelmarin has been reported to be cytotoxic in pancreatic cancer. Coumarins also reduce edema and inflammation by inhibiting the prostaglandins biosynthesis. Hydroxyl aromatic substituted derivatives such as 5-hydroxycoumarin or vicinal dihydroxy coumarins have also been found to be potent antiinflammatory agents. Some coumarins are approved by the FDA as drugs, and warfarin is one such example. It blocks the Vitamin K reductase enzyme thus disrupting the clotting

mechanism. In conclusion, the coumarin class of phytomolecules has a lot of potential to be used as drugs for various diseases (Garga et al., 2020).

In one study, Six fluorescent half-sandwich iridium(III) coumarin-salicylaldehyde Schiff base (O^N) compounds ([(η5- Cp*)Ir(O^N)Cl]) [Ir1-Ir6] were synthesized and stated to have high anticancer activity (IC50: 9.9 ± 0.1 μM–40.7 ± 12.9 μM) with dual functions: lysosomal damage and anti-metastasis (Liu et al., 2020). Lysosomes, organelles present in eukaryotic cells, have significant features in acidic environments (pH: 4.5–5.5), which are conducive to maintaining the activity of a large number of lysosomal hydrolases (Savini et al.,2019; Minchew and Didenko, 2017). Compared with normal cells, tumor cells have high lysosomal contents. Recent studies have demonstrated that weakly basic antitumor drugs can effectively accumulate in the lysosomes, leading to partial lysosomal membrane permeabilization (LMP) (Luzio and Pryor, 2007). Therefore, lysosomes may be potential targets for the selective killing of tumor cells, and the development of lysosome-targeting drugs is expected to become a novel antitumor therapy.

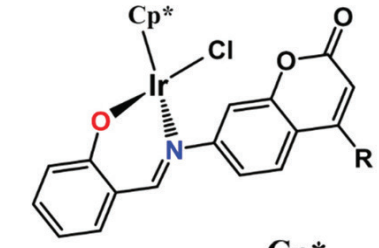

Compound	Cp*	R
Ir1	Cp^{x}	CH_3
Ir2	Cp^{xph}	
Ir3	Cp^{xbiph}	
Ir4	Cp^{x}	CF_3
Ir5	Cp^{xph}	
Ir6	Cp^{xbiph}	

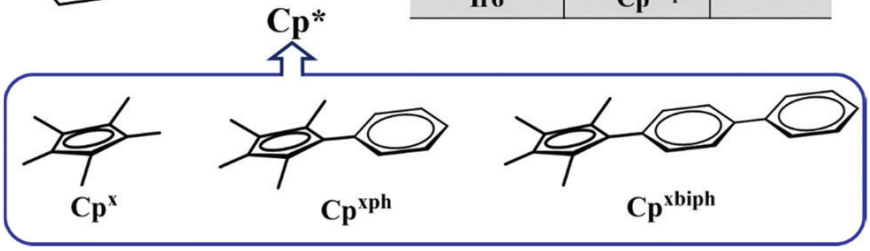

Fig.1: *Ir1 – Ir6 compounds synthesized by Liu et al.*

In a study by Kumari et al., WR (Warfarin) and organotin (IV) complexes [[Me3Sn (WR)] and [Bu3Sn (WR)]] screened for counter cytotoxicity by in vitro MTT assay to HCT-15 (colon adenocarcinoma), MCF-7 (breast cancer), HeLa (cervical cancer), DU145 (prostate cancer) and LNCaP (androgen-sensitive prostate adenocarcinoma). When IC50 values were examined, it was seen that the complexes did not show

cytotoxicity against MCF-7, HeLa and LNCaP cell lines. However, it has been found to cause good cytotoxicity against colon cancer (HCT-15).

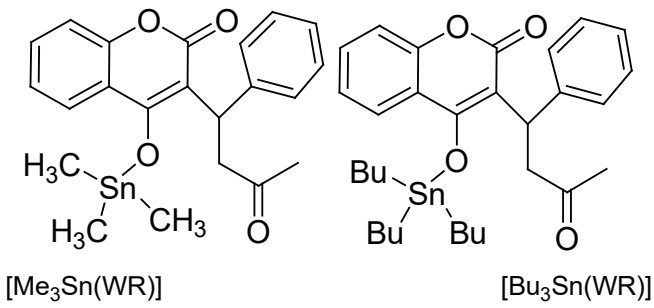

Fig. 2: **[***Me*$_3$*Sn (WR)] and [Bu*$_3$*Sn (WR)]***

There have been many in vitro and in vivo studies showing that Murrayone, a compound containing coumarin and extracted from the plant called Murraya paniculata (L.), which is widely grown in China and used to terminate pregnancy, may be an anticancer reagent. This work will lead the pharmacodynamic studies of the herb (Zhai et al., 2020).

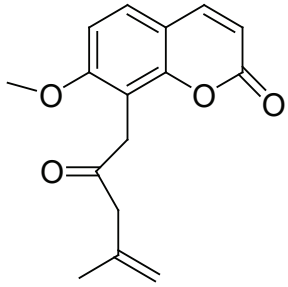

Fig. 3: *Murrayone*

In the study of Mohler et al., a lot of coumarin-modified androgens were prepared and tested for treatment of prostate cancer .Examples; Acetamide, 2-[[(3α,5α,17β)-3-hydroxyandrostan-17-yl]oxy]-N-[2-(2,3,6,7-tetrahydro-11-oxo-1H,5H,11H-[1]benzopyrano[6,7,8-ij]quinolizin-9-yl)ethyl]-,

Acetamide, 2-[[(5α,17β)-3-oxoandrostan-17-yl]oxy]-*N*-[2-(2,3,6,7-tetrahydro-11-oxo-1*H*,5*H*,11*H*-[1]benzopyrano[6,7,8-*ij*]quinolizin-9-yl)ethyl]-, Acetamide, 2-[[[(5α)-3-oxoandrostan-17-ylidene]amino]oxy]

-*N*-[2-(2,3,6,7-tetrahydro-11-oxo-1*H*,5*H*,11*H*-[1]benzopyrano[6,7,8-*ij*] quinolizin-9-yl)ethyl]-, Spiro[androstane-3,4'-[4*H*,7*H*,11*H*]pyrido[3', 4':3,4][1]benzopyrano[6,7,8-*ij*]quinolizin]-5'(1'*H*)-one, 2',3',8',9',12',13'-hexahydro-17-hydroxy-, (3α,5α,17β)-, Spiro[androstane-3,4'-[4*H*,7*H*,11*H*] pyrido[3',4':3,4][1]benzopyrano[6,7,8-*ij*]quinolizine]-5'(1'*H*),17-dione, 2',3',8',9',12',13'-hexahydro-, (3α,5α), Acetamide, *N*-[2-(7-amino-2-oxo-2*H*-1-benzopyran-4-yl)ethyl]-2-,[[(5α,17β)-3-oxoandrostan-17-yl]oxy]-, 2*H*-1-Benzopyran-2-one, 7-amino-4-[2-[[2-[[(5α,17β)-3-oxoandrostan-17-yl]oxy]ethyl]amino]ethyl]-, 2*H*-1-Benzopyran-2-one, 7-methoxy-4-[2-[[2-[[(5α,17β)-3-oxoandrostan-17-yl]oxy]ethyl]amino]ethyl]-, 2*H*-1-Benzopyran-2-one, 7-(dimethylamino)-4-[2-[[2-[[(3α,5α,17β)-3-hydroxyandrostan-17-yl]oxy]ethyl]amino]ethyl]-, and others (Mohler et al., 2020).

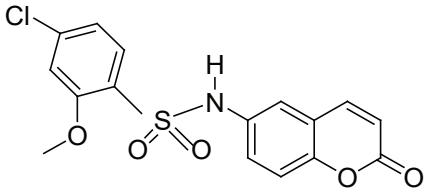

Fig. 4: *Compound 13*

Recent studies have shown that substances derived from natural products are promising in cancer treatment. In this study , reports of studies applying different virtual screening methods to select natural products with potential anticancer activity were presented. Coumarin, quinone, tannins, alkaloids, flavonoids and terpenes are based as natural products (Cavalcanti et al., 2019).

In this study, three new Ru (II) complexes, ($RuCl_2$ [La] [DMSO] $_2$) * H_2O (**Ru1**), ($RuCl_2$[Lb] [DMSO] $_2$) (**Ru2**) and ($RuCl_2$ [Lc][DMSO] $_2$) (**Ru3**), respectively contains 3-(2'-benzimidazolyl)coumarin (La), 3-(2'-benzimidazolyl)-7-fluoro-coumarin(Lb) and 3-(2'-benzimidazolyl)-7-methoxyl-coumarine (Lc) were firstly synthesized. Of these compounds, **Ru2**, in particular, was found to show higher activity even than cisplatin, the reference compound. (inhibition rate Ru2 [IR] = 61.3%) and cisplatin (IR= 25.5%) (Qin et al, 2019).

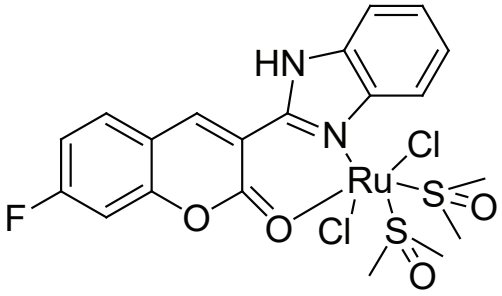

Fig. 5: *Ru2*

Peihong et al. declared that synthesized six new compounds, (2,6-dihydro-8-hydroxy-9-methoxy-2,6-dioxo-4H-Pyrano[3,4,5-de]-1-benzopyran-3-acetic acid methyl ester (**1**), 2,6-dihydro-8-hydroxy-9-methoxy-2,6-dioxo-4H-Pyrano[3,4,5-de]-1-benzopyran-3-acetic acid (**2**), 2,6-dihydro-8-hydroxy-4,9-dimethoxy-2,6-dioxo-,(-)-4H-Pyrano[3,4,5-de]-1-benzopyran-3-acetic acid methyl ester (**3**) , 2,6-dihydro-8-hydroxy-4,9-dimethoxy-2,6-dioxo-, (-)-4H-Pyrano[3,4,5-de]-1-benzopyran-3-acetic acid (**4**), 2,6-dihydro-4,8-dihydroxy-9-methoxy-2,6-dioxo-,(-)-4H-Pyrano[3,4,5-de]-1-benzopyran-3-acetic acid methyl ester (**5**), 2,6-dihydro-4,8-dihydroxy-9-methoxy-2,6-dioxo-, (-)-4H-Pyrano[3,4,5-de]-1-benzopyran-3-acetic acid , could be used as antitumor reagents (Peihong et al., 2019).

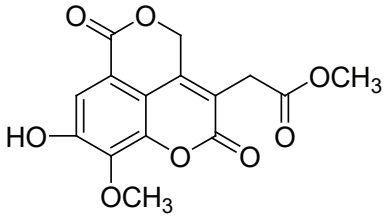

1

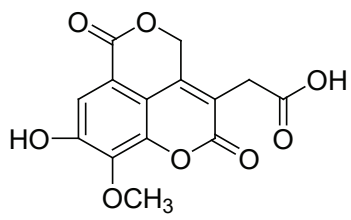

2

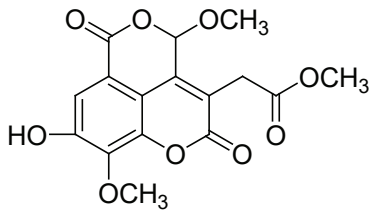

3

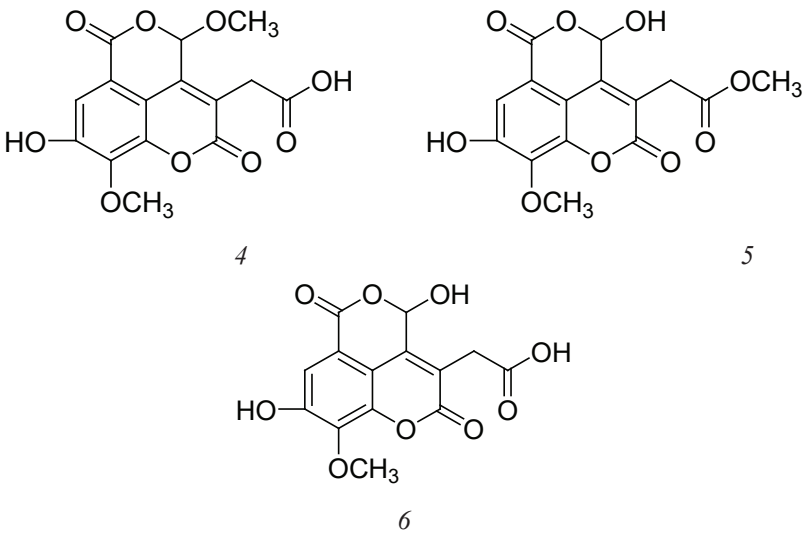

Fig. 6: *Synthesized compounds by Peihong et al.*

This study states that two new substances . (4-(2,5-dihydroxy-4-methylphenyl)-6-hydroxy-8-methyl-2H-1-Benzopyran-2-one and 4-(2,5-dihydroxy-3-methylphenyl)-6-hydroxy-8-methyl-2H-1-Benzopyran-2-one) were extracted from Japanese cockroach beetle and showed antitumor activity (Yongxian et al, 2019).

In this study, it was stated that six compounds (7-[[(2*Z*)-3,7-dimethyl-2,6-octadien-1-yl]oxy]-4-methyl-8-nitro-2*H*-1-Benzopyran-2-one,7-[[(2*Z*)-3,7-dimethyl-2,6-octadien-1-yl]oxy]-5-hydroxy-4-methyl-2*H*-1-Benzopyran-2-one, 5,7-bis[[(2*Z*)-3,7-dimethyl-2,6-octadien-1-yl]oxy]-4-methyl-2*H*-1-Benzopyran-2-one,7-[[(2*Z*)-3,7-dimethyl-2,6-octadien-1-yl]oxy]-4-hydroxy-5-methyl-2*H*-1-Benzopyran-2-one, 8-[(2*Z*)-3,7-dimethyl-2,6-octadien-1-yl]-7-[[(2*Z*)-3,7-dimethyl-2,6-octadien-1-yl]oxy]-4-hydroxy-5-methyl-2*H*-1-Benzopyran-2-one, and 6-[(2*Z*)-3,7-dimethyl-2,6-octadien-1-yl]-7-[[(2*Z*)-3,7-dimethyl-2,6-octadien-1-yl]oxy]-4-hydroxy-5-methyl-2*H*-1-Benzopyran-2-one) were synthesized for the first time and had a good anti-gastric cancer cell proliferation effect and high selectivity (Jianyong et al., 2019).

In the other study, 2-(3-substituted-4-methyl-2-oxo-2H-chromen7-yloxy)-2-methylpropanoic acid derivatives (5a-5f) were synthesized and their structures were identified by mass, ^{1}H NMR, ^{13}C NMR and IR for the first time. Cytotoxic activities of these compounds against MCF-7, MDA-231 (human breast cancer) and HT29 (human colon

adenocarcinoma) cell lines was examined by MTT assay. The results proved these compounds to be potent and selective cytotoxic agents (Venkata et al., 2016).

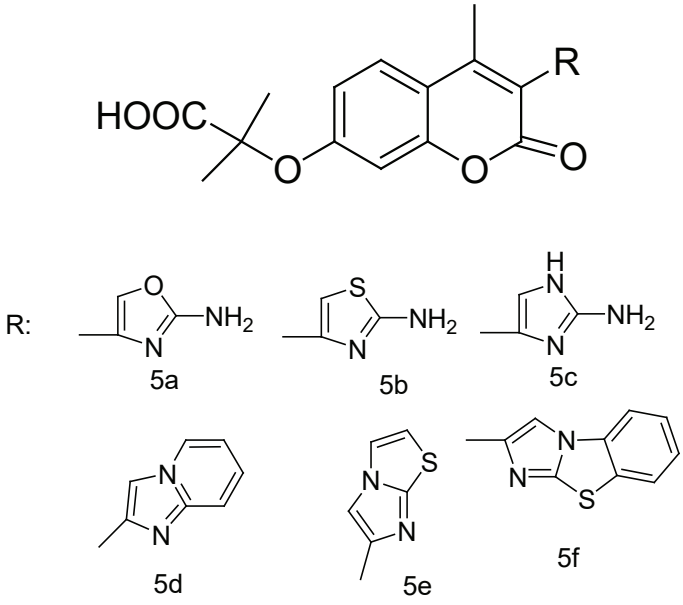

Fig. 7: *5a -5f*

Venkata et al., in this study, Lipophilicity (log P) parameter of the above compounds (5a-5f) was calculated by RP-UFLC method. A good correlation and very close values were obtained between the experimentally determined log P values and values obtained from Chemdraw. These close values found indicate that these compounds have good anticancer activity. The anticancer activity results of these compounds also proved the accuracy of this study. This method is important in terms of providing preliminary information about the biological activities of the compounds to be synthesized (Venkata et al, 2017).

A series of novel coumarin-based hydroxamate derivatives (10a-10e; 11a-11e; 12a-12b) were synthesized as histone deacetylase inhibitors (HDACis). Because, HDAC is one of the hot topics in the field of antitumor research. The experimental results showed that these coumarin derivatives synthesized were anticancer agents (Yang et al., 2019).

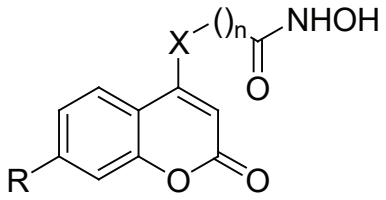

10a: R=H X=NH n=2
10b: R=H X=NH n=5
10c: R=0CH_3 X=NH n=5
10d: R=0CH_3 X=NH n=6
10e: R=0CH_3 X=NH n=7

11a: R=0CH_3 X=O n=4
11b: R=0CH_3 X=O n=5
11c: R=0CH_3 X=O n=6
11d: R=0CH_3 X=O n=7
11e: R=0CH_3 X=O n=8

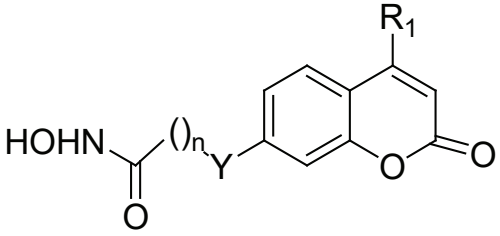

12a: R_1=H Y=O n=7
12b: R_1=CH_3 Y=O n=7

Fig. 8: *10a – 10e , 11a – 11e, 12a – 12b*

Methyl substituted umbelliferone selenocyanate (MUS) was synthesized and examined as anticancer agent against two murine cancers (Dalton's Lymphoma and Sarcoma-180) in vivo. The results were very good (Patra et al., 2018).

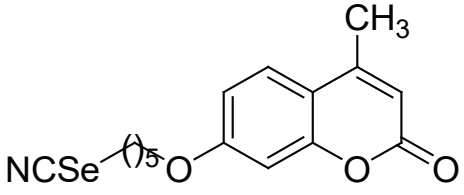

Fig. 9: *MUS*

Clauselenisin A and its five known analogues were isolated from the stems and leaves of plant of Clausena lenis in China. This study suggests that these substances are antitumor agents (Liu et al., 2018).

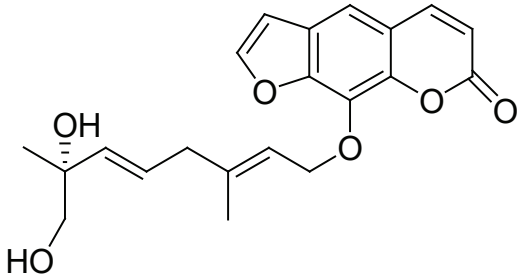

Fig. 10: *Clauselenisin A*

In this study a new synthetic hybrid compound (AD-013) was synthesized which integrates a coumarin moiety and an α-methylene-δ-lactone motif. The cytotoxic activity of this new compound was studied against MCF-7 and HL-60 cancer cells, and the results were compared with novobiosin, a coumarin-based antibiotic. AD-013 was observed to have higher cytotoxic activity (Dlugosz et al., 2018).

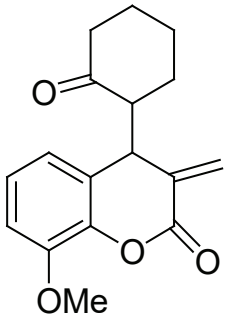

Fig. 11: *AD-013*

Some new alkenylcumarins were synthesized and their anticancer activity against Taq DNA polymerase was investigated. Of the alkenylcumarins synthesized, the most active was 6-(pent-4-enyloxy)-coumarin (Bruna-Haupt et al., 2018).

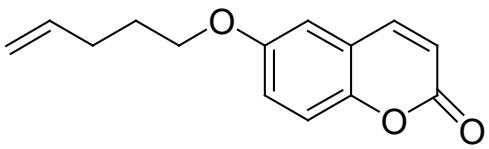

Fig. 12: *6-(pent-4-enyloxy)-coumarin*

Coumarin derivatives synthesized in this study (8-13; 17a-i; 18a-i) were observed to be an inhibitor against human CA IX and CA XII carbonic anhydrases (De Luca et al., 2018).

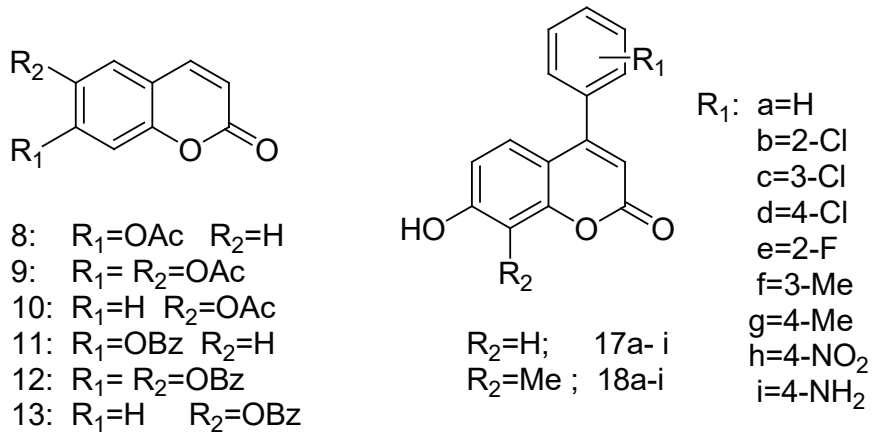

Fig. 13: *8-13, 17a–i, 18a -i*

A series of 6-methyl-4-substituted coumarin and 4-substituted benzocoumarine was synthesized and evaluated in vitro for antitumor activity against MCF-7 and HepG-2 cell line. 5h, 7d, 7h, 9a, 13a and 13d showed strong activity against both MCF-7 and HepG-2 cell line (Morsy et al., 2017).

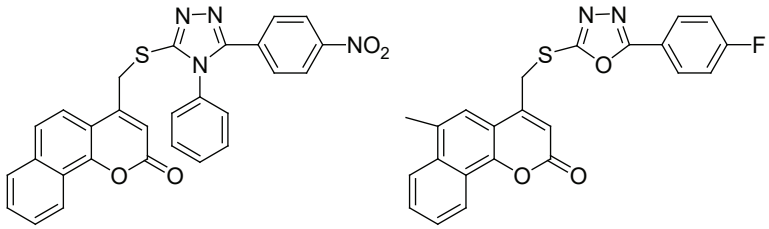

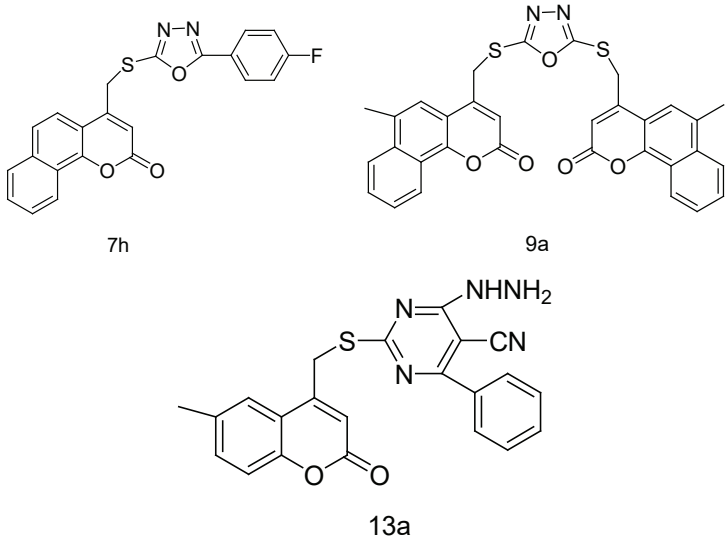

Fig. 14: *5h, 7d, 7h, 9a, 13a*

A series of novel coumarin–1,2,3-triazole hybrids (16a–16e, 17a–17e, 18a–18e, 19a–19d, 20a–20d) was synthesized by the copper(I)-catalyzed Huisgen 1,3-dipolar cycloaddition reaction. these compounds showed unselective cytostatic activities against all tested tumor (HeLa, CaCo-2, K562) and normal (MDCK1) cells (Bistrovic et al., 2017).

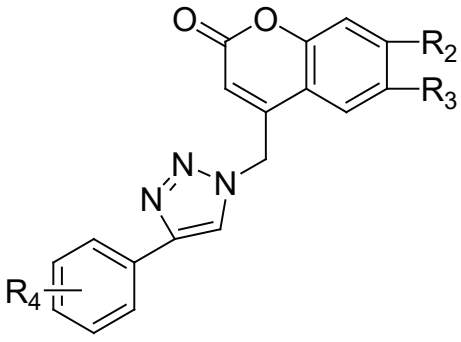

16a-16e; R_2=OCH_3 R_3=H

	16a	16b	16c	16d	16e
R_4	H	p-OCH_3	m-OCH_3	o-OCH_3	m-OH

17a-17e; R_2=H R_3=OCH_3

	17a	17b	17c	17d	17e
R_4	H	p-OCH_3	m-OCH_3	o-OCH_3	m-OH

18a-18e; R_2=OH R_3=H

	18a	18b	18c	18d	18e
R_4	H	p-OCH_3	m-OCH_3	o-OCH_3	m-OH

19a-19d; R_2=H R_3=OH

	19a	19b	19c	19d
R_4	H	p-OCH_3	m-OCH_3	o-OCH_3

20a-20d; R_2=OH R_3=OH

	20a	20b	20c	20d
R_4	H	p-OCH_3	m-OCH_3	o-OCH_3

Fig. 15: *16a–16e, 17a–17e, 18a–18e, 19a–19d, 20a–20d*

In the other study; Raj and Bahulayan synthesized twelve new coumarin tagged peptidomimetic macrocycles (3a-3l) and they observed the excellent cytotoxicity against human breast cancer cell line (MCF-7) (Raj and Bahulayan, 2017).

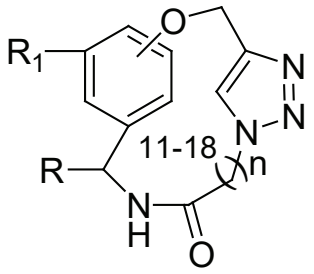

Fig. 16: *Compounds 3a-3l*

Two new dicoumarins (1, 2) and a new tricoumarin (3) have been isolated from Chimonanthus salicifolius by Wang et al. These compounds showed modest cytotoxicity against Hela and HL-60 cell lines, while only (3) had the cytotoxicity against PC-3 cell line (Wang et al., 2016).

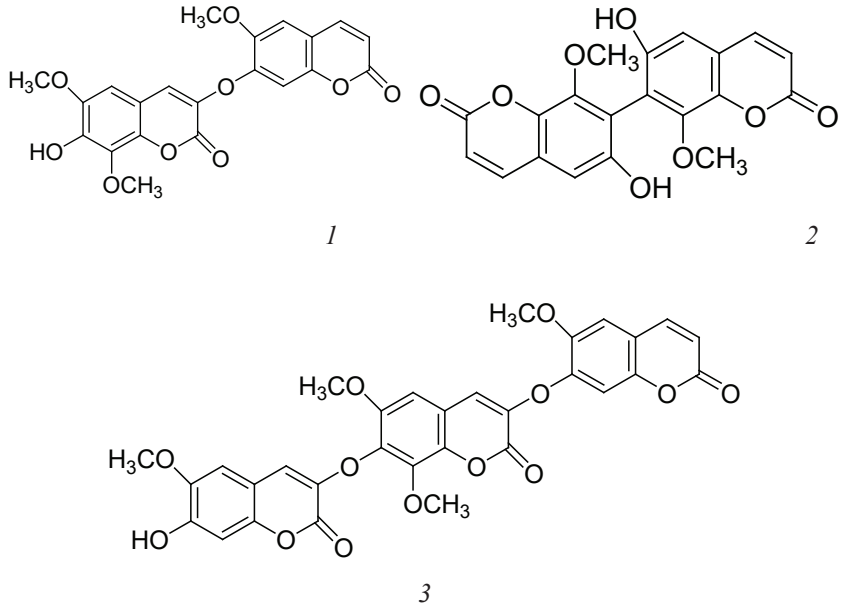

1 *2*

3

Fig. 17: *Compounds 1 - 3*

The anticancer activities of benzimidazole compounds in general, especially 2-arylbenzimidazoles, are well known (Keri et al., 2015). In this study, Eight coumarine-benzimidazole hybrids (7-14) were synthesized and examined in vitro anticancer activity against leukemia cancer cells (CCRF-CEM, HL60(TB), K562, RPMI8226), HCT116, HCT15, melanoma cancer cells (LOX IMVI, UACC257) and breast cancer cells (MCF7, T47D) (Kamaldeep et al., 2013).

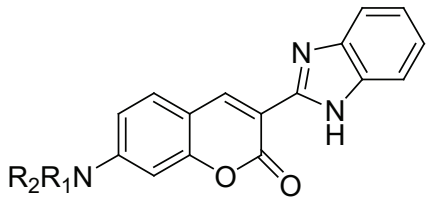

7; NR_1R_2= Ethylenediamine
8; NR_1R_2= Ethanolamine
9; NR_1R_2= n.Butylamine
10; NR_1R_2= Cyclohexylamine
11; NR_1R_2= 4-Fluoroaniline
12; NR_1R_2= Morpholine
13; NR_1R_2= Methylpiperazine
14; NR_1R_2= 2-Aminoethylmorpholine

Fig. 18: *Coumarin-benzimidazole hybrids (7-14)*

In the other study, Bana et al. synthesized coumarin-quinone derivative and declarated that it has good CDC25 phosphatase inhibitory activity (Bana et al., 2015).

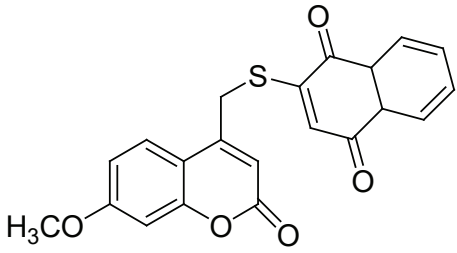

Fig. 19: *Coumarin-quinone derivative*

REFERENCES

Asif, M., 2015. Pharmacological activities and phytochemistry of various plants containing coumarin derivatives. Current Sci. Perspect. 1 (3), 77–90.

Aneko, T.K., Ahara, S.T., Akabayashi, F.T., 2007. Inhibitory effect of natural coumarin compounds, esculetin, and esculin, on oxidative DNA damage and formation of aberrant crypt foci and tumors induced by 1, 2-dimethylhydrazine in rat colons. Biol. Pharm. Bull. 30 (11), 2052–2057.

Bana, E., Sibille, E., Valente, S., Cerella, C., Chaimbault, P., Kirsch, G., Dicato, M., Diederich, M.,

Bagrel, D., 2015. Mol. Carcinog. 54, 229-241.

Bistrovic, A., Stipanicev, N., Opacak-Bernardi, T., Jukic, M., Martinez, S., Glavas-Obrovac, Lj., Raic-Malic, S., 2017. Synthesis of 4-aryl-1, 2,3-triazolyl appended natural coumarin-related compounds with antiproliferative and radical scavenging activities and intracellular ROS production modification, New Journal of Chemistry (2017), 41(15), 7531-7543.

Borges, G., Vianna, R., Medina-remón, A., 2013. The antioxidant activity of coumarins and flavonoids. Mini Rev. Med. Chem. 13, 318–334.

Bruna-Haupt, E., Garro, H.A., Gutierrez, L., Pungitore, C.R., 2018. Collection of alkenylcoumarin derivatives as Taq DNA polymerase inhibitors: SAR and in silico simulations, Medicinal Chemistry Research, 27(5), 1432-1442.

Cavalcanti, É.B.V.S., Félix, M.B., Scotti, L., Scotti, M.T., 2019. Virtual Screening of Natural Products to Select Compounds with Potential Anticancer Activity, Anti-Cancer Agents in Medicinal Chemistry, 19(2), 154-171.

De Luca, L., Mancuso, F., Ferro, S., Buemi, M.R., Angeli, A., Del Prete, S., Capasso, C., Supuran, C.T., Gitto, R., 2018. Inhibitory effects and structural insights for a novel series of coumarin-based compounds that selectively target human CA IX and CA XII carbonic anhydrases, European Journal of Medicinal Chemistry, 143, 276-282.

Dlugosz, A., Gach-Janczak, K., Szymanski, J., Deredas, D., Krawczyk, H., Janecki, T., Janecka, A.,2018. Anticancer Properties of a New Hybrid Analog AD-013 Combining a Coumarin Scaffold with an α-methylene-δ-lactone Motif, Anti-Cancer Agents in Medicinal Chemistry, 18(3), 450 -457.

Garga, S.S., Guptaa, J., Sharmab, S., Sahu, D., 2020. An insight into the therapeutic applications of coumarin compounds and their mechanisms of action. European Journal of Pharmaceutical Sciences 152 (2020) 105424 – 105432.

Iwata, N., Kainuma, M., Kobayashi, D., Kubota, T., 2016. The relation between hepatotoxicity and the total coumarin intake from traditional Japanese medicines containing cinnamon bark. Front. Pharmacol. 1–9.

Jianyong, S., Guangzhi, L., Li, C., 2019. Application of terpenoid coumarin compounds to treating gastric cancer, Faming Zhuanli Shenqing , CN 109223772 A 20190118.

Kamaldeep, P., Shweta, B., Vijay, L., 2013. Synthesis of new conjugated coumarin-benzimidazole hybrids and their anticancer activity, Bioorg Med Chem Lett., 23(12):3667-72

Keri, R.S., Hiremathad, A., Budagumpi, S., Nagaraja, B.M., 2015. Comprehensive review in current developments of benzimidazole-based medicinal chemistry, Chemical Biology and Drug Design, 86 (1), 799-845.

Kumari, R., Banerjee, S., Roy, P., Nath, M., 2020. Organotin(IV) complexes of NSAID, ibuprofen, X-ray structure of Ph3Sn(IBF), binding and cleavage interaction with DNA and in vitro cytotoxic studies of several organotin complexes of drugs, Appl Organometal Chem. e5283-e5307.

Lee, S.Y., Lim, T.G., Chen, H., Jung, S.K., Lee, H.J., Lee, M.H., Kim, D.J., Shin, A., Lee,

K.W., Bode, A.M., Surh, Y.J., Dong, Z., 2013. Esculetin suppresses proliferation of human colon cancer cells by directly targeting β-catenin. Cancer Prev. Res. 6 (12),1356–1364.

Liang, C., Ju, W., Pei, S., Tang, Y., Xiao, Y., 2017. Pharmacological activities and synthesis of esculetin and its derivatives: a mini-review. Molecules 22 (3), 387.

Liu, Y.P., Wen, Q., Hu, S., Ma, Y.L., Jiang, Z.H., Tang, J.Y., Qiu, S.X., 2018. Furanocoumarins with potential antiproliferative activities from Clausena lenis, Natural Product Research, 1–7.

Liu, C., Liu, X., Ge, X., Wang, Q., Zhang, L., Shang, W., Zhang, Y., Yuan, X. A., Tian, L.,

Liu, Z., 2020. Fluorescent iridium(III) coumarin-salicylaldehyde Schiff base compounds as lysosome-targeted antitumor agents. Dalton Trans., 49, 5988-5998.

Luzio, J.P. and Pryor, P.R., 2007. Lysosomes: Fusion and function, Nat. Rev. Mol. Cell Biol., 8, 622–632.

Minchew, C.L. and Didenko, V.V., 2017. Dual detection of nucleolytic and proteolytic markers of lysosomal cell death: DNase II-type breaks and cathepsin D, Methods Mol. Biol., 1554, 229–236.

Mohler, J.L., Fiandalo, M.V., Watt, D., Sviripa, V., 2020. Coumarin-modified androgens for treatment of prostate cancer. PCT Int. Appl. WO 2020223174 A1 20201105.

Morsy, S.A., Farahat, A.A., Nasr, M.N.A., Tantawy, A.S., 2017. Synthesis, molecular modeling and anticancer activity of new coumarin containing compounds, Saudi Pharmaceutical Journal, 25(6), 873–883.

Patra, A.R., Roy, S.S., Basu, A., Bhuniya, A., Bhattacharjee, A., Hajra, S., Ugir H., Baral, R., Bhattacharya, S., 2018. Design and synthesis of coumarin-based organoselenium as a new hit for myeloprotection and synergistic therapeutic efficacy in adjuvant therapy, Scientific Reports, 8(1), 1-12.

Peihong, F., Ting, L., Wencheng, Z., Jingyuan, L., 2019. Coumarin compound (3-(2-R2-2-oxoethyl)-4-R1-8-hydroxy-9-methoxy-2H-pyrano[3,4,5-de]chromene-2,6(4H)-dione) and its preparation method, application as antitumor agent, antiinflammatory agent, and HuR inhibitör, Faming Zhuanli Shenqing, CN 109678873 A 20190426.

Qin,Q.P., Wang, Z.F., Huang, X.L., Tan, M.X., Shi, B.B., Liang, H., 2019. High in Vitro and in Vivo Tumor-Selective Novel Ruthenium(II) Complexes with 3-(2′-Benzimidazolyl)-7-fluoro-coumarin, ACS Med. Chem. Lett., 10, 936−940.

Raj, P.J., Bahulayan, D., 2017. MCR-Click" synthesis of coumarin-tagged macrocycles with large Stokes shift values and cytotoxicity against human breast cancer cell line MCF-7, Tetrahedron Letters, 58(22), 2122–2126.

Savini, M., Zhao, Q., and Wang, M., 2019. Lysosomes: Signaling hubs for metabolic sensing and longevity, Trends Cell Biol., 29, 876–887.

Sollai, F., Zucca, P., Sanjust, E., Steri, D., Rescigno, A., 2008. Umbelliferone and esculetin:inhibitors or substrates for polyphenols oxidases. Biol. Pharma. Bull. 31 (12),2187–2193.

Stefanachi, A., Leonetti, F., Pisani, L., Farmaco, F., Moro, A., Orabona, E., 2018. Coumarin : a natural, privileged and versatile scaffold for bioactive compounds. Molecules 23, 250.

Venkata, S.K., Gurupadayya, B.M., Vishwanathan, B.I., Chandan, R.S., Nagesha, D.K., 2016. Cytotoxicity studies of coumarin analogs: design, synthesis and biological activity. RSC Advances, 6(101), 98816–98828.

Venkata, S.K., Gurupadayya, B.M., Iyer, V.B., Chandan, R.S., 2017. Determination of octanol-water partition coefficient of novel coumarin based anticancer compounds by reversed-phase ultra-fast liquid chromatography, International Journal of Pharmacy and Pharmaceutical Sciences , 9(8), 98-104.

Wang, K.W., Li, D., Wu, B., Cao, X.J., 2016. New cytotoxic dimeric and trimeric coumarins from Chimonanthus salicifolius, Phytochemistry Letters, 16, 115–120.

Yang, F., Zhao, N., Song, J., Zhu, K., Jiang, C., Shan, P., Zhang, H., 2019. Design, Synthesis and Biological Evaluation of Novel Coumarin-Based Hydroxamate Derivatives as Histone Deacetylase (Hdac) Inhibitors with Antitumor Activities, Molecules, 24, 2569- 2584.

Yongxian, C., Yongming, Y., Zhengchao, T., 2019. Coumarin compound and extraction method thereof, Faming Zhuanli Shenqing (2019), CN 109678829 A 20190426.

Zhai, S., Denga, X., Zhang, C., Zhoua, Y., Xie, H., Jianga, Z., Jia, L., 2020. A novel UPLC/MS/MS method for rapid determination of murrayone in rat plasma and its pharmacokinetics, Journal of Pharmaceutical and Biomedical Analysis, 180, 113046-113053.

Zhang, Z., Gu, L., Wang, B., Huang, W., Zhang, Y., Ma, Z., Zeng, S., Shen, Z., 2019. Discovery of novel coumarin derivatives as potent and orally bioavailable BRD4 inhibitor based on scaffold hopping. J. Enzyme Inhib. Med. Chem. 34 (1), 808–817.

Chapter 2

COMPETITION OR COEXISTENCE:

VIRULENCE DYNAMICS OF SARS-COV-2

Emir HALIKI [1]

1 Ege University Faculty of Science Department of Physics

1. Introduction

There are some pathogens more lethal than others and for that reason, a lot number of factors come into play such as immunity, infecting dose, host genetics, medical treatments. However, some pathogens are genuinely more dangerous than others. This subject is easily seen in animal diseases where it is possible to experimentally infect animals with different strains and compare the outcome. For instance, Marek's disease **[1]**, which is caused by a virus. When it was discovered in 1900s, was a relatively lethal mould disease, killing unvaccinated birds easily. Today's strains of this virus kill unvaccinated birds even faster **[2]**. Alongside with that, the high-path bird flu is as lethal as that.

Experimental infection studies usually find that pathogen populations contain strains that are more or less harmful to the hosts they infect, meaning that there is a genetic variation on which natural selection could act. In other words, pathogens could evolve to be nice or dangerous. The question then becomes, why is natural selection favored dangerous strains in some species and nicer strains in others **[3]**. For instance, the factor in the answer of question stops even more dangerous malaria strains from spreading or conversely, stops milder malaria strains from spreading.

When SARS came into the human population in 2002, it killed approximately ten percent of the infected people **[4]**. If that disease become pandemic in humans, would it have evolved to kill more or fewer people? The former answer was an evolution, eventually produces infectious diseases that do not harm their hosts. The thought was that pathogen strains killing the hosts also kill themselves and so become evolutionary impasses. Nice strains come to dominate because they keep their hosts and therefore themselves alive, and so could transmit on to other hosts. In the manner of this old theory, dangerous diseases are explained as being relatively new and are on their way to become nicer. For instance, HIV would be said to be dangerous, because a while ago has it jumped from chimpanzees to humans **[5]**. Given enough time this old thought goes, recent HIV strains that kill would be replaced by new strains that do not.

Now, it is known that this theory is useless. Infectious diseases would not all eventually evolve to be nicer. The first reason is that we

have seen diseases evolved to become dangerous just mentioned in Marek's disease example. Scientists debate about how many thousands of years people have been getting malaria, but even one thousand years is enough time for nicer malaria strains to replace dangerous ones, and malaria still kills hundreds of thousands of people in a year **[6]**. The idea that pathogens always evolved to be nicer could also be wrong in theory. In the limit, it must be true that pathogens' instantly killing their hosts would have no evolutionary future. However, there are no diseases at that limit. Even pretty dangerous diseases could get a lot of transmission process of killing the host. For instance, while a person is dying from malaria they could infect a horde of mosquitos which would pass the disease to other humans **[7]**. The idea that diseases evolved to be nice that well adaptive pathogens do not kill their hosts assumes transmission to a new host is maximized only if the host lives, which is not true. If one considers the opoosite, it is easy to imagine a pathogen that does not kill its host because does not replicate well. No wonder it would not do the host much harm, but also would not transmit much either. Nice pathogens do not need to win the competition.

In the 1980s, people began to realize this case, and the old idea that everything evolved to be nice got replaced by a more complicated one. Pathogens could evolve to be nice, but they could also evolve to be dangerous. This idea is known by biologists as the trade-off hypothesis of virulence evolution **[8]**, which is a cost-benefit argument. Evolutionary costs and benefits are in the infectious disease context measured in terms of new infected hosts. If there are strains more or less dangerous, which would be favored by evolution? It would be the one that leaves more secondary cases. If the nicer strain affects more people it would win, otherwise the dangerous would. It is easy to say the next step is hard to figure out what would happen in any particular disease. One needs to know a lot about the natural history of the system. To explain how this way of thinking works, it is needed to be a focus on a single disease. For instance, the possible cause of Malaria being virulent. It is a disease of human blood caused by single-cell parasites, which are transmitted between humans by mosquitoes. By thinking of the evolutionary cost of virulence, mosquitoes do not bite people who are dead. More virulent malaria strains would have a greater likelihood of killing their hosts and doing so more quickly **[9]**. This means infections caused by really virulent strains would on average be infectious for less time than

infections caused by nicer strains, and this is the evolutionary cost of virulence and because of that cost natural selection would favor less virulent strains.

If one thinks about the evolutionary benefits of virulence, experimental works on mouse malaria **[10, 11]** have found that virulent strains out-compete less virulent strains, they evade immunity better and make more transmission stages per day. They are also debilitating the host which probably makes it an easier target for mosquitoes because a healthy person could easily kill mosquitoes whereas a sick person does not care. Therefore, virulent strains have evolutionary advantages as well as evolutionary disadvantages. Those evolutionary costs and benefits generate a selection in opposing directions. The trade-off hypothesis says that the level of being dangerous we see in any disease is where those costs and benefits balance out. The reason for malaria's dangerousness is that strains, which are nicer than those we see in nature, losing the head-to-head competition, rapidly cleared by immunity, and produce fewer transmission stages per day. The reason why malaria is not even more dangerous is that dangerous strains have shorter infectious periods because they kill their hosts. Consequently, that is how the trade-off hypothesis of virulence evolution **[12]** works.

This hypothesis held up well since it was first proposed in the 1980s **[13, 14]**. It remains the key theory but is controversial as there are some compelling data, which support it for some diseases undoubtedly **[8]**. However, those diseases are of water fleas, chickens, rabbits, mice, or plants. For many diseases of humans, it is not known enough about the evolutionary costs and benefits to know if the model applies, which may certainly would not in many cases. For instance, rabies is a spillover disease in humans, which is not transmitted from person to person, but rather from dog to dog or bat to bat. Thus, humans get this disease when a dog or a bat accidentally bites them. That means the evolutionary reaction is happening in dogs or bats, not humans. The model could not explain why it almost always kills humans. Evolutionary forces shaping virulence is of more than academic interest. For most known diseases, there are variant strains, which are rare. Some evolutionary forces keeping those strains down. When we start to use vaccines, drugs, sewage systems, or airplanes, where we crowd animals onto farms or ourselves into cities, changing the natural history of the disease system. In some cases that might make the new strains even rarer. Diseases, which are under control

in the short term could years or decades later evolve back and infect us. We need to understand what keeps dangerous strains rare, encouraging us to keep them rare.

2. Virulence as the pathogen evolution

The main point of the pathogen evolution is that pathogens have their own agenda and they respond rapidly to things that they encounter, since they have short generation times, vast numbers, and fairly high mutation rates **[15]**. Many of them also have horizontal gene transfer that makes them extraordinarily evolutionary flexible. In order to investigate how that flexibility affects their virulence, the central idea in the evolutionary theory of virulence evolution is that there is a trade-off between virulence and transmission. Other things that affect the virulence of pathogens are whether they are transmitted vertically, horizontally, or by vectors, whether they infect their hosts singly or in the presence of other pathogens that are also infecting the hosts.

The paradigm for virulence transmission trade-off is myxoma virus infecting rabbits. Myxoma is transmitted by mosquitoes, fleas, lice, ticks, and mites, and it causes tumors, but it does not immediately kill cottontail rabbits in North and South America **[16]**. However, in European rabbits, it causes a disease called myxomatosis that has an initial hundred percent lethality rate.

In 1950, myxoma was introduced to Australia to control a devastating outbreak of rabbits, which have escaped from captivity **[17]**. There are no native predators of rabbits in Australia and they had reproduced explosively. Also, they were eating the continent right down to the dust. Then both the pathogen and the host are evolved. There was less virulence in the pathogen and there was better resistance in the host **[18]**. The virulence evolves to an intermediate point and then stops there, where it is still being lethal. Steps of the evolutionary working principle are written below:

- If the rabbit dies quickly, there is little opportunity for fleas and other biting insects to transmit the disease.
- Less virulent strains then outcompete more virulent ones because of their superior transmission.

- They do worse in a single host but better in the population as a whole.
- Hosts also evolve genetic resistance and adaptive immunity.

The main idea of the virulence transmission trade-off is that it often exists and from the pathogens' point of view, it is a major problem if the pathogen is only living in this host. If the pathogen does not solve this problem, then it is going to go locally extinct, considering it is specific to the host.

Vertical transmission is between parent and offspring, then it is going what we are thinking of reproduction as being vertical, and that is a direct way of getting the parasite from one host into the other. It would select for low virulence and eventually for commensalism there. Because the genetic interests of the host and the pathogen are completely identical in this case. There is no reason for the pathogen to do anything to disturb the reproduction and survival of the host. Strictly horizontal transmission selects for high virulence. The thing that would break that would simply be the virulence transmission trade-off. If there is a vector involved, then the impact of the vector's presence depends on the efficiency of the vector to transmitting that given different virulences of the disease. In this case, the disease is evolving both with the vector and the host that scientists are focused on **[19, 20]**.

The virulence evolution is also affected by whether or not the infection is single or multiple. If one looks at it from the pathogens' point of view, multiple infection that is being in there with a competition selects for increased virulence if the impact of the parasites on the host is through lethality **[21]**. Different pathogen strains are competing to be represented in transmission, and that is changing the virulence transmission trade-off in the following way: To be transmitted, the pathogen has to win the competition and make itself more frequent. But in doing so, it has to damage the host more. Therefore, virulence increases and the host dies sooner. However, there is another way that this kind of interaction could be mediated and that is through sub-lethal effects on growth or anything else that has a sub-lethal effect on the host. If those effects feedback to the parasites to reduce their rate of development, meaning that a more slowly growing host is less able to support rapidly growing parasites, then a multiple infection would generally lead to lower virulence. Therefore, one could not say multiple

infection (after a seroconversion it is called superinfection) means higher virulence. It all depends upon whether the impact is on lethality or some sub-lethal effects like growth **[22]**.

One of the most medically interesting evolutionary considerations about the evolution of virulence has to do with how many hosts are being used and what happens in a new host. The idea behind this is a master of everything is not actually a master of anything. A pathogen that does very well in one host would do poorly in another **[23]**, since they adapt locally to that host. The more host species that are regularly infected the less well adapted the pathogen is to any one of them. A pathogen that evolves to be good at exploiting one host would lose efficiency to others. It turns out this is how attenuated live viruses are used for or produced.

An attenuated live vaccine such as the yellow fever vaccine or the saving oral polio vaccine is produced by serial passage **[24]**. Microbiologists have used serial passage for a long time to study pathogen virulence, and it works because pathogens evolve quickly. The fact that it works demonstrates that there are widespread trade-offs in performance on different hosts. Those trade-offs limit host ranges that are how many different kinds of things could this pathogen infect, and they also constrain the emergence of new diseases, since they make it hard for a disease that specialized, such as on an animal reservoir to jump into the human population.

There is a bit more theoretical factor, which is the level of extrinsic risk that the host faces. Thus, things that are not the pathogen that might kill it would affect the virulence evolution of the pathogen. The idea here is that if the host is going to die anyway for some other reason, there is less reason for the pathogen to limit its impact. This means virulence should increase in pathogens infecting hosts whose lifespan is reduced for several reasons that have nothing to do with the virulence **[25, 26]**. In other words, the disease should be a more serious problem in species and populations that are getting hammered for other reasons. There are lots of species in a population that get hammered for other reasons and many of them seem to have solved this problem since they do not necessarily seem to be more susceptible to disease than populations are not. However, there are no any controlled experiments done to test this idea directly, and the effect may be real.

There is a lot of virulence evolution that goes on in other circumstances. For example, there are obligate parasites **[27, 28]**. Some of them are specialists on humans such as *Plasmodium falciparum*, HIV, influenza virus (A, B, and C), *Mycobacterium tuberculosis*, and the recent SARS-CoV-2. They have to complete their life cycle in humans. Some of them are also generalists, which are opportunists such as *Borrelia burgdorferi* (Lyme disease) or rabies, salmonella, bartonella viruses. And there are facultative parasites **[29]** including specialist and generalist ones. Commensal opportunists, which are *Staphylococcus aureus* living in our bodies all the time, then break out when they move between tissues, are specialists. There are also generalists, which are environmental opportunists such as *Pseudomonas aeruginosa* or mycobacterium. Obligate and facultative parasites are shown in more detail in table 1. The important point about where the parasite is that if it is not in the human whole time, the human may not be that important to its life cycle and may not be shaping the evolution of its virulence. It is known that responses to sources are stronger than responses to sinks. If the source is another animal population, then the pathogen would be responding very strongly to that and not very much to humans. In a human, it always goes extinct as Ebola and rabies, which could not evolve. The significance of effects depends on the frequency of encounters. Therefore, it is quite natural to think that the more time something happens the bigger the response to it would be, and if most of the experiences that pathogens are having their frequency of interaction is with some other species and not with humans, then their virulence evolution in humans is going to be trivial, and it would be mostly a byproduct of stuff happening elsewhere.

Table 1. Examples of pathogens and their ecological classification

	Obligate parasites	**Facultative parasites**
Specialists	*Plasmodium falciparum*, HIV, inluenza (A, B, C), *Mycobacterium tuberculosis*, SARS-CoV-2	*Staphylococcus aureus*, *Enterococcus faecalis*, *Haemophillus influenza*, *Streptococcus pneumoniae* *Candida albicans* **[30]**
Generalists	*Borrelia burgdorferi*, rabies virus, *Salmonella spp.*, *Bartonella henselae*	*Pseudomonas aeruginosa*, *Burkholderia cepacia*, *Rhodoccus equi*, *Mycobacterium marinum*

If we intervened, we could trigger the evolution of greater virulence. Anything we do that shifts transmission from vertical towards horizontal would increase virulence. Anything that increases the frequency of multiple infections with more impact on lethality than growth would increase virulence. Anything that reduces hosts' lifespan for some non-pathogen reason would probably increase virulence, and anything that selects for survival is more virulent strains within the host would increase virulence. They are all we do that would cause pathogens to react to what we are up to.

3. The new coronavirus

Coronaviruses are a large family of common viruses that are found in humans and animals. Many cases of the common cold are due to pathogenicity of a coronavirus. They have caused two large-scale outbreaks in the past two decades. The SARS (Severe Acute Respiratory Syndrome) virus in 2002 and the MERS (Middle East Respiratory Syndrome) virus in 2012 **[31, 32]**. It is generally been considered that these coronaviruses could cause future disease outbreaks because they are known to be able to evolve within animals and then jump to humans. In SARS palm civets and raccoon dogs were identified as the intermediate. Covid-19 is an example of this which is believed to have jumped from bats to pangolins to humans in a local seafood market in Wuhan China during 2019. Covid-19 refers to the coronavirus infectious disease found in 2019.

The actual disease itself is referred to as Covid-19, but the virus is called the SARS-CoV-2, which stands for severe acute respiratory syndrome coronavirus 2, and was named because its structure very closely resembles that of the SARS virus from 2002. This is the seventh known coronavirus to infect humans **[33]**. Two of which were similarly highly pathogenic (MERS and SARS), the other four are of low pathogenicity and endemic in humans.

A high level of infectiousness of the new coronavirus is enabled by its virulence factors, which are being studied in detail. One of the famous ones is the health of the host, indicating older people and people with immune dysfunctions appear to be more susceptible to worse effects of Covid-19. Another potential virulence factor of the disease is the nutritional status of the host. This is not uncommon among viruses since

the immune defenses that need to be mounted against viral infections could be energetically expensive. In many coronaviruses, the intestine is a common location for viral proliferation. If this is the case for Covid-19, nutritional status could be even more important as a virulence factor. Another postulated virulence factor is related to T cells. In many patients with Covid-19, there is a decrease in CD4 T cells following infection as conditions become critical. This is believed to be an important virulence factor, but the working principles of its mechanism are not well understood yet. Some postulate this is linked to nutrition, as some evidence exists showing reduced iron and zinc lead to decreases in CD4 T cells in mice **[34]**.

Based on all these, one could understand that the SARS-CoV-2 is an obligate and specialist parasite. It needs to enter a plant or animal cell in order to reproduce. Its RNA or DNA encodes for various proteins that are made by the host cell. Spike protein of SARS-CoV-2 binds to receptors on human cells (acetylcholine-esterase-2, ACE2) with a much higher affinity than other coronaviruses **[35]**. Another reason is that due to the higher lethality rate in SARS disease compared to Covid-19, it has been observed that its spread is limited at the epidemic level and does not cause a pandemic **[36]**.

4. Mathematical model of virulence dynamics

When examining virulence dynamics by creating a mathematical model, two basic assumptions are required. First, any host could not evolve on the evolutionary timescale of the virus. Because, as in all parasites, viruses evolve much faster than their hosts. Second, viruses have small sizes, short generation times, and high rates of direct reproduction in comparison with their hosts **[37]**.

Case I: A virus as an infectious agent in a population of hosts

Here, the case where only one virus is present in the population is examined. In the basic model of infection dynamics, some parameters are needed to describe the host-virus interaction. Those are:

k: rate of uninfected hosts' entering into the population,
u: the natural death rate of uninfected hosts,
v: virulence (disease-induced mortality),

$u + v$: the death rate of infected hosts,
β: infectivity (rate constant of infection),
S: uninfected (susceptible) hosts,
I: infected hosts,
βSI: the rate that infected hosts transmit the virus to uninfected.

Therefore, host-virus interaction could be described by those ordinary differential equations below.

$$\frac{dS}{dt} = k - uS - \beta SI \tag{1}$$

$$\frac{dI}{dt} = \beta SI - I(u + v) \tag{2}$$

Moreover, $\frac{1}{u+v}$ is the average lifetime of an infected host and βS is the rate at which one infected host produces new infections. The product of these two is the average number of new infections caused by a single infected host in its lifetime if there are S uninfected. This is called the reproductive ratio (R_0).

$$R_0 = \frac{\beta}{u + v}\frac{k}{u} \tag{3}$$

If $R_0 < 1$, the virus could not spread, the transmission chain would die out. The chain reaction is sub-critical. If $R_0 > 1$, there would be an exponential increase in infected hosts. A pandemic would occur and the chain reaction is super-critical. After some time the number of infected would peak and then decline, finally leading to a stable state. A graph for a relatively high value of the R_0 (5.7 for SARS-CoV-2) **[38]** is shown below (Figure 1).

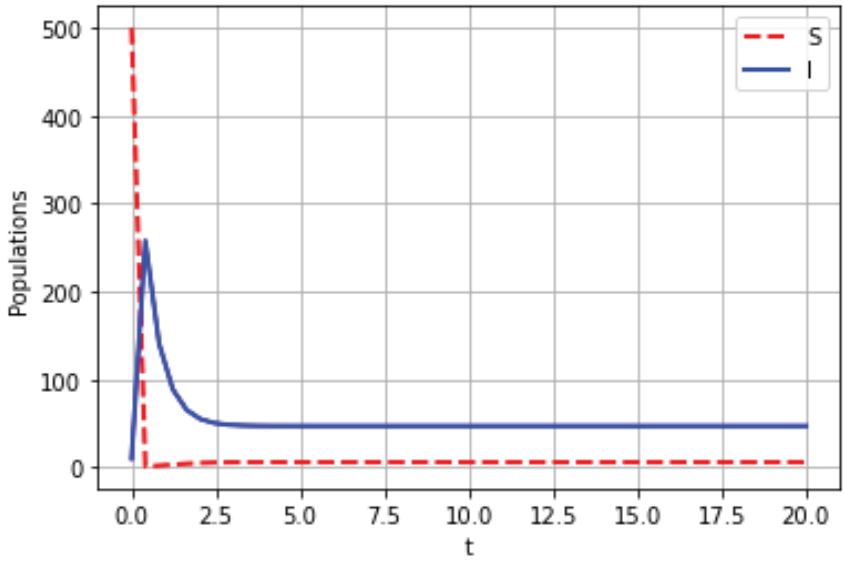

Figure 1. Graph of uninfected and infected populations over time (days) for an R_0 value of 5.7, indicating a situation where the pandemic would be dangerous. Here $S(0) = 500$ and $I(0) = 10$.

As seen in figure 1, after some time the number of infected people would peak and then decline. Finally, lead to a stable state given by

$$I^* = \frac{\beta k - u(u+v)}{\beta(u+v)} \tag{4}$$

Also, the S has a stable state which is $\frac{u+v}{\beta}$. The overall reproductive ratio of SARS-CoV-2 is greater than common influenza. However, estimates for both Covid-19 and influenza viruses are very context and time-specific, making direct comparisons more difficult.

Case II: Two viruses competing in a population of hosts

If there are two viruses competing for the same hosts, equations (1) and (2) could be extended to obtain

$$\frac{dS}{dt} = k - uS - S(\beta_1 I_1 + \beta_2 I_2) \tag{5}$$

$$\frac{dI_1}{dt} = \beta_1 S I_1 - I_1(u + v_1) \tag{6}$$

$$\frac{dI_2}{dt} = \beta_2 S I_2 - I_2(u + v_2) \tag{7}$$

Two viruses would differ in their virulences (v_1 and v_2) and infectivities (β_1 and β_2). Therefore, their reproductive ratios are

$$R_{0,1} = \frac{\beta_1}{u + v_1}\frac{k}{u}, \quad R_{0,2} = \frac{\beta_2}{u + v_2}\frac{k}{u} \tag{8}$$

Their coexistence is only possible in $R_{0,1} = R_{0,2}$. At equilibrium time derivatives of I_1 and I_2 must be zero.

$$\frac{dI_1}{dt} = 0 \Longrightarrow S = \frac{u + v_1}{\beta_1} \tag{9}$$

$$\frac{dI_2}{dt} = 0 \Longrightarrow S = \frac{u + v_2}{\beta_2} \tag{10}$$

Those equations prove that their ratios are equal. Also, $\frac{dS}{dt} = 0$. This condition where the reproductive ratios are equal is non-generic. It is even a condition that has never been encountered. Generally $R_{0,1} \neq R_{0,2}$, where coexistence is not possible. Here are the possible scenarios of competition:

If $R_{0,1} < 1$ and $R_{0,2} < 1$, then the stable states are

$$S = \frac{k}{u}, \quad I_1 = 0, \quad I_2 = 0 \tag{11}$$

indicating the population become uninfected.

If $R_{0,1} > 1 > R_{0,2}$, then the stable states are

$$S^* = \frac{u + v_1}{\beta_1}, \quad I_1^* = \frac{\beta_1 - u(u + v_1)}{\beta_1(u + v_1)} \tag{12}$$

indicating virus 2 (2nd strain) becomes extinct.

If $R_{0,1} < 1 < R_{0,2}$, then the stable states are

$$S^* = \frac{u + v_2}{\beta_2}, \quad I_2^* = \frac{\beta_2 - u(u + v_2)}{\beta_2(u + v_2)} \tag{13}$$

indicating virus 1 becomes extinct.

If both reproductive ratios exceed one ($R_{0,1} > 1$ and $R_{0,2} > 1$), then the higher one would out-compete the lower. For instance, in the case of $R_{0,2} > R_{0,1}$ the system would converge to the stable state of $R_{0,1} < 1 < R_{0,2}$ scenario. Virus 2 would out-compete virus 1.

If there is a competition between coronavirus and influenza in the current time, the final scenario, $R_{0,1} > 1$ and $R_{0,2} > 1$, could be expected to occur. Because while the R_0 values of both viruses are greater than 1, the reproductive ratio of coronavirus is also greater than that of influenza. When the necessary calculations are made by accepting the $R_{0,1}$ value of influenza as 1.3 **[39]** and the $R_{0,2}$ value of the coronavirus as 5.7, and when 10 infected from each in the sample population of 500 in case I were determined as the initial condition, the resultant graphic is shown in figure 2.

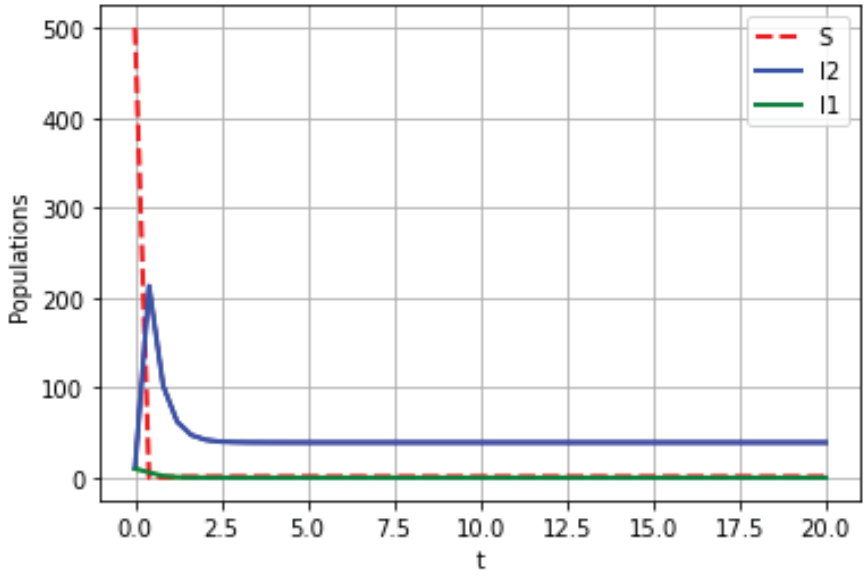

Figure 2. The coronavirus strain (with the number of infected is I_2) with the higher reproductive ratio is out-competing the influenza strain (with the number of infected is I_1). In this diagram, all infected individuals would eventually carry the SARS-CoV-2, while influenza becomes extinct. The system would converge to the stable states of equation (13).

Note that this also indicates the evolution would tend to increase its reproductive ratio. If there is no constraint between virulence and infectivity, β would increase and v would decrease. However, they have an association between them in general. Selection would always favor the more virulent virus.

Case III: The coexistence of two viruses with superinfection

In this case an infected host could be infected again by other virus. Selection no longer maximizes the reproductive ratio. But anyways, more virulent viruses out-compete less virulent ones within an infected individual, keeping the less virulent ones out of extinction. For a superinfection of n viruses, these equations could be written below.

$$\frac{dS}{dt} = k - uS - S\sum_{i=1}^{n} \beta_i I_i \tag{14}$$

$$\frac{dI_i}{dt} = I_i\left(\beta_i S - u - v_i + r\beta_i \sum_{j=1}^{i-1} I_j - r \sum_{j=i+1}^{n} \beta_j I_j\right), \quad i = 1,2,\dots,n \tag{15}$$

where v_i is the virulence of ith virus, r is the superinfection rate relative to uninfected hosts' infection (could be $r < 1$ or $r > 1$ for biological robustness of hosts against infections).

In superinfection one may assume a functional relation between overall virulence and infectivity, which could be

$$\beta_i = \frac{\alpha v_i}{c + v_i} \tag{16}$$

For a low virulence, infectivity increases with it, and for high, there is a saturation at maximum level. Therefore, the reproductive ratio could be written as

$$R_{0.i} = \frac{\alpha k v_i}{u(c + v_i)(u + v_i)} \tag{17}$$

where α and c are constants. The optimal virulence, which maximizes the R_0 is then $v_{opt} = \sqrt{cu}$. By considering the initial parameters in the previous cases, the change of virulence according to the overall reproductive ratio is shown in Figure 3.

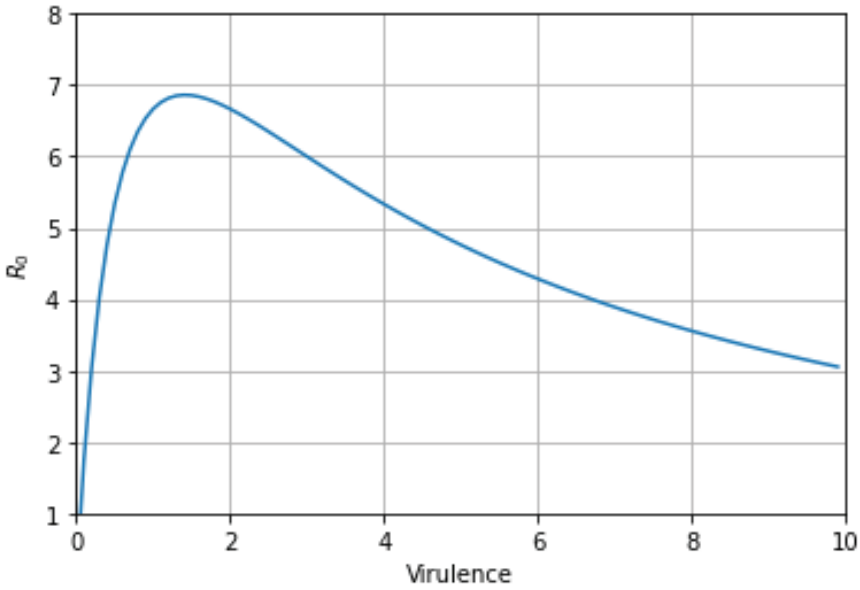

Figure 3. Virulence-R_0 graph in the coexistence of multiple viruses (here $\alpha = 8$ and $c = 1$). In case of a coexistence between the coronavirus and influenza, this should be an expected behavior. When the coronavirus was handled individually, that is, when the pandemic was the strongest, the R_0 value increased up to 7.8 in Shanghai **[40]**.

5. Conclusion

Since the first days of the pandemic, there have been many studies on the contagiousness parameters of the coronavirus, which were also cited in the previous sections. Even in the mathematical epidemiology model of the disease, entropy-based metric and global transmission have been tried to be predicted **[41]**. The distribution and consequences of the epidemic vary according to various factors such as: the number of households, humidity, temperature, season, hygiene, access to health facilities and isolation capacity, demographic population characteristics, smoking, the host's ability to transmit infection, immunity, nutritional status, accompanying diseases, prevalence, pathogenicity, route of transmission, transmission characteristics and virulence factors **[42]**. Moreover, in this study, a virulence model for influenza, which may be one of the accompanying diseases, has been tried to be created. It is still

not completely clear what would happen when two viruses encounter each other on the same host.

Both the coronavirus and influenza have similar transmission characteristics and clinical manifestations. But , a statistics from Turkey shows that their coinfection may be limited. In a two month period, only 6 of 1103 Covid-19 cases were diagnosed with influenza, indicating the coexistence (coinfection) seems to be rare **[43]**. However, some of them could be undiagnosed. There are some other coexistence reports from other countries as well. Alongside with that, influenza coexist with some other respiratory pathogens like mycoplasma, legionella CMV, parainfluenza, RSV, EBV, rhinovirus and other coronavirus strains. In short, since coexistence between coronavirus and influenza is rarely seen in certain cases, it does not seem possible to talk about a competition between them much.

Within the scope of all these data, the superinfection scenario, that is, if a patient with influenza or coronavirus is infected by another, seems a more likely situation. It is now known that the measures taken against Covid-19 and the examinations performed cause a decrease in respiratory diseases such as influenza **[44]**. This is proof that the two viruses would coexist with each other. Coronavirus is also known to coexist with other respiratory viruses. Therefore, it is predicted that, like other members of the coronavirus family, SARS-CoV-2 will naturally avoid competition with other viruses, but would increase virulence on hosts.

References

1) Osterrieder, N., Kamil, J. P., Schumacher, D., Tischer, B. K., & Trapp, S. (2006). Marek's disease virus: from miasma to model. Nature Reviews Microbiology, 4(4), 283-294.
2) Bertzbach, L. D., van Haarlem, D. A., Härtle, S., Kaufer, B. B., & Jansen, C. A. (2019). Marek's Disease Virus Infection of Natural Killer Cells. Microorganisms, 7(12), 588.
3) Levin, B. R. (1996). The evolution and maintenance of virulence in microparasites. Emerging infectious diseases, 2(2), 93.
4) Anderson, R. M., Fraser, C., Ghani, A. C., Donnelly, C. A., Riley, S., Ferguson, N. M., ... & Hedley, A. J. (2004). Epidemiology, transmission dynamics and control of SARS: the 2002–2003 epidemic. Philosophical Transactions of the Royal Society of London. Series B: Biological Sciences, 359(1447), 1091-1105.
5) Wain, L. V., Bailes, E., Bibollet-Ruche, F., Decker, J. M., Keele, B. F., Van Heuverswyn, F., ... & Sharp, P. M. (2007). Adaptation of HIV-1 to its human host. Molecular biology and evolution, 24(8), 1853-1860.
6) World Health Organization. (2016). World malaria report 2015. World Health Organization.
7) Churcher, T. S., Trape, J. F., & Cohuet, A. (2015). Human-to-mosquito transmission efficiency increases as malaria is controlled. Nature communications, 6(1), 1-8.
8) Alizon, S., Hurford, A., Mideo, N., & Van Baalen, M. (2009). Virulence evolution and the trade-off hypothesis: history, current state of affairs and the future. Journal of evolutionary biology, 22(2), 245-259.
9) Mackinnon, M. J., & Marsh, K. (2010). The selection landscape of malaria parasites. Science, 328(5980), 866-871.
10) Abkallo, H. M., Tangena, J. A., Tang, J., Kobayashi, N., Inoue, M., Zoungrana, A., ... & Culleton, R. (2015). Within-host competition does not select for virulence in malaria parasites; studies with Plasmodium yoelii. PLoS Pathog, 11(2), e1004628.
11) Barclay, V. C., Sim, D., Chan, B. H., Nell, L. A., Rabaa, M. A., Bell, A. S., ... & Read, A. F. (2012). The evolutionary consequences of blood-stage vaccination on the rodent malaria Plasmodium chabaudi. PLoS Biol, 10(7), e1001368.
12) Alizon, S., & Michalakis, Y. (2015). Adaptive virulence evolution: the good old fitness-based approach. Trends in ecology & evolution, 30(5), 248-254.
13) Schönpflug, W. (1986). The trade-off between internal and external information storage. Journal of Memory and Language, 25(6), 657-675.

14) Ellis, M. E. (1982). Evolution of aversive information processing: a temporal trade-off hypothesis. Brain, behavior and evolution, 21(2-3), 151-160.
15) McDonald, B. A., & Linde, C. (2002). Pathogen population genetics, evolutionary potential, and durable resistance. Annual review of phytopathology, 40(1), 349-379.
16) Kerr, P. J., Liu, J., Cattadori, I., Ghedin, E., Read, A. F., & Holmes, E. C. (2015). Myxoma virus and the Leporipoxviruses: an evolutionary paradigm. Viruses, 7(3), 1020-1061.
17) Fenner, F., & Woodroofe, G. M. (1965). Changes in the virulence and antigenic structure of strains of myxoma virus recovered from Australian wild rabbits between 1950 and 1964. Australian Journal of Experimental Biology and Medical Science, 43, 359-370.
18) Kerr, P. J., Ghedin, E., DePasse, J. V., Fitch, A., Cattadori, I. M., Hudson, P. J., ... & Holmes, E. C. (2012). Evolutionary history and attenuation of myxoma virus on two continents. PLoS Pathog, 8(10), e1002950.
19) Stewart, A. D., Logsdon, J. M., & Kelley, S. E. (2005). An empirical study of the evolution of virulence under both horizontal and vertical transmission. Evolution, 59(4), 730-739.
20) Lipsitch, M., Siller, S., & Nowak, M. A. (1996). The evolution of virulence in pathogens with vertical and horizontal transmission. Evolution, 50(5), 1729-1741.
21) Alizon, S., de Roode, J. C., & Michalakis, Y. (2013). Multiple infections and the evolution of virulence. Ecology letters, 16(4), 556-567.
22) Brown, S. P., Hochberg, M. E., & Grenfell, B. T. (2002). Does multiple infection select for raised virulence?. Trends in microbiology, 10(9), 401-405.
23) Guiqing, W. A. N. G. (2009). The Stability of Pathogenic of Gray Leaf Spot Pathogens [J]. Acta Agriculturae Boreali-Occidentalis Sinica, 3.
24) Kollaritsch, H., Que, J. U., Kunz, C., Wiedermann, G., Herzog, C., & Cryz Jr, S. J. (1997). Safety and immunogenicity of live oral cholera and typhoid vaccines administered alone or in combination with antimalarial drugs, oral polio vaccine, or yellow fever vaccine. Journal of Infectious Diseases, 175(4), 871-875.
25) Halstead, S. B. (2009). Antibodies determine virulence in dengue. Ann NY Acad Sci, 1171(Suppl 1), E48-56.
26) Gonçalves, I. R., Dantas, R. C. C., Ferreira, M. L., Batistão, D. W. D. F., Gontijo-Filho, P. P., & Ribas, R. M. (2017). Carbapenem-resistant Pseudomonas aeruginosa: association with virulence genes and biofilm formation. brazilian journal of microbiology, 48(2), 211-217.

27) Becker, Y. E. C. H. I. E. L. (1978). The chlamydia: molecular biology of procaryotic obligate parasites of eucaryocytes. Microbiological Reviews, 42(2), 274.
28) Bouayed, J., & Bohn, T. (2020). Behavioral manipulation—key to the successful global spread of the new coronavirus SARS-CoV-2?. Journal of medical virology.
29) Luong, L. T., & Mathot, K. J. (2019). Facultative parasites as evolutionary stepping-stones towards parasitic lifestyles. Biology letters, 15(4), 20190058.
30) Abaci, Ö., Halki-Uztan, A., & Ates, M. (2008). Specific identification of Candida albicans and Candida dubliniensis by PCR using species-specific primers. Annals of microbiology, 58(2), 325.
31) Tseng, C. T., Sbrana, E., Iwata-Yoshikawa, N., Newman, P. C., Garron, T., Atmar, R. L., ... & Couch, R. B. (2012). Immunization with SARS coronavirus vaccines leads to pulmonary immunopathology on challenge with the SARS virus. PloS one, 7(4), e35421.
32) Mackay, I. M., & Arden, K. E. (2015). MERS coronavirus: diagnostics, epidemiology and transmission. Virology journal, 12(1), 1-21.
33) Burki, T. K. (2020). Coronavirus in China. The Lancet. Respiratory Medicine, 8(3), 238.
34) Briguglio, M., Pregliasco, F. E., Lombardi, G., Perazzo, P., & Banfi, G. (2020). The malnutritional status of the host as a virulence factor for new coronavirus SARS-CoV-2. Frontiers in Medicine, 7, 146.
35) Walls, A. C., Park, Y. J., Tortorici, M. A., Wall, A., McGuire, A. T., & Veesler, D. (2020). Structure, function, and antigenicity of the SARS-CoV-2 spike glycoprotein. Cell.
36) World Health Organization. (2003). Consensus document on the epidemiology of severe acute respiratory syndrome (SARS) (No. WHO/CDS/CSR/GAR/2003.11). World Health Organization.
37) Nowak, M. A. (2006). Evolutionary dynamics: exploring the equations of life. Harvard university press.
38) Bulut, C., & Kato, Y. (2020). Epidemiology of COVID-19. Turkish journal of medical sciences, 50(SI-1), 563-570.
39) Lee, B. Y., Brown, S. T., Cooley, P. C., Zimmerman, R. K., Wheaton, W. D., Zimmer, S. M., ... & Burke, D. S. (2010). A computer simulation of employee vaccination to mitigate an influenza epidemic. American journal of preventive medicine, 38(3), 247-257.
40) Zhang, J., Litvinova, M., Liang, Y., Wang, Y., Wang, W., Zhao, S., ... & Yu, H. (2020). Changes in contact patterns shape the dynamics of the COVID-19 outbreak in China. Science.
41) Wang, Z., Broccardo, M., Mignan, A., & Sornette, D. (2020). The dynamics of entropy in the COVID-19 outbreaks. Nonlinear Dynamics, 101(3), 1847-1869.

42) Türken, M., & Köse, Ş. (2020). Covid-19 bulaş yolları ve önleme. Tepecik Eğitim ve Araştırma Hastanesi Dergisi, 30, 36-42.
43) Ozaras, R., Cirpin, R., Duran, A., Duman, H., Arslan, O., Bakcan, Y., ... & Bilir, S. (2020). Influenza and COVID-19 Co-infection: Report of 6 cases and review of the Literature. Journal of Medical Virology.
44) Soo, R. J. J., Chiew, C. J., Ma, S., Pung, R., & Lee, V. (2020). Decreased influenza incidence under COVID-19 control measures, Singapore. Emerging infectious diseases, 26(8), 1933.

Chapter 3

NOTES ON THE ALMOST LORENTZIAN R-PARACONTACT STRUCTURES ON TANGENT BUNDLE

Haşim ÇAYIR[1]

1 Giresun University, Faculty of Arts and Sciences, Department of Mathematics, Turkey, E-mail:hasim.cayir@giresun.edu.tr, ORCID ID: 0000-0003-0348-8665

1 Introduction

Let f be a function in M, we write f^V in $T(M)$ obtained by forming the composition of $\pi: T(M) \to M$ and $f: M \to R$, so that

$$f^V = f o \pi. \tag{1.1}$$

Thus, if a point $\tilde{p} \in \pi^{-1}(U)$ has induced coordinates (W^h, θ^h), then

$$f^V(\tilde{p}) = f^V(W, \theta) = f o \pi(\tilde{p}) = f(p) = f(W). \tag{1.2}$$

We called f^V the vertical lift of the function f [9].

Let $W \in \Im_0^1(T(M))$ be such that $Wf^V = 0$ for all $f \in \Im_0^0(M)$. Then, W is a vertical vector field. Let $\begin{pmatrix} W^h \\ W^{\bar{h}} \end{pmatrix}$ be components of W according to the induced coordinates. Then W is vertical if and only if its components in $\pi^{-1}(U)$ satisfy

$$\begin{pmatrix} W^h \\ W^{\bar{h}} \end{pmatrix} = \begin{pmatrix} 0 \\ W^{\bar{h}} \end{pmatrix}. \tag{1.3}$$

Let $\tilde{\omega} \in \Im_1^0(T(M))$ be such that $\tilde{\omega}(W)^V = 0$ for all $W \in \Im_0^1(M)$. Then, $\tilde{\omega}$ is a vertical $1-$form in $T(M)$. We define the ω^V of the $1-$form ω by

$$\omega^V = (\omega_i)^V (dW^i)^V \tag{1.4}$$

in each open set $\pi^{-1}(U)$. The ω^V of ω with local expression $\omega = \omega_i dW^i$ has components

$$\omega^V: (\omega^i, 0) \tag{1.5}$$

according to the induced coordinates in $T(M)$. The F^V of an element $F \in \Im_1^1(M)$ with local components F_i^h has components [9]

$$F^V: \begin{pmatrix} 0 & 0 \\ F_i^h & 0 \end{pmatrix}. \tag{1.6}$$

If f is a function in M, we write f^C in $T(M)$ defined by

$$f^C = \iota(df) \tag{1.7}$$

and call f^C the complete lift of the function f. The f^C of a function f has the local expression

$$f^C = \theta^i \partial_i f = \partial f \tag{1.8}$$

according to the induced coordinates in $T(M)$.

Let $W \in \Im_0^1(M)$. We define a vector field W^C in $T(M)$ by

$$W^C f^C = (Wf)^C, \tag{1.9}$$

f being an arbitrary function in M, W^C is called as the complete lift of W in $T(M)$ [2,9].

ω^C of ω with components ω_i in M has components of the form

$$\omega^C : (\partial\omega_{i,} \omega_i) \tag{1.10}$$

according to the induced coordinates in $T(M)$ [2].

The F^C of an element $F \in \Im_1^1(M)$ with local components F_i^h has the components

$$F^C : \begin{pmatrix} F_i^h & 0 \\ \partial F_i^h & F_i^h \end{pmatrix}. \tag{1.11}$$

The f^H of $f \in \Im_0^0(M)$ to $T(M)$ is given by

$$f^H = f^C - \nabla_\gamma f,$$

where

$$\nabla_\gamma f = \gamma \nabla f. \tag{1.12}$$

Let $W \in \Im_0^1(M)$. Then the W^H of W is defined by

$$W^H = W^C - \nabla_\gamma W \tag{1.13}$$

in $T(M)$.

Let $\omega \in \Im_1^0(M)$ with affine connection ∇. Then, ω^H of ω is defined by

$$\omega^H = \omega^C - \nabla_\gamma \omega \tag{1.14}$$

on $T(M)$, where $\nabla_\gamma \omega = \gamma \nabla \omega$.

Proposition 1.1 For any $W \in \Im_0^1(M)$, $f \in \Im_0^0(M)$ and ∇^C is the complete lift of the ∇ to $T(M)$ [9]

$$\nabla^C_{W^V} f^C = (\nabla_W f)^V, \nabla^C_{W^C} f^V = (\nabla_W f)^V, \nabla^C_{W^C} f^C = (\nabla_W f)^C, \nabla^C_{W^V} f^V = 0. \tag{1.15}$$

Proposition 1.2 For any $W, \theta \in \Im_0^1(M_n)$ and ∇^C is the complete lift of the ∇ to $T(M)$ [9]

$$\nabla^C_{W^V} \theta^V = 0, \nabla^C_{W^V} \theta^C = (\nabla_W \theta)^V, \tag{1.16}$$

$$\nabla^C_{W^C} \theta^V = (\nabla_W \theta)^V, \nabla^C_{W^C} \theta^C = (\nabla_W \theta)^C.$$

Proposition 1.3 The horizontal lift of an affine connection ∇ in M to $T(M)$, denoted by ∇^H, defined by

$$\nabla^H_{W^V} \theta^V = 0, \nabla^H_{W^V} \theta^H = 0, \tag{1.17}$$

$$\nabla^H_{W^H} \theta^V = (\nabla_W \theta)^V, \nabla^H_{W^H} \theta^H = (\nabla_W \theta)^H$$

for any $W, \theta \in \Im_0^1(M)$ [9].

2. Main Results

Let F be a tensor field of type $(1,1)$ on a manifold $\bar{M}$ of dimension $(2n+r)$. If there exists on $\bar{M}$ the vector fields (σ_a) and the 1- forms (η^a) such that

$$\eta^\alpha(\sigma_\beta) = -\delta^\alpha_\beta, F(\sigma_\alpha) = 0, \eta^\alpha oF = 0, F^2 = I^2 - \sum_{\alpha=1}^{r} \sigma_\alpha \otimes \eta^r, \tag{2.1}$$

then the structure $(F, \sigma_\alpha, \eta^\alpha)$ is also called a Lorentzian almost r-paracontact structure, where $(\alpha, \beta = 1,2,\ldots,r)$ and δ_β^α denotes Kronecker delta.

2.1 Complete Lifts and Covarient Derivatives

From (2.1) and lifts of the paracomplex tensor fields, we obtain

$$(F^2)^C = \left(I - \sum_{\alpha=1}^{r} \sigma_\alpha \otimes \eta^\alpha\right)^C,$$

$$(F^2)^C = I - \sum_{\alpha=1}^{r} (\sigma_\alpha^V \otimes \eta^{\alpha C} + \sigma_\alpha^C \otimes \eta^{\alpha V})$$

$$(F^2)^C W^C = W^C - \sum_{\alpha=1}^{r} ((\eta^\alpha W)^C \sigma_\alpha^V + (\eta^\alpha W)^V \sigma_\alpha^C) \tag{2.3}$$

and

$$F^C(\sigma_\alpha^V) = 0, F^C(\sigma_\alpha^C) = 0, \tag{2.4}$$

$$\eta^{\alpha V} \circ F^C = 0, \eta^{\alpha C} \circ F^V = 0, \eta^{\alpha C} \circ F^C = 0, \tag{2.5}$$

$$\eta^{\alpha V}(\sigma_\beta^V) = 0, \eta^{\alpha V}(\sigma_\beta^C) = -\delta_\beta^\alpha, \eta^{\alpha C}(\sigma_\beta^V) = -\delta_\beta^\alpha, \eta^{\alpha C}(\sigma_\beta^C) = 0. \tag{2.6}$$

Theorem 2.1 Let $\bar{M}$ be differentiable manifold endowed with almost Lorentzian r-paracontact structure $(F, \sigma_\alpha, \eta^\alpha)$ for any $W \in \Im_0^1(\bar{M}), W^V, W^C \in \Im(T(\bar{M}))$, then a structure $\widehat{\Psi}$ of $\Im_1^1(T(\bar{M}))$ defined by

$$\widehat{\Psi} = F^C - \sum_{\alpha=1}^{r} (\sigma_\alpha^V \otimes \eta^{\alpha V} - \sigma_\alpha^C \otimes \eta^{\alpha C}) \tag{2.7}$$

is an almost paracomplex structure in $T(\bar{M}).\rho$

Proof. For $W \in \Im_0^1(\bar{M})$ and W^V, W^C are the vertical and complete lifts of W, respectively.

$$\hat{\Psi}^2(W^C) = \hat{\Psi}(\hat{\Psi}W^C)$$

$$= \hat{\Psi}((FW)^C - \sum_{\alpha=1}^{r}((\eta^\alpha(W))^V\sigma_\alpha^V - (\eta^\alpha(W))^C\sigma_\alpha^C))$$

$$= (F^C - \sum_{\alpha=1}^{r}\sigma_\alpha^V \otimes \eta^{\alpha V} - \sigma_\alpha^C \otimes \eta^{\alpha C}).((FW)^C - \sum_{\alpha=1}^{r}((\eta^\alpha(W))^V\sigma_\alpha^V - (\eta^\alpha(W))^C\sigma_\alpha^C))$$

$$= (F^C)^2W^C + \sum_{\alpha=1}^{r}(-F^C((\eta^\alpha(W))^V\sigma_\alpha^V + F^C(\eta^\alpha(W))^C\sigma_\alpha^C - (\eta^{\alpha V}(FW)^C)\sigma_\alpha^V$$

$$+\sigma_\alpha^V \otimes \eta^{\alpha V}((\eta^\alpha(W))^V\sigma_\alpha^V) - \sigma_\alpha^V \otimes \eta^{\alpha V}((\eta^\alpha(W))^C\sigma_\alpha^C) + (\eta^{\alpha C}(FW)^C)\sigma_\alpha^C$$

$$-\sigma_\alpha^C \otimes \eta^{\alpha C}((\eta^\alpha(W))^V\sigma_\alpha^V) + \sigma_\alpha^C \otimes \eta^{\alpha C}((\eta^\alpha(W))^C\sigma_\alpha^C))$$

$$= W^C - \sum_{\alpha=1}^{r}((\eta^\alpha W)^C\sigma_\alpha^V + (\eta^\alpha W)^V\sigma_\alpha^C) + \sum_{\alpha=1}^{r}(-(\eta^\alpha W)^V(F^C\sigma_\alpha^V) + ((\eta^\alpha W))^C(F^C\sigma_\alpha^C)$$

$$-(\eta^\alpha(F(W)))^V\sigma_\alpha^V + (\eta^\alpha(W))^V(\eta^{\alpha V}(\sigma_\alpha)^V)\sigma_\alpha^V - (\eta^\alpha(W))^C(\eta^{\alpha V}(\sigma_\alpha)^C)\sigma_\alpha^V$$

$$+\left(\eta^\alpha(F(W))\right)^C\sigma_\alpha^C - (\eta^\alpha(W))^V(\eta^{\alpha C}(\sigma_\alpha^V))\sigma_\alpha^C - (\eta^\alpha(W))^C(\eta^{\alpha C}(\sigma_\alpha^C))\sigma_\alpha^C)$$

$$= W^C - \sum_{\alpha=1}^{r}((\eta^\alpha(W))^C\sigma_\alpha^V + (\eta^\alpha(W))^V\sigma_\alpha^C + (\eta^\alpha(W))^V(F^C\sigma_\alpha^V) - (\eta^\alpha(W))^C(F^C\sigma_\alpha^C)$$

$$+\left(\eta^\alpha(F(W))\right)^V\sigma_\alpha^V - (\eta^\alpha(W))^V(\eta^{\alpha V}(\sigma_\alpha)^V)\sigma_\alpha^V + (\eta^\alpha(W))^C(\eta^{\alpha V}(\sigma_\alpha)^C)\sigma_\alpha^V$$

$$-(\eta^\alpha(F(W)))^C\sigma_\alpha^C + \left(\eta^\alpha(W)\right)^V(\eta^{\alpha C}(\sigma_\alpha^V))\sigma_\alpha^C + \left(\eta^\alpha(W)\right)^C(\eta^{\alpha C}(\sigma_\alpha^C)\sigma_\alpha^C$$

By means of (2.1),(2.3),(2.4),(2.5) and (2.6), we have

$$\hat{\Psi}^2 = I \tag{2.8}$$

So, $\hat{\Psi}$ is an almost paracomplex structure in $T(\bar{M})$, the proof is completed. Similarly $\hat{\Psi}^2 W^V = W^V$ is proved. Considering lift properties of tensor fields and the equation (2.7), we get

$$\hat{\Psi}W^V = (FW)^V + \left(\eta^\alpha(W)\right)^V\sigma_\alpha^C, \tag{2.9}$$

$$\hat{\Psi}W^C = (FW)^C - \left(\eta^\alpha(W)\right)^V\sigma_\alpha^V + \left(\eta^\alpha(W)\right)^C\sigma_\alpha^C, \tag{2.10}$$

where $W \in \Im_0^1(\bar{M}), W^V, W^C \in \Im(T(\bar{M}))$.

If $\eta^\alpha(W) = 0$, we have

$$\widehat{\Psi}W^V = (FW)^V, \widehat{\Psi}W^C = (FW)^C. \tag{2.11}$$

If we put $W = \sigma_\alpha$, i.e. $\eta^a(\sigma_\beta) = -\delta_\beta^a$ and σ_α has the conditions of (2.1), then we have

$$\widehat{\Psi}\sigma_\alpha^V = -\delta_\beta^\alpha \sigma_\alpha^C = -\sigma_\beta^C, \widehat{\Psi}\sigma_\alpha^C = \delta_\beta^\alpha \sigma_\alpha^V = \sigma_\beta^V, \alpha, \beta = 1,2,\dots,r. \tag{2.12}$$

Theorem 2.2 Let the $T(\bar{M})$ tangent bundle of the manifold $\bar{M}$ admits $\widehat{\Psi}$ defined by (2.7). For any vector fields W, θ such that $\eta^\alpha(\theta) = 0$, we get

$$i)(\nabla_{W^V}^C \widehat{\Psi})\theta^V = 0,$$

$$ii)(\nabla_{W^V}^C \widehat{\Psi})\theta^C = ((\nabla_W F)\theta)^V + \sum_{\alpha=1}^{r} ((\nabla_W \eta^\alpha)\theta)^V \sigma_\alpha^C,$$

$$iii)(\nabla_{W^C}^C \widehat{\Psi})\theta^V = ((\nabla_W F)\theta)^V + \sum_{\alpha=1}^{r} ((\nabla_W \eta^\alpha)\theta)^V \sigma^C,$$

$$iv)(\nabla_{W^C}^C \widehat{\Psi})\theta^C = ((\nabla_W F)\theta)^C - \sum_{\alpha=1}^{r} ((\nabla_W \eta^\alpha)\theta)^V \sigma_\alpha^V + \sum_{\alpha=1}^{r} ((\nabla_W \eta^\alpha)\theta)^C \sigma_\alpha^C,$$

where $W, \theta \in \Im_0^1(\bar{M})$, $F \in \Im_1^1(\bar{M})$, a $1-$form $\eta^\alpha \in \Im_1^0(\bar{M})$, a vector field σ_α and ∇^C is the complete lift of the ∇ to $T(\bar{M})$.

Proof. For $\widehat{\Psi} \in \Im_1^1(T(\bar{M}))$ defined by (2.7), we have

$$i)(\nabla_{W^V}^C \widehat{\Psi})\theta^V = \nabla_{W^V}^C (F^C - \sum_{\alpha=1}^{r} (\sigma_\alpha^V \otimes \eta^{\alpha V} - \sigma_\alpha^C \otimes \eta^{\alpha C}))\theta^V$$

$$-(F^C - \sum_{\alpha=1}^{r} (\sigma_\alpha^V \otimes \eta^{\alpha V} - \sigma_\alpha^C \otimes \eta^{\alpha C}))\nabla_{W^V}^C \theta^V$$

$$= \nabla_{W^V}^C (F\theta)^V - \sum_{\alpha=1}^{r} \nabla_{W^V}^C (\eta^{\alpha V}(\theta)^V)\sigma_\alpha^V + \sum_{\alpha=1}^{r} \nabla_{W^V}^C (\eta^\alpha(\theta))^V)\sigma_\alpha^C$$

$$= 0,$$

$$ii)(\nabla_{W^V}^C \widehat{\Psi})\theta^C = \nabla_{W^V}^C (F^C - \sum_{\alpha=1}^{r} (\sigma_\alpha^V \otimes \eta^{\alpha V} - \sigma_\alpha^C \otimes \eta^{\alpha C})\theta^C$$

$$-(F^C - \sum_{\alpha=1}^{r} (\sigma_\alpha^V \otimes \eta^{\alpha V} - \sigma_\alpha^C \otimes \eta^{\alpha C})\nabla_{W^V}^C \theta^C$$

$$= \nabla^C_{W^V} F^C \theta^C - \sum_{\alpha=1}^{r} \nabla^C_{W^V} (\eta^\alpha(\theta))^V \sigma_\alpha^V + \sum_{\alpha=1}^{r} \nabla^C_{W^V} (\eta^\alpha(\theta))^C \sigma_\alpha^C$$

$$-F^C \nabla^C_{W^V} \theta^C + \sum_{\alpha=1}^{r} (\eta^{\alpha V} (\nabla_W \theta)^V) \sigma_\alpha^V - \sum_{\alpha=1}^{r} (\eta^\alpha (\nabla_W \theta))^V \sigma_\alpha^C$$

$$= \left(\nabla^C_{W^C} F^C\right)\theta^C - F^C \nabla^C_{W^V} \theta^C + F^C \nabla^C_{W^V} \theta^C$$

$$- \sum_{\alpha=1}^{r} (\nabla_W (\eta^\alpha(\theta)))^V \sigma_\alpha^C + \sum_{\alpha=1}^{r} ((\nabla_W \eta^\alpha)\theta)^V \sigma_\alpha^C$$

$$= ((\nabla_W F)\theta)^V + \sum_{\alpha=1}^{r} ((\nabla_W \eta^\alpha)\theta)^V \sigma_\alpha^C,$$

$$iii)(\nabla^C_{W^C} \hat{c})\theta^V = \nabla^C_{W^C} (F^C - \sum_{\alpha=1}^{r} (\sigma_\alpha^V \otimes \eta^{\alpha V} - \sigma_\alpha^C \otimes \eta^{\alpha C}))\theta^V$$

$$-(F^C - \sum_{\alpha=1}^{r} (\sigma_\alpha^V \otimes \eta^{\alpha V} - \sigma_\alpha^C \otimes \eta^{\alpha C}) \nabla^C_{W^C} \theta^V$$

$$= \nabla^C_{W^C} F^C \theta^V - \sum_{\alpha=1}^{r} \nabla^C_{W^C} (\eta^{\alpha V} (\theta^V)) \sigma_\alpha^V + \sum_{\alpha=1}^{r} \nabla^C_{W^C} (\eta^\alpha(\theta))^V \sigma_\alpha^C$$

$$-F^C \nabla^C_{W^C} \theta^V + \sum_{\alpha=1}^{r} \eta^{\alpha V} (\nabla_W \theta)^V \sigma_\alpha^V - \sum_{\alpha=1}^{r} (\eta^\alpha (\nabla_W \theta))^V \sigma_\alpha^C$$

$$= \left(\nabla^C_{W^C} F^C\right)\theta^V - F^C \nabla^C_{W^C} \theta^V + F^C \left(\nabla^C_{W^C} \theta^V\right)$$

$$- \sum_{\alpha=1}^{r} (\nabla_W (\eta^\alpha(\theta))^V \sigma_\alpha^C + \sum_{\alpha=1}^{r} ((\nabla_W \eta^\alpha)\theta)^V \sigma_\alpha^C$$

$$= ((\nabla_W F)\theta)^V + \sum_{\alpha=1}^{r} ((\nabla_W \eta^\alpha)\theta)^V \sigma^C,$$

$$\imath v)(\nabla^C_{W^C} \widehat{\Psi})\theta^C = \nabla^C_{W^C} (F^C - \sum_{\alpha=1}^{r} (\sigma_\alpha^V \otimes \eta^{\alpha V} - \sigma_\alpha^C \otimes \eta^{\alpha C}))\theta^C$$

$$-(F^C - \sum_{\alpha=1}^{r} (\sigma_\alpha^V \otimes \eta^{\alpha V} - \sigma_\alpha^C \otimes \eta^{\alpha C})) \nabla^C_{W^C} \theta^C$$

$$= \nabla^C_{W^C} F^C \theta^C - \sum_{\alpha=1}^{r} \nabla^C_{W^C} (\eta^\alpha(\theta))^V \sigma_\alpha^V + \sum_{\alpha=1}^{r} \nabla^C_{W^C} (\eta^\alpha(\theta))^C \sigma_\alpha^C$$

$$-F^C\nabla^C_{W^C}\theta^C+\sum_{\alpha=1}^{r}(\eta^\alpha(\nabla_W\theta))^V\sigma_\alpha^V-\sum_{\alpha=1}^{r}(\eta^\alpha(\nabla_W\theta))^C\sigma_\alpha^C$$

$$=\left(\nabla^C_{W^C}F^C\right)\theta^C+F^C\left(\nabla^C_{W^C}\theta^C\right)-F^C\nabla^C_{W^C}\theta^C+\sum_{\alpha=1}^{r}(\nabla_W(\eta^\alpha(\theta)))^V\sigma_\alpha^V$$

$$-\sum_{\alpha=1}^{r}((\nabla_W\eta^\alpha)\theta)^V\sigma_\alpha^V-\sum_{\alpha=1}^{r}(\nabla_W(\eta^\alpha(\theta)))^C\sigma_\alpha^C+\sum_{\alpha=1}^{r}((\nabla_W\eta^\alpha)\theta)^C\sigma_\alpha^C$$

$$=((\nabla_WF)\theta)^C-\sum_{\alpha=1}^{r}((\nabla_W\eta^\alpha)\theta)^V\sigma_\alpha^V+\sum_{\alpha=1}^{r}((\nabla_W\eta^\alpha)\theta)^C\sigma_\alpha^C,$$

where $\eta^\alpha(\nabla_W\theta)=\nabla_W(\eta^\alpha\theta)-(\nabla_W\eta^\alpha)\theta$ and $F\theta\in\Im_0^1(\bar{M})$.

Corollary 2.1 If we put $\theta=\sigma_\alpha$, i.e. $\eta^\alpha(\sigma_\beta)=-\delta^\alpha_\beta$ and σ_α has the conditions of (2.1), we get

$$i)(\nabla^C_{W^V}\tilde{\Phi})\sigma_\alpha^V=-\sum_{\alpha=1}^{r}(\nabla_W\sigma_\alpha)^V,$$

$$ii)(\nabla^C_{W^V}\tilde{\Phi})\sigma_\alpha^C=((\nabla_WF)\sigma_\alpha)^V+\sum_{\alpha=1}^{r}((\nabla_W\eta^\alpha)\sigma_\alpha)^V\sigma_\alpha^C,$$

$$iii)(\nabla^C_{W^C}\tilde{\Phi})\sigma_\alpha^V=((\nabla_WF)\sigma_\alpha)^V-\sum_{\alpha=1}^{r}(\nabla_W\sigma_\alpha)^C+\sum_{\alpha=1}^{r}((\nabla_W\eta^\alpha)\sigma_\alpha)^V\sigma_\alpha^C,$$

$$iv)(\nabla^C_{W^C}\tilde{\Phi})\sigma_\alpha^C=((\nabla_WF)\sigma_\alpha)^C+\sum_{\alpha=1}^{r}(\nabla_W\sigma_\alpha)^V-\sum_{\alpha=1}^{r}((\nabla_W\eta^\alpha)\sigma_\alpha)^V$$
$$+\sum_{\alpha=1}^{r}((\nabla_W\eta^\alpha)\sigma_\alpha)^C\sigma_\alpha^C.$$

2.2 Horizontal Lifts and Covarient Derivatives

From (2.1) and lifts of the paracomplex tensor fields, we obtain

$$(F^2)^H=\left(I-\sum_{\alpha=1}^{r}\sigma_\alpha\otimes\eta^\alpha\right)^H,$$

$$(F^2)^H = I - \sum_{\alpha=1}^{r} (\sigma_\alpha^V \otimes \eta^{\alpha H} + \sigma_\alpha^H \otimes \eta^{\alpha V}), \tag{2.13}$$

$$(F^2)^H W^H = W^H - \sum_{\alpha=1}^{r} (\eta^\alpha W)^V \sigma_\alpha^H \tag{2.14}$$

and

$$F^H(\sigma_\alpha^H) = 0, F^H(\sigma_\alpha^V) = 0, \tag{2.15}$$

$$\eta^{\alpha H} \circ F^H = 0, \eta^{\alpha V} \circ F^H = 0, \tag{2.16}$$

$$\eta^{\alpha H}(\sigma_\beta^H) = 0, \eta^{\alpha H}(\sigma_\beta^V) = -\delta_\beta^\alpha, \eta^{\alpha V}(\sigma_\beta^H) = -\delta_\beta^\alpha. \tag{2.17}$$

Theorem 2.3 Let $\bar{M}$ be differentiable manifold endowed with almost Lorentzian r-paracontact structure $(F, \sigma_\alpha, \eta^\alpha)$ for any $W \in \Im_0^1(\bar{M}), W^V, W^H \in \Im(T(\bar{M}))$, then a structure Ψ of $\Im_1^1(T(\bar{M}))$ defined by

$$\Psi = F^H - \sum_{\alpha=1}^{r} (\sigma_\alpha^V \otimes \eta^{\alpha V} - \sigma_\alpha^H \otimes \eta^{\alpha H}) \tag{2.18}$$

is an almost paracomplex structure in $T(\bar{M})$.

Proof. For $W \in \Im_0^1(\bar{M})$ and W^V, W^H are vertical and horizontal lifts of W, respectively, we have

$$\Psi^2(W^H) = \Psi(\Psi(W^H))$$

$$= \Psi((FW)^H - \sum_{\alpha=1}^{r} (\eta^\alpha(W))^V \sigma_\alpha^V)$$

$$= (F^H - \sum_{\alpha=1}^{r} (\sigma_\alpha^V \otimes \eta^{\alpha V} - \sigma_\alpha^H \otimes \eta^{\alpha H})((FW)^H - \sum_{\alpha=1}^{r} (\eta^\alpha(W))^V (\sigma_\alpha)^V)$$

$$= W^H - \sum_{\alpha=1}^{r} (\eta^\alpha(W))^V \sigma_\alpha^H + \sum_{\alpha=1}^{r} (-(\eta^\alpha(W))^V F^H \sigma_\alpha^V - (\eta^\alpha(FW))^V \sigma_\alpha^V$$

$$+(\eta^\alpha(W))^V (\eta^{\alpha V}(\sigma_\alpha^V))\sigma_\alpha^V + (\eta^{\alpha H}(FW)^H)\sigma_\alpha^H - (\eta^\alpha(W))^V (\eta^{\alpha H}(\sigma_\alpha^V)\sigma_\alpha^H$$

$$= W^H - \sum_{\alpha=1}^{r} ((\eta^\alpha(W))^V \sigma_\alpha^H + (\eta^\alpha(W))^V F^H \sigma_\alpha^V + (\eta^\alpha(FW))^V \sigma_\alpha^V$$

$$-\left(\eta^{\alpha}(W)\right)^{V}(\eta^{\alpha V}(\sigma_{\alpha}^{V}))\sigma_{\alpha}^{V}-(\eta^{\alpha H}(FW)^{H})\sigma_{\alpha}^{H}+\left(\eta^{\alpha}(W)\right)^{V}(\eta^{\alpha}(\sigma_{\alpha}))^{V}\sigma_{\alpha}^{H}$$

By means of (2.1),(2.14),(2.15),(2.16),(2.17) and (2.18), we have

$$\Psi^{2}(W^{H})=W^{H}$$

$$\Psi^{2}=I$$

So, Ψ is an almost paracomplex structure in $T(\bar{M})$, the proof is completed. Similarly $\Psi^{2}W^{V}=W^{V}$ is proved. Considering lift properties of tensor fields and the equation (2.18), we get

$$\Psi W^{V}=(FW)^{V}+\left(\eta^{\alpha}(W)\right)^{V}\sigma_{\alpha,}^{H} \tag{2.19}$$

$$\Psi W^{H}=(FW)^{H}-\left(\eta^{\alpha}(W)\right)^{V}\sigma_{\alpha}^{V}, \tag{2.20}$$

where $W\epsilon\Im_{0}^{1}(\bar{M}),W^{V},W^{H}\epsilon\Im(T(\bar{M}))$.

If $\eta^{\alpha}(W)=0$, we have

$$\Psi W^{V}=(FW)^{V},\Psi W^{H}=(FW)^{H}. \tag{2.21}$$

If we put $W=\sigma_{\alpha}$, i.e. $\eta^{\alpha}(\sigma_{\beta})=-\delta_{\beta}^{\alpha}$ and σ_{α} has the conditions of (2.1), then we have

$$\Psi\sigma_{\alpha}^{V}=-\delta_{\beta}^{\alpha}\sigma_{\alpha}^{H}=-\sigma_{\beta}^{H},\Psi\sigma_{\alpha}^{H}=\delta_{\beta}^{\alpha}\sigma_{\alpha}^{V}=\sigma_{\beta}^{V},\alpha,\beta=1,2,\dots,r. \tag{2.22}$$

Theorem 2.4 Let the tangent bundle $T(\bar{M})$ of the manifold $\bar{M}$ admits Ψ defined by (2.18). For any vector fields W,θ such that $\eta^{\alpha}(\theta)=0$, we have

$$i)(\nabla_{W^{H}}^{H}\Psi)\theta^{V}=((\nabla_{W}F)\theta)^{V}+\sum_{\alpha=1}^{r}((\nabla_{W}\eta^{\alpha})\theta)^{V}\sigma_{\alpha}^{H},$$

$$ii)(\nabla_{W^{H}}^{H}\Psi)\theta^{H}=((\nabla_{W}F)\theta)^{H}-\sum_{\alpha=1}^{r}\left((\nabla_{W}\eta^{\alpha})\theta\right)^{V}\sigma_{\alpha}^{V},$$

$$iii)(\nabla_{W^{V}}^{H}\Psi)\theta^{V}=0,$$

$$iv)(\nabla^H_{W^V}\Psi)\theta^H = 0,$$

where $W,\theta \in \Im^1_0(\bar{M})$, a tensor field $F \in \Im^1_1(\bar{M})$, a vector field σ_α, a $1-$form $\eta^\alpha \in \Im^0_1(\bar{M})$ and ∇^H is the horizontal lift of ∇ to $T(\bar{M})$.

Proof. For $\Psi \in \Im^1_1(T(\bar{M}))$ defined by (2.18) and $\eta^\alpha(\theta) = 0$, we get

$$i)(\nabla^H_{W^H}\Psi)\theta^V = \nabla^H_{W^H}\Psi\theta^V - \Psi\nabla^H_{W^H}\theta^V$$

$$= \nabla^H_{W^H}((F\theta)^V + \sum_{\alpha=1}^{r}\left(\eta^\alpha(\theta)\right)^V\sigma^H_\alpha)$$

$$-(F^H - \sum_{\alpha=1}^{r}(\sigma^V_\alpha \otimes \eta^{\alpha V} - \sigma^H_\alpha \otimes \eta^{\alpha H}))\nabla^H_{W^H}\theta^V$$

$$= \nabla^H_{W^H}(F\theta)^V + \sum_{\alpha=1}^{r}\nabla^H_{W^H}\left(\eta^\alpha(\theta)\right)^V\sigma^H_\alpha$$

$$-(F^H - \sum_{\alpha=1}^{r}\sigma^V_\alpha \otimes \eta^{\alpha V} - \sigma^H_\alpha \otimes \eta^{\alpha H}))\nabla^H_{W^H}\theta^V$$

$$= (\nabla_W(F\theta))^V + \sum_{\alpha=1}^{r}\nabla^H_{W^H}\left(\left(\eta^\alpha(\theta)\right)\sigma_\alpha\right)^H - F^H(\nabla_W\theta)^V$$

$$+\sum_{\alpha=1}^{r}(\eta^{\alpha V}(\nabla_W\theta)^V)\sigma^V_\alpha - \sum_{\alpha=1}^{r}(\eta^{\alpha H}(\nabla_W\theta)^V)\sigma^H_\alpha$$

$$= ((\nabla_W F)\theta)^V + \sum_{\alpha=1}^{r}((\nabla_W\eta^\alpha)\theta)^V\sigma^H_\alpha,$$

$$ii)(\nabla^H_{W^H}\Psi)\theta^H = \nabla^H_{W^H}\Psi\theta^H - \Psi\nabla^H_{W^H}\theta^H$$

$$= \nabla^H_{W^H}(F\theta)^H - \sum_{\alpha=1}^{r}\left(\eta^\alpha(\theta)\right)^V\sigma^V_\alpha$$

$$-(F^H - \sum_{\alpha=1}^{r}(\sigma^V_\alpha \otimes \eta^{\alpha V} - \sigma^H_\alpha \otimes \eta^{\alpha H}))\nabla^H_{W^H}\theta^H$$

$$= (\nabla_W F\theta)^H - \sum_{\alpha=1}^{r}\nabla^H_{W^H}((\eta^\alpha(\theta)\sigma_\alpha))^V$$

$$-(F^H - \sum_{\alpha=1}^{r} (\sigma_\alpha^V \otimes \eta^{\alpha V} - \sigma_\alpha^H \otimes \eta^{\alpha H}))\nabla_{W^H}^H \theta^H$$

$$= (\nabla_W F\theta)^H - \sum_{\alpha=1}^{r} \nabla_{W^H}^H ((\eta^\alpha(\theta))\sigma_\alpha)^V - (F\nabla_W \theta)^H$$

$$+ \sum_{\alpha=1}^{r} (\eta^{\alpha V}((\nabla_W \theta)^H))\sigma_\alpha^V - \sum_{\alpha=1}^{r} (\eta^{\alpha H}(\nabla_W \theta)^H)\sigma_\alpha^H$$

$$= ((\nabla_W F)\theta)^H + \big(F(\nabla_W \theta)\big)^H - \big(F(\nabla_W \theta)\big)^H$$

$$+ \sum_{\alpha=1}^{r} \big(\eta^\alpha(\nabla_W \theta)\big)^V \sigma_\alpha^V$$

$$= ((\nabla_W F)\theta)^H - \sum_{\alpha=1}^{r} \big((\nabla_W \eta^\alpha)\theta\big)^V \sigma_\alpha^V,$$

$$iii)(\nabla_{W^V}^H \Psi)\theta^V = \nabla_{W^V}^H \Psi\theta^V - \Psi\nabla_{W^V}^H \theta^V$$

$$= \nabla_{W^V}^H (F\theta)^V + \sum_{\alpha=1}^{r} \big(\eta^\alpha(\theta)\big)^V \sigma_\alpha^H$$

$$-(F^H - \sum_{\alpha=1}^{r} (\sigma_\alpha^V \otimes \eta^{\alpha V} - \sigma_\alpha^H \otimes \eta^{\alpha H}))\nabla_{W^V}^H \theta^V$$

$$= \nabla_{W^V}^H (F\theta)^V + \sum_{\alpha=1}^{r} \nabla_{W^V}^H \Big(\big(\eta^\alpha(\theta)\big)\sigma_\alpha\Big)^H$$

$$= \nabla_{W^V}^H (F\theta)^V$$

$$= 0,$$

$$iv)(\nabla_{W^V}^H \Psi)\theta^H = \nabla_{W^V}^H \Psi\theta^H - \Psi\nabla_{W^V}^H \theta^H$$

$$= \nabla_{W^V}^H (F\theta)^H - \sum_{\alpha=1}^{r} \big(\eta^\alpha(\theta)\big)^V \sigma_\alpha^V$$

$$-(F^H - \sum_{\alpha=1}^{r} (\sigma_\alpha^V \otimes \eta^{\alpha V} - \sigma_\alpha^H \otimes \eta^{\alpha H}))\nabla_{W^V}^H \theta^H$$

$$= \nabla^H_{W^V}(F\theta)^H - \sum_{\alpha=1}^{r} \nabla^H_{W^V}\left((\eta^\alpha(\theta))\sigma_\alpha\right)^V$$

$$= \nabla^H_{W^V}(F\theta)^H$$

$$= 0,$$

where $\eta^\alpha \nabla_W \theta = \nabla_W(\eta^\alpha \theta) - (\nabla_W \eta^\alpha)\theta$ and $F\theta \in \Im_0^1(\bar{M})$.

Corollary 2.2 If we put $\theta = \sigma_\alpha$, i.e. $\eta^\alpha(\sigma_\beta) = -\delta^\alpha_\beta$ and σ_α has the conditions of (2.1), we obtain

$$i)(\nabla^H_{W^H}\Psi)\sigma^V_\alpha = ((\nabla_W F)\sigma_\alpha)^V - \sum_{\alpha=1}^{r}(\nabla_W \sigma_\alpha)^H + \sum_{\alpha=1}^{r}((\nabla_W \eta^\alpha)\sigma_\alpha)^V \sigma^H_\alpha$$

$$ii)(\nabla^H_{W^H}\Psi)\sigma^H_\alpha = ((\nabla_W F)\sigma_\alpha)^H + \sum_{\alpha=1}^{r}(\nabla_W \sigma_\alpha)^V - \sum_{\alpha=1}^{r}\left((\nabla_W \eta^\alpha)\sigma_\alpha\right)^V \sigma^V_\alpha$$

$$iii)(\nabla^H_{W^V}\Psi)\sigma^V_\alpha = 0$$

$$iv)(\nabla^H_{W^V}\Psi)\sigma^H_\alpha = 0$$

References

[1] Blair D.E., Contact Manifolds in Riemannian Geometry. *Lecture Notes in Math, New York, Springer Verlag,* 509.1976.

[2] Das Lovejoy, S., Fiberings on almost r-contact manifolds. *Publicationes Mathematicae, Debrecen, Hungary*, 43(1993), 161-167.

[3] Oproiu, V., Some remarkable structures and connexions, defined on the tangent bundle. *Rendiconti di Matematica*, 3, 6 VI, 1973.

[4] Omran, T., Sharffuddin A., Husain, S.I., Lift of Structures on Manifolds. *Publications de 1'Instıtut Mathematıqe, Nouvelle serie*, 360(1984), no.50, 93 – 97.

[5] Salimov, A.A., Tensor Operators and Their applications. *Nova Science Publ, New York* .2013.

[6] Sasaki, S., On The Differantial Geometry of Tangent Boundles of Riemannian Manifolds. *Tohoku Math. J.* 10(1958), 338-358.

[7] Salimov, A.A., Çayır H., Some Notes On Almost Paracontact Structures, *Comptes Rendus de 1'Acedemie Bulgare Des Sciences*, 66(2013), no.3, 331-338.

[8] Tekkoyun, M., Lifts of Almost r-Contact and r-Paracontact Structures, arXiv:0902.4123v1 [math.DS] 24 Feb. 2009

[9] Yano, K., Ishihara, S., Tangent and Cotangent Bundles. *New York, Marcel Dekker Inc*. 1973.

Chapter 4

SUFFICIENT AND NECESSARY CONDITIONS TO ANALYSE THE STRUCTURE OF DELTA -SOFT SETS

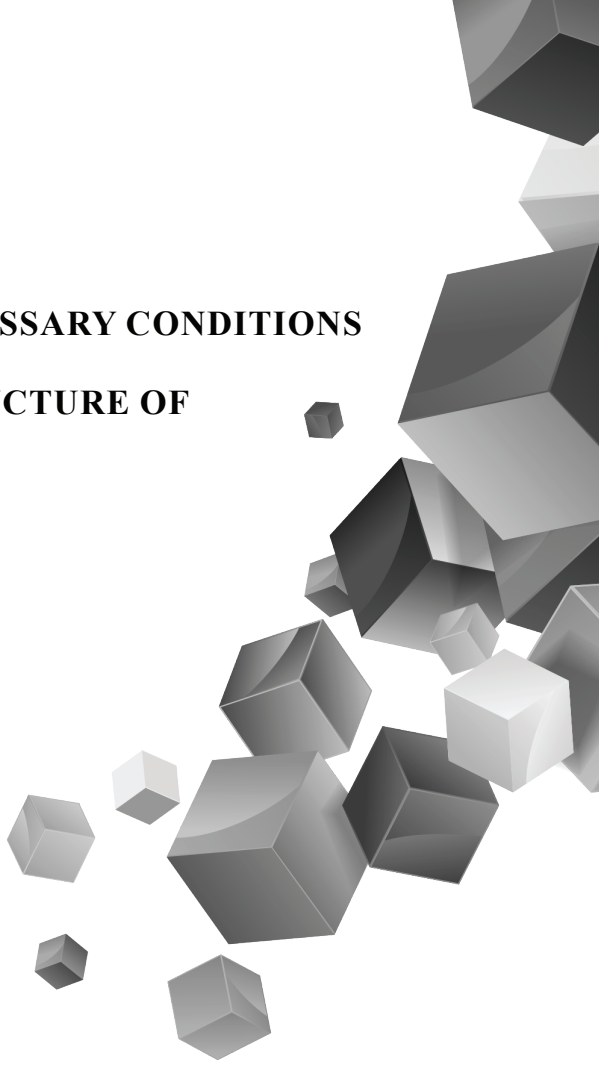

Güzide ŞENEL[1]

1 Faculty of Science, Department of Mathematics, Amasya University, Amasya, Turkey
Corresponding author, g.senel@amasya.edu.tr, Güzide Şenel ORCID: 0000-0003-4052-2631.

1. Introduction

Soft sets which are firstly defined by Molodtsov [1] are integral to solve the problems contain uncertainties that are not successfully modelled in classical mathematics. Hereupon, the properties and applications of soft sets have been studied increasingly ([2] - [11], [26] - [28]). The first interference to soft set operations was done by Maji et al. (2003) [12]. In the studies on [12], most of the attention was devoted to analysing the robustness of soft operations on various models whose parameters carry uncertainties induced by different sources. This development has shifted the perspective of soft sets to introduce the soft topological structure. The application of soft sets to topology is not a new endeavour; there is a long history of mathematical descriptions of valuable scientists. Successful applications include Shabir and Naz [13]'s description in which soft topological space over an initial universe with a fixed set of parameters is illustrated. The shift toward to this perspective was gradual; it passed a turning point at the first quarter of the 21st century when newly developed theories provided observations of applications of soft set in soft topological spaces in the works of ([14] - [19]). It is obvious that soft set theory is becoming an increasingly valuable tool for topology from the works on this section. Thanks to the improvement of the theory and the application of soft topology, the question of whether or not there is any additional topology on the soft set has occurred. As a result of which, soft bitopological and soft ditopological (SDT) space on a soft set were introduced in the works of ([20] - [21] - [22]). The concept of SDT - space on a soft set consists of with two structures on it - a soft topology and a soft subspace topology. The first one is used to describe soft openness properties of a soft topological space while the second one deals with its sub-soft openness properties. In the course of writing this paper, I learned that several authors in [23] and [24] has simultaneously obtained results on soft sets in soft bitopological spaces similar to soft set structures defined in SDT-space in certain respects. In consideration of the foregoing, $\tilde{\delta}$-soft sets in SDT- spaces proposed in [25]. This present study builds on previous analysis by defining their different characterizations and properties by theorems and examples. Also, the qualitative analysis of $\tilde{\delta}$-soft sets has been carried out; in particular, the structure of $\tilde{\delta}$-soft semi closure ($\tilde{\delta}$-sscl), $\tilde{\delta}$-soft semi interior ($\tilde{\delta}$-ssint), $\tilde{\delta}$-soft pre-closure ($\tilde{\delta}$-spcl) and $\tilde{\delta}$-ssoft pre-interior ($\tilde{\delta}$-sspint) has been

identified. The main threshold theorems which are sufficient and necessary to analyse the structure of all defined $\tilde{\delta}$-soft sets have been provided. Moreover, some additional remarks have been reported, regarding the role of characterization $\tilde{\delta}$-soft sets with respect to the threshold results.

This paper is organised as follows: The second section covers the basics of soft sets, soft topology and soft ditopology. These should be read sequentially. In Section 3, the key features of $\tilde{\delta}$-soft sets have been presented. In Section 4, theorems and examples which are sufficient and necessary to analyse the structure of all defined $\tilde{\delta}$-soft sets have been provided. Moreover, some additional remarks have been reported, regarding the role of characterization $\tilde{\delta}$-soft sets with respect to the threshold results. I hope that, after studying this article, the reader will be prepared to engage with published works of SDT-spaces. By 'engage', I mean not only to understand these $\tilde{\delta}$-soft sets but also to analyse them critically (both their construction and their interpretation). Readers should also be in a position to construct and analyse their own $\tilde{\delta}$-soft sets, given appropriate experimental data.

Definition 2.1. ([1]; [3]) A soft set f on the universe U is a set defined by $f_A: E \to \mathcal{P}(U)$ such that $f(e) = \emptyset$ if $e \in E \setminus A$.

Here f_A is also called an approximate function and if $A = E$, then we use f instead of f_E. A soft set over U can be represented by the set of ordered pairs $f = \{(e, f(e)): e \in E\}$. We will identify any soft set f with the function $f(e)$ and we shall use that concept as interchangeable. Soft sets are denoted by the letters $f, g, h, \ldots$ and the corresponding functions by $f(e), g(e), h(e), \ldots$

Throughout this paper, the set of all soft sets over U parameterized by E (briefly over U) will be denoted by $\mathbb{S}$.

Definition 2.2. ([3]) Let $f \in \mathbb{S}$. Then, if $f(e) = \emptyset$ for all $e \in E$, then f is called an empty set, denoted by Φ and if $f(e) = U$ for all $e \in E$, then f is called universal soft set, denoted by $\tilde{E}$.

Definition 2.3. ([3]) Let $f, g \in \mathbb{S}$. Then, f is a soft subset of g, denoted by $f \tilde{\subseteq} g$, if $f(e) \subseteq g(e)$ for all $e \in E$, and f and g are equal, denoted by $f = g$, if $f(e) = g(e)$ for all $e \in E$.

Definition 2.4. ([3]) Let $f, g \in \mathbb{S}$. Then, the intersection of f and g, denoted $f \tilde{\cap} g$, is defined by $(f \tilde{\cap} g)(e) = f(e) \cap g(e)$ for all $e \in E$, and the union of f and g, denoted $f \tilde{\cup} g$, is defined by $(f \tilde{\cup} g)(e) = f(e) \cup g(e)$ for all $e \in E$.

Definition 2.5. ([3]) Let $f \in \mathbb{S}$. Then, the soft complement of f, denoted $f^{\tilde{c}}$, is defined by $f^{\tilde{c}}(e) = U \setminus f(e)$ for all $e \in E$.

Definition 2.6. ([3]) Let$f \in \mathbb{S}$. The power soft set of f is defined by $\mathcal{P}(f) = \{f_i \tilde{\subseteq} f : i \in I\}$ and its cardinality is defined by $|\mathcal{P}(f)| = 2^{\sum_{e \in E} |f(e)|}$ where $|f(e)|$ is the cardinality of $f(e)$.

Example 2.7. ([3]) Let $U = \{u_1, u_2, u_3\}$, $E = \{e_1, e_2\}$, $f \in \mathbb{S}$, and $f = \{(e_1, \{u_1, u_2\}), (e_2, \{u_2, u_3\})\}$. Then,

$$
\begin{aligned}
f_1 &= \{(e_1, \{u_1\})\}, \\
f_2 &= \{(e_1, \{u_2\})\}, \\
f_3 &= \{(e_1, \{u_1, u_2\})\}, \\
f_4 &= \{(e_2, \{u_2\})\}, \\
f_5 &= \{(e_2, \{u_3\})\}, \\
f_6 &= \{(e_2, \{u_2, u_3\})\}, \\
f_7 &= \{(e_1, \{u_1\}), (e_2, \{u_2\})\}, \\
f_8 &= \{(e_1, \{u_1\}), (e_2, \{u_3\})\}, \\
f_9 &= \{(e_1, \{u_1\}), (e_2, \{u_2, u_3\})\}, \\
f_{10} &= \{(e_1, \{u_2\}), (e_2, \{u_2\})\}, \\
f_{11} &= \{(e_1, \{u_2\}), (e_2, \{u_3\})\}, \\
f_{12} &= \{(e_1, \{u_2\}), (e_2, \{u_2, u_3\})\}, \\
f_{13} &= \{(e_1, \{u_1, u_2\}), (e_2, \{u_2\})\}, \\
f_{14} &= \{(e_1, \{u_1, u_2\}), (e_2, \{u_3\})\}, \\
f_{15} &= f, \\
f_{16} &= \Phi
\end{aligned}
\tag{8}
$$

are all soft subsets of f. So, $|\tilde{P}(f)| = 2^4 = 16$.

Definition 2.8. ([13]) Let $f \in \mathbb{S}$. A soft topology on f, denoted by $\tilde{\tau}$, is a collection of soft subsets of f having following properties:

i. $f, \Phi \in \tilde{\tau}$,

ii. $\{g_i\}_{i \in I} \subseteq \tilde{\tau} \Rightarrow \tilde{\cup}_{i \in I} g_i \in \tilde{\tau}$,

iii. $\{g_i\}_{i=1}^{n} \subseteq \tilde{\tau} \Rightarrow \tilde{\cap}_{i=1}^{n} g_i \in \tilde{\tau}$.

The pair $(f, \tilde{\tau})$ is called a soft topological space.

Example 2.9. Refer example Example 2.7., $\tilde{\tau}^1 = \tilde{\mathcal{P}}(f)$, $\tilde{\tau}^0 = \{\Phi, f\}$ and $\tilde{\tau} = \{\Phi, f, f_2, f_{11}, f_{13}\}$ are soft topologies on f.

Definition 2.10. ([13]) Let $(f,\tilde{\tau})$ be a soft topological space. Then, every element of $\tilde{\tau}$ is called soft open set. Clearly, Φ and f are soft open sets.

Definition 2.11. (Şenel, 2016) Let f be a nonempty soft set over the universe U, $g \,\tilde{\subseteq}\, f$, $\tilde{\tau}$ be a soft topology on f and $\tilde{\tau}_g$ be a soft subspace topology on g. Then, $(f,\tilde{\tau},\tilde{\tau}_g)$ is called a soft ditopological space which is abbreviated as SDT-space.

A pair $\tilde{\delta} = (\tilde{\tau},\tilde{\tau}_g)$ is called a soft ditopology over f and the members of $\tilde{\delta}$ are said to be $\tilde{\delta}$-soft open in f. The complement of $\tilde{\delta}$-soft open set is called $\tilde{\delta}$-soft closed soft set.

Example 2.12. ([18]) Let us consider all soft subsets on f in the example Example 2.7. Let $\tilde{\tau} = \{\Phi, f, f_2, f_{11}, f_{13}\}$ be a soft topology on f. If $g = f_9$, then $\tilde{\tau}_g = \{\Phi, f_5, f_7, f_9\}$, and $(g,\tilde{\tau}_g)$ is a soft topological subspace of $(f,\tilde{\tau})$. Hence, we get soft ditopology over f as $\tilde{\delta} = \{\Phi, f, f_2, f_5, f_7, f_9, f_{11}, f_{13}\}$.

Definition 2.13. ([18]) Let $h \,\tilde{\subseteq}\, f$. Then, $\tilde{\delta}$- soft interior ($\tilde{\delta}$- int) of h, denoted by $(h)^{\circ}_{\tilde{\delta}}$, is defined by $(h)^{\circ}_{\tilde{\delta}} = \tilde{\cup}\{k : k \,\tilde{\subset}\, h, k \text{is} \tilde{\delta}\text{-soft open}\}$. The $\tilde{\delta}$-soft closure ($\tilde{\delta}$- cl) of h, denoted by $(\bar{h})_{\tilde{\delta}}$, is defined by $(\bar{h})_{\tilde{\delta}} = \tilde{\cap}\{k : h \,\tilde{\subset}\, k, k \text{is} \tilde{\delta} - \text{soft closed}\}$.

Note that $(h)^{\circ}_{\tilde{\delta}}$ is the biggest $\tilde{\delta}$-soft open set that contained in h and $(\bar{h})_{\tilde{\delta}}$ is the smallest $\tilde{\delta}$-soft closed set that containing h.

3. $\tilde{\delta}$- Soft Sets in SDT-Spaces

Soft set theory can be used for developing SDT-spaces by using $\tilde{\delta}$-b-open set, $\tilde{\delta}$-b-closed set, $\tilde{\delta}$-b-dense set, $\tilde{\delta}$-regular- open set, $\tilde{\delta}$-preopen set, $\tilde{\delta}$-semi open set, $\tilde{\delta}$ - α-open set and $\tilde{\delta}$-β- open set which are first mentioned in the work (Şenel, n.d.). In this section, properties of these $\tilde{\delta}$- soft sets and their relationship which are fundamental for research on soft ditopology are analysed.

Definition 3.1. ([25]) Let $(f,\tilde{\delta})$ be an SDT-space, $h \,\tilde{\subseteq}\, f$. Then h is called $\tilde{\delta}$-soft-b-open set (briefly $\tilde{\delta}$-sb-open) if $h \,\tilde{\subseteq}\, \tilde{\delta}\text{- int}\left(\tilde{\delta}\text{- cl}(h)\right) \tilde{\cup}\, \tilde{\delta}\text{- cl}\left(\tilde{\delta}\text{- int}(h)\right)$. The set of all $\tilde{\delta}$- soft b-open sets are denoted by $\tilde{\delta}$-SbO(f).

The complement of $\tilde{\delta}$- soft b-open set is called $\tilde{\delta}$- soft b-closed set.

Example 3.2. ([25]) Consider the SDT-space $(f, \tilde{\delta})$ and the Example 2.7, $g = f_9$, $\tilde{\tau} = \{f, \Phi, f_4, f_{10}\}$, $\tilde{\tau}_g = \{f, \Phi, f_1, f_7, f_{13}\}$. Then, we get soft ditopology over f as $\hat{\delta} = \{f, \Phi, f_1, f_4, f_7, f_{10}, f_{13}\}$ and $\hat{\delta}$-closed set are $\{f, \Phi, f_{12}, f_{14}, f_{11}, f_8, f_5\}$. $\hat{\delta}$-soft b-open sets are $\{f, \Phi, f_1, f_4, f_7, f_6, f_8, f_9, f_{12}, f_{10}, f_{13}\}$ and $\hat{\delta}$-soft b-closed sets are $\{f, \Phi, f_1, f_2, f_7, f_3, f_8, f_5, f_{10}\ f_{12}, f_{14}\}$.

Definition 3.3. ([25]) Let $(f, \tilde{\delta})$ be an SDT-space and$h \cong f$. Then,

i. h is $\hat{\delta}$-soft regular open ($\hat{\delta}$-sr-open) set if $h = \tilde{\delta}\text{-int}\left(\tilde{\delta}\text{-cl}(h)\right)$ and $\hat{\delta}$-soft regular closed $\hat{\delta}$-sr-closed) set if $h = \tilde{\delta}\text{-cl}\left(\tilde{\delta}\text{-int}(h)\right)$.

ii. h is $\hat{\delta}$-soft α-open ($\hat{\delta}$-sα-open) set if $h \cong \tilde{\delta}\text{-int}\left(\tilde{\delta}\text{-cl}\left(\tilde{\delta}\text{-int}(h)\right)\right)$ and h is $\hat{\delta}$-soft α-closed ($\hat{\delta}$-sα-closed) set if $h \cong \tilde{\delta}\text{-cl}\left(\tilde{\delta}\text{-int}\left(\tilde{\delta}\text{-cl}(h)\right)\right)$.

iii. h is $\hat{\delta}$-soft preopen ($\hat{\delta}$-sp-open) set if $h \cong \tilde{\delta}\text{-int}\left(\tilde{\delta}\text{-cl}(h)\right)$ and $h$is $\hat{\delta}$-soft preclosed ($\hat{\delta}$-sp-closed) set if $h \cong \tilde{\delta}\text{-cl}\left(\tilde{\delta}\text{-int}(h)\right)$.

iv. h is $\hat{\delta}$-soft semi open ($\hat{\delta}$-ss-open) set if $h \cong \tilde{\delta}\text{-cl}\left(\tilde{\delta}\text{-int}(h)\right)$ and $h$is $\hat{\delta}$-soft semi closed ($\hat{\delta}$-ss-closed) set if $h \cong \tilde{\delta}\text{-int}\left(\tilde{\delta}\text{-cl}(h)\right)$.

v. h is $\hat{\delta}$-soft β-open ($\hat{\delta}$-sβ-open) set if $h \cong \tilde{\delta}\text{-cl}\left(\tilde{\delta}\text{-int}\left(\tilde{\delta}\text{-cl}(h)\right)\right)$ and $h$is $\hat{\delta}$-soft β-closed ($\hat{\delta}$-sβ-closed) set if $h \cong \tilde{\delta}\text{-int}\left(\tilde{\delta}\text{-cl}\left(\tilde{\delta}\text{-int}(h)\right)\right)$.

Theorem 3.4. ([25]) Let $(f, \tilde{\delta})$ be an SDT-space. Then, the $\hat{\delta}$-soft sets have the following properties:

i. Every $\hat{\delta}$-soft preopen set is $\hat{\delta}$-soft β -open.

ii. Every $\hat{\delta}$-soft semi open set is $\hat{\delta}$-soft β -open.

iii. Every $\hat{\delta}$-soft α open set is $\hat{\delta}$-soft preopen.

PROOF. Let $(f, \tilde{\delta})$ be an SDT-space and$h \cong f$. Then,

i. Let h be a $\hat{\delta}$-soft preopen set. This implies,

$$h \cong \tilde{\delta}\text{-int}\left(\tilde{\delta}\text{-cl}(h)\right) \cong \tilde{\delta}\text{-cl}\left(\tilde{\delta}\text{-int}\left(\tilde{\delta}\text{-cl}(h)\right)\right)$$

Thus, h is $\hat{\delta}$-soft β -open set.

ii. Let h be a $\tilde{\delta}$-soft semi open set. This implies,

$$h \tilde{\subseteq} \tilde{\delta}\text{-cl}\left(\tilde{\delta}\text{-int}(h)\right) \tilde{\subseteq} \tilde{\delta}\text{-cl}\left(\tilde{\delta}\text{-int}\left(\tilde{\delta}\text{-cl}(h)\right)\right)$$

Thus, $h$is $\tilde{\delta}$-soft β -open set.

iii. Let h be a $\tilde{\delta}$-soft α-open set. This implies,

$$h \tilde{\subseteq} \tilde{\delta}\text{-int}\left(\tilde{\delta}\text{-cl}\left(\tilde{\delta}\text{-int}(h)\right)\right) \tilde{\subseteq} \tilde{\delta}\text{-int}\left(\tilde{\delta}\text{-cl}(h)\right)$$

Thus, h is $\tilde{\delta}$-soft preopen set.

Remark 3.5. ([25]) The converse of the above theorem is need not be true as seen in the following example:

Example 3.6. ([25]) Consider the SDT-space $(f, \tilde{\delta})$ and the Example 2.7, $g = f_9$, $\tilde{\tau} = \{f, \Phi, f_4, f_{10}\}$, $\tilde{\tau}_g = \{f, \Phi, f_1, f_7, f_{13}\}$. Then, we get soft ditopology over f as $\tilde{\delta} = \{f, \Phi, f_1, f_4, f_7, f_{10}, f_{13}\}$ and $\tilde{\delta}$-closed set are $\{f, \Phi, f_5, f_8, f_{11}, f_{12}, f_{14}\}$.

(i) f_6 is $\tilde{\delta}$-soft β open but not $\tilde{\delta}$-soft preopen.

For proving the converse of the (ii) and (iii), we need to generate new SDT-spaces:

Example 3.7. ([25]) Let us consider the soft subsets of f that are given in Example 2.7. $(f, \tilde{\delta})$ is an SDT-space, where $g = f_2$, $\tilde{\tau} = \{f, \Phi, f_1\}$ $\tilde{\tau}_g = \{f, \Phi, f_2\}$. Then, $\tilde{\delta}$- soft open sets are $\{f, \Phi, f_1, f_2, f_3\}$, $\tilde{\delta}$-soft closed set are $\{f, \Phi, f_6, f_9, f_{12}\}$.

ii. The soft subset f_4 is $\tilde{\delta}$-soft β-open set but not $\tilde{\delta}$-soft semi open.

Example.3.8.. ([25]) Let $U = \{u_1, u_2, u_3, u_4\}$, $E = \{e_1, e_2, e_3\}$, and $f = \{(e_1, \{u_1, u_2, u_3, u_4\})(e_2, \{u_1, u_2, u_3, u_4\}), (e_3, \{u_1, u_2, u_3, u_4\})\}$.

Then, $\tilde{\tau}_1 = \{f, \Phi, f_1, f_2, f_3, f_4, f_5, f_6, f_7, f_8, f_9, f_{10}, f_{11}, f_{12}, f_{13}, f_{14}, f_{15}\}$ and $\tilde{\tau}_2 = \{f, \Phi\}$. Where,

$f_1 = \{(e_1, \{u_1\}), (e_2, \{u_2, u_3\}), (e_3, \{u_1, u_4\})\}$

$f_2 = \{(e_1, \{u_2, u_4\}), (e_2, \{u_1, u_3, u_4\}), (e_3, \{u_1, u_2, u_4\})\}$

$f_3 = \{(e_2, \{u_3\}), (e_3, \{u_1\})\}$

$f_4 = \{(e_1, \{u_1, u_2, u_4\}), (e_2, U), (e_3, U)\}$

$f_5 = \{((e_1, \{u_1, u_3\})), (e_2, \{u_2, u_4\}), (e_3, U)\}$

$f_6 = \{((e_1, \{u_1\})), (e_2, \{u_2\})\}$

$f_7 = \{(e_1, \{u_1, u_3\}), (e_2, \{u_2, u_3, u_4\}), (e_3, \{u_1, u_2, u_4\})\}$

$f_8 = \{((e_2,\{u_4\})),(e_3,\{u_2\})\}$

$f_9 = \{(e_1,U),(e_2,U),(e_3,\{u_1,u_2,u_3\})\}$

$f_{10} = \{(e_1,\{u_1,u_3\}),(e_2,\{u_2,u_3,u_4\}),(e_3,\{u_1,u_2\})\}$

$f_{11} = \{(e_1,\{u_2,u_3,u_4\}),(e_2,U),(e_3,\{u_1,u_2,u_3\})\}$

$f_{12} = \{(e_1,\{u_1\}),(e_2,\{u_2,u_3,u_4\}),(e_3,\{u_1,u_2,u_4\})\}$

$f_{13} = \{(e_1,\{u_1\}),(e_2,\{u_2,u_4\}),(e_3,\{u_2\})\}$

$f_{14} = \{(e_1,\{u_3,u_4\}),(e_2,\{u_1,u_2\})\}$

$f_{15} = \{(e_1,\{u_1\}),(e_2,\{u_2,u_3\}),(e_3,\{u_1\})\}$

Then, the pair $\tilde{\delta} = (\tilde{\tau},\tilde{\tau}_g)$ is an SDT-space over f. Let $h \tilde{\subseteq} f$. Then,

$h = \{(e_1,\{u_4\}),(e_2,\{u_1,u_2,u_3\}),(e_3,\{u_2,u_4\})\}$,

$\tilde{\delta}\text{-int}\left(\tilde{\delta}\text{-cl}(h)\right) = f$,

and

$\tilde{\delta}\text{-int}\left(\tilde{\delta}\text{-cl}\left(\tilde{\delta}\text{-int}(h)\right)\right) = \Phi$

Hence h is $\tilde{\delta}$-soft preopen set but not $\tilde{\delta}$-soft α -open.

Theorem 3.9. ([25]) Let $(f,\tilde{\delta})$ be an SDT-space. Then,

i. Every $\tilde{\delta}$-soft preopen set is $\tilde{\delta}$-soft b-open set.

ii. Every $\tilde{\delta}$-soft b-open set is $\tilde{\delta}$-soft β -open set.

iii. Every $\tilde{\delta}$-soft semi open set is $\tilde{\delta}$-soft b-open set.

PROOF. Let $(f,\tilde{\delta})$ be an SDT-space and$h \tilde{\subseteq} f$ and h is a $\tilde{\delta}$-soft preopen set. Then,

$h \tilde{\subseteq} \tilde{\delta}\text{-int}\left(\tilde{\delta}\text{-cl}(h)\right) \tilde{\subseteq} \tilde{\delta}\text{-int}\left(\tilde{\delta}\text{-cl}(h)\right) \tilde{\cup} \tilde{\delta}\text{-int}(h) \tilde{\subseteq} \tilde{\delta}\text{-int}\left(\tilde{\delta}\text{-cl}(h)\right) \tilde{\cup} \tilde{\delta}\text{-cl}\left(\tilde{\delta}\text{-int}(h)\right)$

Thus (i) proved.

Let h be a $\tilde{\delta}$-soft b-open set. Then,

$h \tilde{\subseteq} \tilde{\delta}\text{-cl}\left(\tilde{\delta}\text{-int}(h)\right) \tilde{\cup} \tilde{\delta}\text{-int}\left(\tilde{\delta}\text{-cl}(h)\right) \tilde{\subseteq} \tilde{\delta}\text{-cl}\left(\tilde{\delta}\text{-int}\left(\tilde{\delta}\text{-cl}(h)\right)\right) \tilde{\cup} \tilde{\delta}\text{-int}\left(\tilde{\delta}\text{-cl}(h)\right) \tilde{\subseteq} \tilde{\delta}\text{-cl}\left(\tilde{\delta}\text{-int}\left(\tilde{\delta}\text{-cl}(h)\right)\right)$

Thus (ii) proved.

Let h be a $\tilde{\delta}$-soft semi open set. This implies

$h \tilde{\subseteq} \tilde{\delta}\text{-}cl\left(\tilde{\delta}\text{-}int(h)\right) \tilde{\subseteq} \tilde{\delta}\text{-cl}\left(\tilde{\delta}\text{-int}(h)\right) \tilde{\cup} \tilde{\delta}\text{-int}(h) \tilde{\subseteq} \tilde{\delta}\text{-cl}\left(\tilde{\delta}\text{-int}(h)\right) \tilde{\cup} \tilde{\delta}\text{-int}\left(\tilde{\delta}\text{-cl}(h)\right)$

Thus (iii) proved.

Remark 3.10. ([25]) The converse of the Theorem 3.9 is need not be true as seen in the following example:

Example 3.11. ([25]) us consider the soft subsets of f that are given in Example 2.7. $(f, \tilde{\delta})$ is an SDT-space, where $g = f_2$, $\tilde{\tau} = \{f, \Phi, f_1\}, \tilde{\tau}_g = \{f, \Phi, f_2\}$. Then, $\tilde{\delta}$- soft open sets are $\{f, \Phi, f_1, f_2, f_3\}$, $\tilde{\delta}$-soft closed set are $\{f, \Phi, f_6, f_9, f_{12}\}$.

(i) The soft set f_7 in f is $\tilde{\delta}$-soft b-open set but not $\tilde{\delta}$-soft preopen set.

(ii) The soft set f_5 in f is $\tilde{\delta}$-soft β -open set but not $\tilde{\delta}$-soft b-open set.

(iii) The soft set f_4 in f is $\tilde{\delta}$-soft b-open set but not $\tilde{\delta}$-soft semi open set.

The following remark gives the relationship between $\tilde{\delta}$-soft sets:

Remark 3.12. (Şenel, n.d.) The above discussions are summarized in the following diagrams:

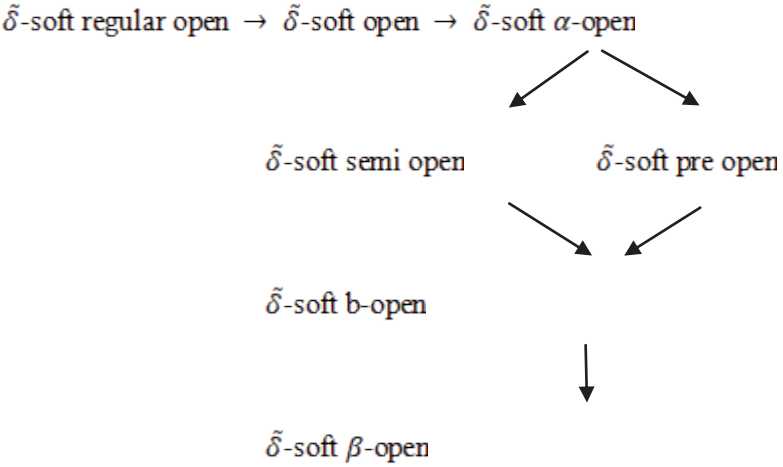

4. Sufficient and Necessary Conditions to Analyse the Structure of $\tilde{\delta}$-soft sets

In this section, the qualitative analysis of $\tilde{\delta}$-soft sets has been carried out; in particular the structure of $\tilde{\delta}$-soft semi closure ($\tilde{\delta}$-sscl), $\tilde{\delta}$-soft semi interior ($\tilde{\delta}$-ssint), $\tilde{\delta}$-soft pre-closure ($\tilde{\delta}$-spcl) and $\tilde{\delta}$-ssoft pre-interior ($\tilde{\delta}$-sspint) has been identified. The main threshold theorems which are sufficient and necessary to analyse the structure of all defined $\tilde{\delta}$-soft sets have been provided. Also, some additional remarks have been reported, regarding the role of characterization $\tilde{\delta}$-soft sets with respect to the threshold results.

Theorem 4.1. Let $(f, \tilde{\delta})$ be an SDT-space, $h \tilde{\subseteq} f$. Then, an arbitrary union of $\tilde{\delta}$-soft-b-open sets are $\tilde{\delta}$-soft-b-open set.

PROOF. Let $\{(h)_\alpha\}$ be a collection of $\tilde{\delta}$-soft-b-open sets. Then, for each α, $(h)_\alpha \tilde{\subseteq} \tilde{\delta}\text{-int}(\tilde{\delta}\text{-cl}(h)_\alpha) \tilde{\cup} \tilde{\delta}\text{-cl}(\tilde{\delta}\text{-int}(h)_\alpha)$.

$$\bigcup_\alpha((h)_\alpha) \tilde{\subseteq} \bigcup_\alpha\{\tilde{\delta}\text{- int}(\tilde{\delta}\text{- cl}(h)_\alpha) \tilde{\cup} \tilde{\delta}\text{- cl}(\tilde{\delta}\text{- int}(h)_\alpha)\}$$

$$\tilde{\subseteq} \bigcup_\alpha\{\tilde{\delta}\text{- int}(\tilde{\delta}\text{- cl}(h)_\alpha)\} \tilde{\cup} \bigcup_\alpha\{\tilde{\delta}\text{- cl}(\tilde{\delta}\text{- int}(h)_\alpha)\}$$

$$\tilde{\subseteq} \left[\tilde{\delta}\text{- int}\left\{\bigcup_\alpha(\tilde{\delta}\text{- cl}(h)_\alpha)\right\}\right] \tilde{\cup} \left[\tilde{\delta}\text{- cl}\left\{\bigcup_\alpha(\tilde{\delta}\text{- int}(h)_\alpha)\right\}\right]$$

$$\tilde{\subseteq} \left[\tilde{\delta}\text{- int}\left\{\tilde{\delta}\text{- cl}\left\{\bigcup_\alpha(h)_\alpha\right\}\right\}\right] \tilde{\cup} \left[\tilde{\delta}\text{- cl}\left\{\tilde{\delta}\text{- int}\left\{\bigcup_\alpha(h)_\alpha\right\}\right\}\right]$$

Remark 4.2. The intersection of two $\tilde{\delta}$-soft b-open sets need not be $\tilde{\delta}$-soft b-open set. In Example 3.2, $f_6 \tilde{\cap} f_8 = f_5$, which is not $\tilde{\delta}$-soft b-open set.

Theorem 4.3. Let $(f, \tilde{\delta})$ be an SDT-space. Then,

i. The intersection of $\tilde{\delta}$-soft open set and $\tilde{\delta}$-sb-open set is $\tilde{\delta}$-sb-open set.

ii. The intersection of $\tilde{\delta}$-sα -open set and $\tilde{\delta}$-sb-open set is $\tilde{\delta}$-sb-open set.

PROOF. Let $(f, \tilde{\delta})$ be an SDT-space and $h, k \widetilde{\subseteq} f$. h is a $\tilde{\delta}$-soft open set and k is a $\tilde{\delta}$-sb-open set. Then,

$$h \tilde{\cap} k \tilde{\subseteq} h \tilde{\cap} \left[\tilde{\delta}\text{-cl}\left(\tilde{\delta}\text{-int}(k)\right) \tilde{\cup} \tilde{\delta}\text{-int}\left(\tilde{\delta}\text{-cl}(k)\right)\right]$$

$$= \left[h \tilde{\cap} \tilde{\delta}\text{-cl}\left(\tilde{\delta}\text{-int}(k)\right)\right] \tilde{\cup} \left[h \tilde{\cap} \tilde{\delta}\text{-int}\left(\tilde{\delta}\text{-cl}(k)\right)\right]$$

$$\tilde{\subseteq} \left[\tilde{\delta}\text{-cl}\left(\tilde{\delta}\text{-int}(h) \tilde{\cap} \text{cl}\left(\tilde{\delta}\text{-int}(k)\right)\right)\right] \tilde{\cup} \left[\tilde{\delta}\text{-int}\left(\tilde{\delta}\text{-cl}(h)\right) \tilde{\cap} \tilde{\delta}\text{-int}\left(\tilde{\delta}\text{-cl}(k)\right)\right]$$

$$\tilde{\subseteq} \left[\tilde{\delta}\text{-cl}\left(\tilde{\delta}\text{-int}(h \tilde{\cap} k)\right)\right] \tilde{\cup} \left[\tilde{\delta}\text{-int}\left(\tilde{\delta}\text{-cl}(h \tilde{\cap} k)\right)\right]$$

Thus (i) proved.

Let $(f, \tilde{\delta})$ be an SDT-space and$h, k \widetilde{\subseteq} f$. h is a $\tilde{\delta}$-soft α -open set and $\tilde{\delta}$-sb-open set. Then,

$$h \tilde{\cap} k \tilde{\subseteq} \left[\tilde{\delta}\text{-int}\left(\tilde{\delta}\text{-cl}\left(\tilde{\delta}\text{-int}(h)\right)\right)\right] \tilde{\cap} \left[\tilde{\delta}\text{-cl}\left(\tilde{\delta}\text{-int}(k)\right) \tilde{\cup} \tilde{\delta}\text{-int}\left(\tilde{\delta}\text{-cl}(k)\right)\right]$$

$$= \left[\tilde{\delta}\text{-int}\left(\tilde{\delta}\text{-cl}\left(\tilde{\delta}\text{-int}(h) \tilde{\cap} \tilde{\delta}\text{-cl}\left(\tilde{\delta}\text{-int}(k)\right)\right)\right)\right] \tilde{\cup} \left[\tilde{\delta}\text{-int}\left(\tilde{\delta}\text{-cl}\left(\tilde{\delta}\text{-int}(h) \tilde{\cap} \tilde{\delta}\text{-int}\left(\tilde{\delta}\text{-cl}(k)\right)\right)\right)\right]$$

$$\tilde{\subseteq} \left[\left(\tilde{\delta}\text{-cl}\left(\tilde{\delta}\text{-int}(h)\right) \tilde{\cap} \left(\tilde{\delta}\text{-cl}\left(\tilde{\delta}\text{-int}(k)\right)\right)\right)\right] \tilde{\cup} \left[\left(\tilde{\delta}\text{-int}\left(\tilde{\delta}\text{-cl}(h)\right) \tilde{\cap} \left(\tilde{\delta}\text{-int}\left(\tilde{\delta}\text{-cl}(k)\right)\right)\right)\right]$$

$$\tilde{\subseteq}\left[\tilde{\delta}\text{-cl}\left(\tilde{\delta}\text{-int}(h\,\tilde{\cap}\,k)\right)\right]\tilde{\cup}\left[\tilde{\delta}\text{-int}\left(\tilde{\delta}\text{-cl}(h\,\tilde{\cap}\,k)\right)\right]$$

Thus (ii) proved.

Theorem 4.4. Any $\tilde{\delta}$-sb-open set h in an SDT-space, $\tilde{\delta}\text{-cl}(h)$ is a $\tilde{\delta}$-sr-closed set.

PROOF. Let h be a $\tilde{\delta}$-sb-open set. This implies,

$$h\,\tilde{\subseteq}\,\tilde{\delta}\text{-cl}\left(\tilde{\delta}\text{-int}(h)\right)\tilde{\cup}\,\tilde{\delta}\text{-int}\left(\tilde{\delta}\text{-cl}(h)\right)$$

Also,

$$\tilde{\delta}\text{-cl}(h)\,\tilde{\subseteq}\,\tilde{\delta}\text{-cl}\left(\tilde{\delta}\text{-cl}\left(\tilde{\delta}\text{-int}(h)\right)\right)\tilde{\cup}\,\tilde{\delta}\text{-cl}\left(\tilde{\delta}\text{-int}\left(\tilde{\delta}\text{-cl}(h)\right)\right)\tilde{\subseteq}\,\tilde{\delta}\text{-cl}\left(\tilde{\delta}\text{-int}\left(\tilde{\delta}\text{-cl}(h)\right)\right)$$

and

$$\tilde{\delta}\text{-cl}\left(\tilde{\delta}\text{-int}\left(\tilde{\delta}\text{-cl}(h)\right)\right)\tilde{\subseteq}\,\tilde{\delta}\text{-cl}(h)$$

Therefore, $\tilde{\delta}\text{-cl}(h)=\tilde{\delta}\text{-cl}\left(\tilde{\delta}\text{-int}\left(\tilde{\delta}\text{-cl}(h)\right)\right)$. So, $\tilde{\delta}\text{-cl}(h)$ is a $\tilde{\delta}$-sr-closed set.

Theorem 4.5. Let $(f,\tilde{\delta})$ be an SDT-space, $h\,\tilde{\subseteq}\,f$ and h is a $\tilde{\delta}$-sb-open set. Then,

i. If $\tilde{\delta}\text{-cl}(h)=\phi$ then h is a $\tilde{\delta}$-ss-open set.

ii. If $\tilde{\delta}\text{-int}(h)=\phi$ then h is a $\tilde{\delta}$-sp-open set.

PROOF. Let h be a $\tilde{\delta}$-sb-open set. This implies,

$$h\,\tilde{\subseteq}\,\tilde{\delta}\text{-cl}\left(\tilde{\delta}\text{-int}(h)\right)\tilde{\cup}\,\tilde{\delta}\text{-int}\left(\tilde{\delta}\text{-cl}(h)\right)$$

Since $\tilde{\delta}\text{-cl}(h)=\phi$, $h\,\tilde{\subseteq}\,\tilde{\delta}\text{-cl}\left(\tilde{\delta}\text{-int}(h)\right)$. Thus (i) proved. Since $\tilde{\delta}\text{-int}(h)=\phi$, $h\,\tilde{\subseteq}\,\tilde{\delta}\text{-int}\left(\tilde{\delta}\text{-cl}(h)\right)$. Thus (ii) proved.

Theorem 4.6. Let $(f,\tilde{\delta})$ be an SDT-space, $h\,\tilde{\subseteq}\,f$ and h is a $\tilde{\delta}$-sb-open set. Then,

(i) If h is a $\tilde{\delta}$-sr-closed set, then h is a $\tilde{\delta}$-sp-open set.

(ii) If h is a $\tilde{\delta}$-sp-open set, then h is a $\tilde{\delta}$-ss-open set.

PROOF. Since h is a $\tilde{\delta}$-sb-open set. Then, $h\,\tilde{\subseteq}\,\tilde{\delta}\text{-cl}\left(\tilde{\delta}\text{-int}(h)\right)\tilde{\cup}\,\tilde{\delta}\text{-int}\left(\tilde{\delta}\text{-cl}(h)\right)$. Let h be a $\tilde{\delta}$-sr-closed set, $h=\tilde{\delta}\text{-cl}\left(\tilde{\delta}\text{-int}(h)\right)$. Then, $h\,\tilde{\subseteq}\,h\,\tilde{\cup}\,\tilde{\delta}\text{-int}\left(\tilde{\delta}\text{-cl}(h)\right)$, which implies, $h\,\tilde{\subseteq}\,\tilde{\delta}\text{-int}\left(\tilde{\delta}\text{-cl}(h)\right)$. Thus (i) proved. Let h be a $\tilde{\delta}$-sp-open set,

$h = \tilde{\delta}\text{-int}\left(\tilde{\delta}\text{-cl}(h)\right)$. $h \tilde{\subseteq} h \tilde{\cup} \tilde{\delta}\text{-cl}\left(\tilde{\delta}\text{-int}(h)\right)$, which implies, $h \tilde{\subseteq} \tilde{\delta}\text{-cl}\left(\tilde{\delta}\text{-int}(h)\right)$. Thus (ii) proved.

Theorem 4.7. Let $(f, \tilde{\delta})$ be an SDT-space, $h \tilde{\subseteq} f$ and h is a $\tilde{\delta}$-sb-closed set. Then,$\tilde{\delta}\text{-int}(h)$ is a $\tilde{\delta}$-sr-open set.

PROOF. Let h is a $\tilde{\delta}$-sb-closed set. This implies,

$$\tilde{\delta}\text{-cl}\left(\tilde{\delta}\text{-int}(h)\right) \tilde{\cap} \tilde{\delta}\text{-int}\left(\tilde{\delta}\text{-cl}(h)\right) \tilde{\subseteq} h$$

Moreover,

$$\tilde{\delta}\text{-int}(h) \tilde{\subseteq} \tilde{\delta}\text{-int}\left(\tilde{\delta}\text{-cl}\left(\tilde{\delta}\text{-int}(h)\right)\right) \tilde{\cap} \tilde{\delta}\text{-int}\left(\tilde{\delta}\text{-int}\left(\tilde{\delta}\text{-cl}(h)\right)\right) \tilde{\subseteq} \tilde{\delta}\text{-int}(h)$$

Thus,

$$\tilde{\delta}\text{-int}\left(\tilde{\delta}\text{-cl}\left(\tilde{\delta}\text{-int}(h)\right)\right) \tilde{\subseteq} \tilde{\delta}\text{-int}(h)$$

Furthermore,

$$\tilde{\delta}\text{-int}(h) \tilde{\subseteq} \tilde{\delta}\text{-int}\left(\tilde{\delta}\text{-cl}\left(\tilde{\delta}\text{-int}(h)\right)\right)$$

Therefore, $\tilde{\delta}\text{-int}(h) = \tilde{\delta}\text{-int}\left(\tilde{\delta}\text{-cl}\left(\tilde{\delta}\text{-int}(h)\right)\right)$. So, $\tilde{\delta}\text{-int}(h)$ is a $\tilde{\delta}$-sr-open set.

The following lemma is used in the sequel.

Lemma 4.8. Let $(f, \tilde{\delta})$ be an SDT-space, $h \tilde{\subseteq} f$. Then,

i. $\tilde{\delta}\text{-sscl}(h) = h \tilde{\cup} \tilde{\delta}\text{-int}\left(\tilde{\delta}\text{-cl}(h)\right)$

ii. $\tilde{\delta}\text{-ssint}(h) = h \tilde{\cap} \tilde{\delta}\text{-cl}\left(\tilde{\delta}\text{-int}(h)\right)$

iii. $\tilde{\delta}\text{-spcl}(h) = h \tilde{\cup} \tilde{\delta}\text{-cl}\left(\tilde{\delta}\text{-int}(h)\right)$

iv. $\tilde{\delta}\text{-spint}(h) = h \tilde{\cap} \tilde{\delta}\text{-int}\left(\tilde{\delta}\text{-cl}(h)\right)$.

Theorem 4.9. Let $(f, \tilde{\delta})$ be an SDT-space, $h \tilde{\subseteq} f$. Then,

i. $\tilde{\delta}\text{-sbcl}(h) = h \tilde{\cup} \left[\tilde{\delta}\text{-int}\left(\tilde{\delta}\text{-cl}(h)\right) \tilde{\cap} \tilde{\delta}\text{-cl}\left(\tilde{\delta}\text{-int}(h)\right)\right]$.

ii. $\tilde{\delta}\text{-sbint}(h) = h \tilde{\cap} \left[\tilde{\delta}\text{-int}\left(\tilde{\delta}\text{-cl}(h)\right) \tilde{\cup} \tilde{\delta}\text{-cl}\left(\tilde{\delta}\text{-int}(h)\right)\right]$.

PROOF. Proof is obvious.

Theorem 4.10. Let $(f, \tilde{\delta})$ be an SDT-space, $h, k \tilde{\subseteq} f$. Then,

i. $\tilde{\delta}\text{-sbcl}(h \tilde{\cup} k) \tilde{\supseteq} \tilde{\delta}\text{-sbcl}(h) \tilde{\cup} \tilde{\delta}\text{-sbcl}(k)$.

ii. $\tilde{\delta}\text{-sbcl}(h \tilde{\cap} k) \tilde{\supseteq} \tilde{\delta}\text{-sbcl}(h) \tilde{\cap} \tilde{\delta}\text{-sbcl}(k)$.

iii. $\tilde{\delta}\text{-sbint}(h \tilde{\cup} k) \tilde{\supseteq} \tilde{\delta}\text{-sbint}(h) \tilde{\cup} \tilde{\delta}\text{-sbint}(k)$.

iv. $\tilde{\delta}\text{-sbint}(h \tilde{\cap} k) \tilde{\supseteq} \tilde{\delta}\text{-sbint}(h) \tilde{\cap} \tilde{\delta}\text{-sbint}(k)$.

PROOF. Since $h \tilde{\subseteq} h \tilde{\cup} k$ or $k \tilde{\subseteq} h \tilde{\cup} k$. This implies $\tilde{\delta}\text{-sbcl}(h) \tilde{\subseteq} \tilde{\delta}\text{-sbcl}(h \tilde{\cup} k)$ or $\tilde{\delta}\text{-sbcl}(k) \tilde{\subseteq} \tilde{\delta}\text{-sbcl}(h \tilde{\cup} k)$.

Thus, $\tilde{\delta}\text{-sbcl}(h \tilde{\cup} k) \tilde{\supseteq} \tilde{\delta}\text{-sbcl}(h) \tilde{\cup} \tilde{\delta}\text{-sbcl}(k)$.

(ii) Similar to that of (i).

Since $h \tilde{\subseteq} h \tilde{\cup} k$ or $k \tilde{\subseteq} h \tilde{\cup} k$. This implies $\tilde{\delta}\text{-sbint}(h) \tilde{\subseteq} \tilde{\delta}\text{-sbint}(h \tilde{\cup} k)$ or $\tilde{\delta}\text{-sbint}(k) \tilde{\subseteq} \tilde{\delta}\text{-sbint}(h \tilde{\cup} k)$.

Thus, $\tilde{\delta}\text{-sbint}(h \tilde{\cup} k) \tilde{\supseteq} \tilde{\delta}\text{-sbint}(h) \tilde{\cup} \tilde{\delta}\text{-sbint}(k)$.

(iv) Similar to that of (iii).

Theorem 4.11. Let $(f, \tilde{\delta})$ be an SDT-space, $h \tilde{\subseteq} f$. Then,

i. $\tilde{\delta}\text{-sbcl}(h) \tilde{\subseteq} \tilde{\delta}\text{-sscl}(h) \tilde{\cap} \tilde{\delta}\text{-spcl}(h)$

ii. $\tilde{\delta}\text{-sbint}(h) \tilde{\supseteq} \tilde{\delta}\text{-ssint}(h) \tilde{\cup} \tilde{\delta}\text{-spint}(h)$

PROOF.

(i) $\tilde{\delta}\text{-ssd}(h) \tilde{\cap} \tilde{\delta}\text{-spd}(h) \tilde{\supseteq} \left[h \tilde{\cup} \tilde{\delta}\text{-int}\left(\tilde{\delta}\text{-cl}(h)\right) \tilde{\cap} h \tilde{\cup} \tilde{\delta}\text{-cl}\left(\tilde{\delta}\text{-int}(h)\right)\right]$

$= h \tilde{\cup} \left[\tilde{\delta}\text{-int}\left(\tilde{\delta}\text{-cl}(h)\right) \tilde{\cap} \tilde{\delta}\text{-cl}\left(\tilde{\delta}\text{-int}(h)\right)\right]$

$= \tilde{\delta}\text{-sbd}(h)$

(ii) $\tilde{\delta}\text{-ssint}(h) \tilde{\cup} \tilde{\delta}\text{-spint}(h) \tilde{\subseteq} \left[h \tilde{\cap} \tilde{\delta}\text{-int}\left(\tilde{\delta}\text{-cl}(h)\right) \tilde{\cap} h \tilde{\cap} \tilde{\delta}\text{-cl}\left(\tilde{\delta}\text{-int}(h)\right)\right]$

$= h \tilde{\cap} \left[\tilde{\delta}\text{-int}\left(\tilde{\delta}\text{-cl}(h)\right) \tilde{\cup} \tilde{\delta}\text{-cl}\left(\tilde{\delta}\text{-int}(h)\right)\right]$

$= \tilde{\delta}\text{-sbint}(h)$

4. Conclusion

This study addresses the properties and characterizations of $\tilde{\delta}$-soft sets by defining sufficient and necessary theorems and examples. The mathematical prerequisite for this text is a working knowledge of soft set and soft topology. In addition to this knowledge a brief review of some fundamental soft ditopological notions is included in Section 2. Properties of $\tilde{\delta}$- soft sets and their relationship which are fundamental for research on soft ditopology are analysed in Section 3. The qualitative analysis of $\tilde{\delta}$-soft sets has been carried out; in particular the structure of $\tilde{\delta}$ -soft semi closure ($\tilde{\delta}$-sscl), $\tilde{\delta}$-soft semi interior ($\tilde{\delta}$-ssint), $\tilde{\delta}$-soft pre-closure ($\tilde{\delta}$-spcl) and $\tilde{\delta}$-ssoft pre-interior ($\tilde{\delta}$-sspint) has been defined in

Section 4. To encourage interaction with the $\tilde{\delta}$-soft sets, exercises are included throughout the manuscript. I hope that interested researchers at all levels will find this manuscript useful for self-study and a deeper understanding of these residues will help establish new results about the distribution of soft set theory.

Funding: This work is supported by the author.

Conflict of interest: The author declares that there is no conflict of interest.

Ethical standard: This article does not contain any studies with human participants or animals performed by the author.

References

[1] Molodtsov, D. .Soft Set Theory-First Results. *Computers and Mathematics with Applications* 37(4-5) (1999) 19-31.

[2] Ali, M. I., Feng, F., Liu, X., Min, W. K.. Shabir, M., On Some New Operations in Soft Set Theory, *Computers and Mathematics with Applications* 57(9) (2009) 1547-1553.

[3] Çağman, N., Enginoğlu, S.. Soft Set Theory and Uni-Int Decision Making. *European Journal of Operational Research* 207(2) (2010) 848-855.

[4] Çağman, N., Enginoğlu, S.. Soft Matrix Theory and Its Decision Making. *Computer and Mathematics with Applications* 59(10) (2010) 3308-3314.

[5] Jiang, Y., Tang, Y., Chen, Q., Wang, J., Tang, S.. Extending Soft Sets with Description Logics, *Computers and Mathematics with Applications* 59(6) (2010) 2087-2096.

[6] Majumdar, P., Samanta, S. K., Similarity measure of soft sets, *New Mathematics and Natural Computation* 4(1) (2008) 1-12.

[7] Xiao, Z., Gong, K., Xia, S., Zou, Y.. Exclusive Disjunctive Soft Sets, *Computers and Mathematics with Applications* 59(6) (2010) 2128-2137.

[8] Zou, Y., Xiao, Z.. Data Analysis Approaches of Soft Sets Under Incomplete Information. *Knowledge-Based Systems* 21(8) (2008) 941-945.

[9] Enginoğlu, S., Soft matrices. PhD Dissertation, Tokat Gaziosmanpaşa University, *Graduate School of Natural and Applied Sciences* Tokat, Turkey (In Turkish). (2012) 1-89.

[10] Enginoğlu, S., Çağman, N. (n.d.) Fuzzy Parameterized Fuzzy Soft Matrices and Their Application in Decision-Making. *TWMS Journal of Applied and Engineering Mathematics*, In Press.

[11] Enginoğlu, S., Memiş, S.. A Configuration of Some Soft Decision-Making Algorithms via *fpfs*-matrices. *Cumhuriyet Science Journal* 39(4) (2018) 871-881.

[12] Maji, P.K., Biswas, R., Roy, A.R.. Soft Set Theory. *Computer and Mathematics with Applications* 45(4-5) (2003) 555-562.

[13] Shabir, M., Naz, M.. On soft topological spaces, *Computers and Mathematics with Applications*, 61(7) (2011) 1786-1799.

[14] Aygünoglu, A. Aygun, H..Some Notes on Soft Topological Spaces, *Neural Computation and Application,* 21(Supplement 1) (2012) 113-119.

[15] Çağman, N., Karataş, S., Enginoğlu, S.. Soft Topology, *Computers and Mathematics with Applications* 62(1), (2011), 351-358.

[16] Hussain, S., Ahmad, B.. Some Properties of Soft Topological Spaces, *Computers and Mathematics with Applications* 62(11) (2011) 4058-4067.

[17] Min, W., K.. A Note on Soft Topological Spaces, *Computers and Mathematics with Applications* 62(9) (2011) 3524-3528.

[18] Şenel, G.. A New Approach to Hausdorff Space Theory via the Soft Sets. *Mathematical Problems in Engineering.* Article ID 2196743, (2016) 1-6.

[19] Zorlutuna, I., Akdağ, M., Min, W. K., Atmaca, S.. Remarks on Soft Topological Spaces, *Annals of Fuzzy Mathematics and Informatics* 3(2) (2012) 171-185.
[20] Basavaraj M. Ittanagi. Soft Bitopological Spaces, *International Journal of Computer Applications* 107(7) (2014) 1-4.
[21] Dizman, T. S., Šostak, A., Yuksel, Ş.. Soft Ditopological Spaces, *Filomat* 30(1) (2016) 209-222.
[22] Şenel, G., The Theory of Soft Ditopological Spaces, *International Journal of Computer Applications*, 150(4) (2016) 1-6.
[23] Revathi, N., Bageerathi, K.. Extremally Disconnected Space in Soft Bitopological Spaces, *International Journal of Advanced Scientific Research and Management* 4(4) (2019) 51-56.
[24] Revathi N., Bageerathi K.. On Soft B-Open Sets in Soft Bitopological Space, *International Journal of Applied Research* 1(11) (2015) 615-623.
[25] Şenel, G., An Approach to Generate New Soft Sets and Spaces in Soft Ditopological Spaces, *Journal of Mathematical Extension(JME),* in press.
[26] T. M. Al-shami, Compactness on Soft Topological Ordered Spaces and Its Application on the Information System, Journal of Mathematics, Volume 2021(2) (2021).
[27] T. M. Al-shami, Ljubisa D.R. Kocinac, The equivalence between the enriched and extended soft topologies, Applied and Computational Mathematics 18(2):149-162 (2019).
[28] O. Göçür, Amply soft set and its topologies: AS and PAS topologies, AIMS Mathematics 6(4):3121-3141 (2021).

Chapter 5

CHEMICAL AND BIOLOGICAL PROPERTIES OF FUROSEMIDE AND COMPLEX FORMATION

Berat İLHAN CEYLAN [1]

1 Istanbul University-Cerrahpaşa, Faculty of Engineering, Department of Chemistry, Inorganic Chemistry Division, 34320 Avcilar, Istanbul, Turkey. ORCID: 0000-0003-2893-3788. beril@istanbul.edu.tr.

Drugs having an effect of the changing volume and position of bodily fluids and which are used in hypertension, acute and chronic heart failure, acute and chronic renal failure, nephrotic syndrome, and cirrhosis, have great importance in medicine and pharmacology. Furosemide is one of these drugs and one of the most used drug molecules in hypertension treatment (Figure 1).

Despite its importance in medicine and pharmacology, furosemide's molecular structure, and experimental and theoretical methods to investigate the vibrational spectrum and molecular structure, are rare (Lamotte et al., 1978; Latosińska et al., 2006).

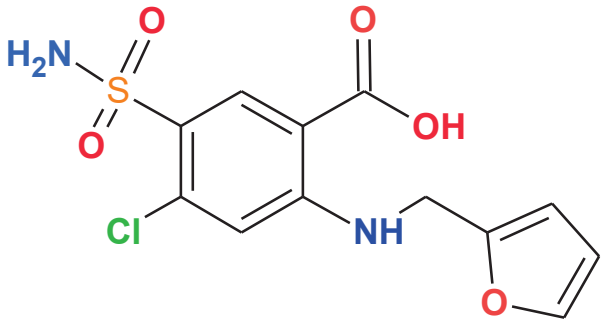

Figure 1. Molecular structure of furosemide.

In basic media, furosemide loses the carboxylic acid proton and forms an anion, thereby its solubility is greatly enhanced (Scheme 1). In a study about the furosemide-silver complex (Ag-FSE), the complex formation was reported, and biological properties were examined *in vitro*. The molecular formula of $AgC_{12}H_{10}ClN_2O_5S$ and 1:1 metal/ligand composition were proposed after elemental analysis, thermal studies, and mass spectrometry (Figure 2).

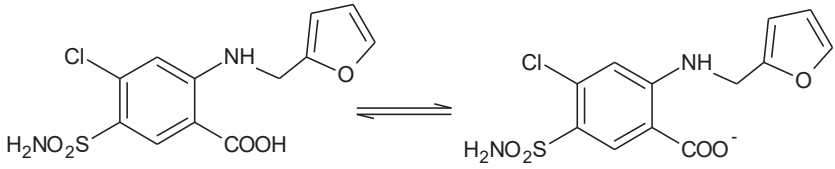

Scheme 1. Proton dissociation of free ligand Furosemide.

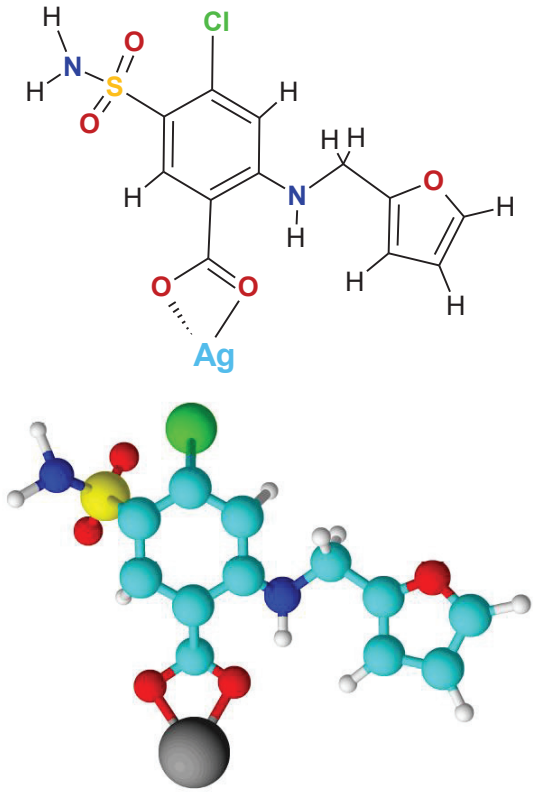

Figure 2. Molecular depiction and ball-and-stick model of Ag-furosemide complex (Ag-FSE).

Infrared spectroscopy and nuclear magnetic resonance studies showed that the carboxylate moiety coordinated to the silver ion. Density functional theory (DFT) included the Ag-FSE complex structure in a detailed manner. The antibacterial activity of the complex was assessed by antibiogram analyses by using minimum inhibitory concentration (MIC) and disc diffusion method. The Ag-FSE complex was found to be significantly effective against Gram-positive bacteria *Staphylococcus aureus*, Gram-negative bacteria *Escherichia coli, Pseudomonas aeruginosa,* and the yeast *Candida albicans*. In Ames experiment, the observation that Ag-FSE did not have a mutagenic activity against *Salmonella typhimurium* bacterial strain is a very important finding of the molecule for projections of a drug in the medical sector (Lustri et al., 2017).

Furosemide as an endogenous candidate molecule was tested within silico docking simulations and anti-pro-inflammatory activity. Furosemide has

a suppressing effect on M1 polarization. Furosemide also promoted the production of anti-inflammatory cytokine products and causing the polarization of M2. The authors have concluded that furosemide is a safe, inexpensive, and well-studied agent. Against COVID-19, furosemide should be considered as a repurposed inhaled therapy with the help of preclinical data (Wang et al., 2020).

Spectral studies

In a study by Bölükbaşı and Yılmaz, furosemide's FT-IR (between 4000 and 650 cm^{-1}), FAR-IR (700 and 150 cm^{-1}), and FT-Raman (between 4000 and 150 cm^{-1}) spectra were recorded. The single crystal X-ray structure of this molecule was also determined. The X-ray analysis revealed E and Z forms constituting a dimeric structure through OH·····O hydrogen bonds. Theoretical analysis of furosemide's probable stable conformers was performed by the DFT method with the 6-31G(d,p) basis set. DFT/B3LYP method was run with 6-31G(d,p), 6-31G(d), and Sadlej PVTZ as the worked basis sets for quantum chemical calculations of the geometric structure and wavenumbers of vibration. What is more, the same theory with 6-31G(d,p) as the basis set was employed for the calculation of the anharmonic wavenumbers. Total energy distribution (TED) was used to provide a detailed interpretation of the infrared and Raman spectra of furosemide. NBO analysis was performed to examine the probable donor–acceptor interactions of E and Z forms. X-ray crystallography provided E- and Z-furosemide by experimental means. Gas-phase theoretical calculations helped obtain the stable E- and Z-furosemides in the solid phase. Different conformers and energy barriers linking them were examined by the authors. The stability of the dimeric structure is supplied by the intermolecular hydrogen bonding effects. The theoretical and experimental results were in remarkable harmony (Bolukbasi & Yilmaz, 2012).

Complex formation

Raymoni et al. have studied zinc complexes of furosemide in which there were two furosemide molecules in the complex, along with some auxiliary ligands like 2-aminopyridine, 2-aminomethylpyridine, 2,2'-bipyridine, 4,4'-bipyridine, 1,10-phenanthroline, and quinoline. A standard set of characterization techniques was applied to shed light on the structure. Single-crystal X-ray diffraction and antibacterial activity were also reported (Raymoni & Abu Ali, 2019).

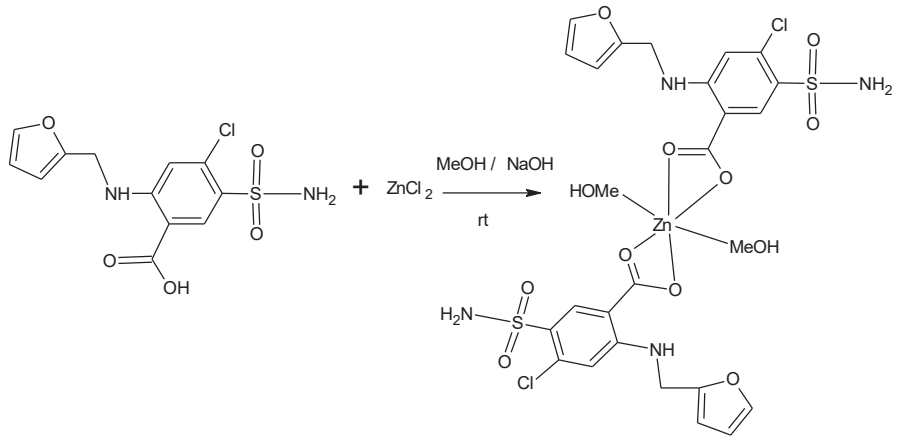

Figure 3. Proposed synthesis of $[Zn(fur)_2(MeOH)_2]$.

Li and co-workers have prepared the 1:1 Pd:furosemide anionic chelate complex in pH 4.5 to 7.0 Britton-Robinson buffers. Basic triphenylmethane dyes like ethyl violet and such were reacted with this chelate for 1:1 ion-association complexes. The absorption spectra had a drastic change, but Rayleigh scattering, second-order scattering, and frequency doubling scattering also changed. According to the concentration of furosemide, the RRS, SOS, and FDS intensities were detected directly proportional to it. These methods could be used for detecting trace amounts of furosemide.
The research allows for determining furosemide in tablets, injection forms, human serums, and urine samples (Li et al., 2010).

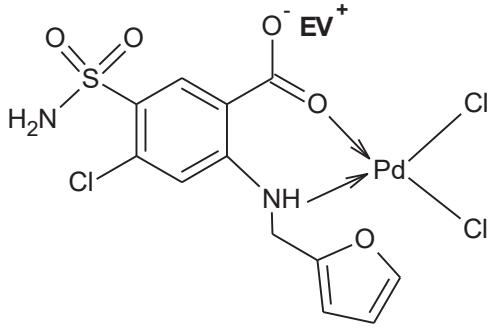

Figure 4. The structure of an ion-association complex of $[Fur \cdot PdCl_2] \cdot EV$.

Hondrellis and co-workers have prepared a series of furosemide complexes with Co, Ni, Cd, Mn, Hg, Pd, and Rh. The furosemide anion

binds to the metals in a chelated bidentate fashion through carboxylato and imino groups.

$$M(fur)_2.3H_2O \rightarrow M(fur)_2.2H_2O + H_2O\uparrow$$
$$Pd(fur)Cl.H_2O \rightarrow Pd(fur)Cl + H_2O\uparrow$$

Scheme 2. Furosemide hydrate complexes lose a molecule of water; M: Co, Ni, Cd

The bis(furosemide) trihydrate complex loses one molecule of water to become the corresponding dihydrate for M = Co, Ni, and Cd. The furosemide monohydrate complex loses a molecule of water to be converted into the anhydrous complex for M = Pd.

The closed formulas for complexes obtained were as follows:

$Mn(fur)_2.2H_2O$, $Co(fur)_2.3H_2O$, $Ni(fur)_2.3H_2O$, $Cu(fur)_2.2H_2O$, $Zn(fur)_2.2H_2O$, $Cd(fur)_2.3H_2O$
$Hg_2(fur)_3Cl.2H_2O$, $Pd(fur)Cl.H_2O$, $Rh(fur)_3.3H_2O$ (Hondrellis et al., 1988)

Analytical procedures
A potentiometric study between furosemide and amino acids as secondary ligands in the mixed ligand complexes in 80% (v/v) ethanol-water medium was reported (Khade et al., 2011).

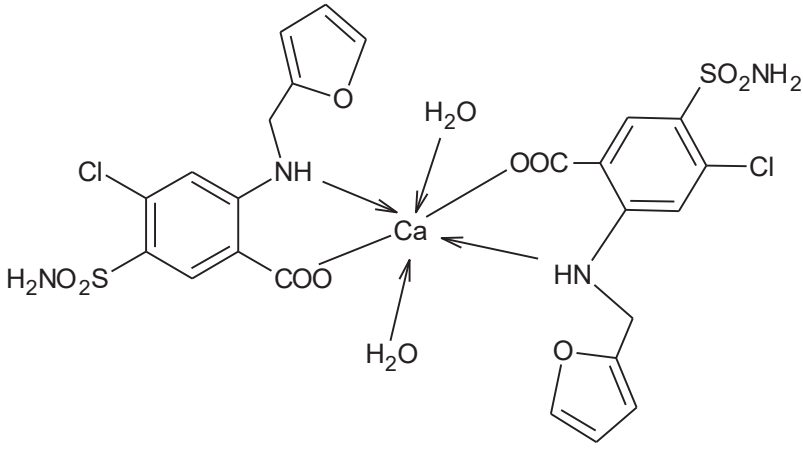

Figure 5. Proposed structure of binary complex formation of furosemide.

Silva Semaan and Cavalhero described a fast flow-injection procedure with spectrophotometric detection for furosemide's complex formation with iron(III) ions in ethanol. Four commercial samples were subjected to the proposed method. Tablets, ampoules, and synthetic urine samples that were spiked with the analyte, posing no ill effects by the presence of the other substances in the formulation. 95 measurements per hour were achieved with the proposed procedure. The results obtained were in harmony with the label and the spectrophotometric comparative procedure. For the commercial formulations and synthetic urine matrixes, the recoveries were reported up to 100% (Silva Semaan & Cavalheiro, 2006).

Furosemide was complexed with copper(II) ions at pH 3.2 in a Mclivaine buffer, producing a green-colored adduct to give way to a sensitive, simple, and accurate spectrophotometric method. Within 5-30 µg/mL, the system displays a maximum absorbance at 790 nm and shows obedience to Beer's law. A correlation coefficient of r = 0.9997 was obtained by the regression analyses; the maximum detection limit was 0.23 µg/mL. The procedure was applied successfully to the drug in tablet form. The structure of the copper complex was revealed to be $Cu(fur)_2(MeOH)_2$ with spectral data and stability constant measurements (Gölcü, 2006).

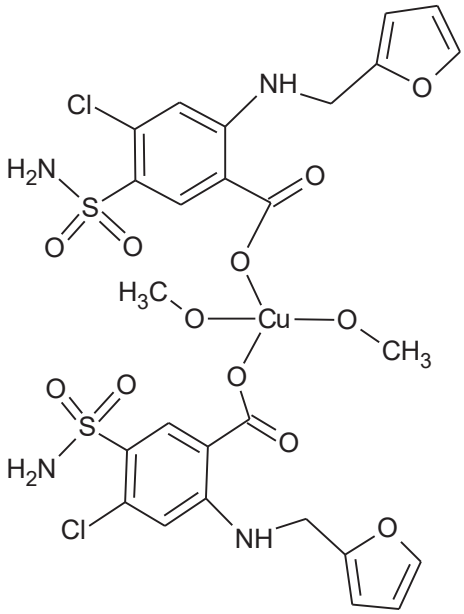

Figure 6. The structure of $Cu(Fur)_2(MeOH)_2$

Mishra and co-workers investigated the complex behavior of furosemide with copper ions in dosage forms. The complex had maximum absorbance at 742 and 730 nm in ethanol and ethyl acetate, respectively (Mishra et al., 1989).

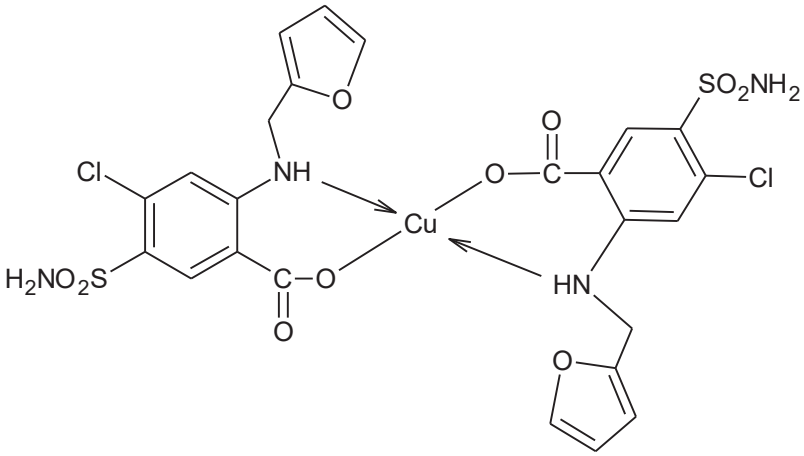

Figure 7. Proposed structure of the Furosemide-copper complex.

Khade conducted a potentiometric study in which Cr(III) reacted with furosemide in the presence of several amino acids in 80% (v/v) ethanol-water mixture at 27 °C at fixed ionic strength supplied by 0.1 M sodium perchlorate. No complex structure was provided (Khade, 2015).

Agatonovic-Kustrin et al. studied the spectrophotometric determination of the palladium(II) complex of furosemide. The standard solution of 10^{-2} M furosemide (3.3 mg of furosemide per milliliter) and the solution, with 2 M sodium hydroxide, was made alkaline to pH 9. 0.4 mg mL^{-1} furosemide-containing sample solution was also prepared and made alkaline to pH 9.0. A $PdCl_2$ solution (5 x 10^{-2} M) was prepared by heating the compound and adding 2 mL of 2 M HCl and diluting up to 50 mL with water. The ionic strength was rendered constant with 2 M KCl solution. Britton-Robinson buffer solutions were prepared by including 0.8 M orthophosphoric acid, boric acid, and acetic acid and 0.4 M sodium hydroxide and an adequate amount of 2 M KCl to keep the ionic strength constant. The complex has a maximum absorption at 527 nm and is soluble in Britton-Robinson buffer within the pH range of 9 to 13. Job's constant changes method revealed that the complex had a 1:2 formation ratio. The spectrophotometric method was applied to Lasix tablets and ampoules, and is suitable for routine and control analyses (Agatonovic-Kustrin et al., 1990).

Malik and Wankhede attempted to synthesize and characterize furosemide and its Fe(III) and Co(II) complexes. Furosemide behaved as a bidentate N, O donor ligand. The complexes had 1:2 M:L content. The synthesized ligand, as well as their metal complexes was screened for diuretic activity. According to the results, the complexes were more active than the ligand (Malik & Wankhede, 2015).

Liu and co-workers described a furosemide determination method with spectrofluorimetry. Zinc complex with 1,4-bis(imidazol-1-ylmethyl)benzene led to an enhancement of the fluorescent emission of furosemide. Optimal conditions tell that fluorescent intensity has a linear relationship with furosemide concentration. The presence of furosemide in pharmaceutical products was demonstrated. The possible mechanism was briefly related to the fluorescent spectroscopy, UV-Vis spectrophotometry, and FTIR (Liu et al., 2013).

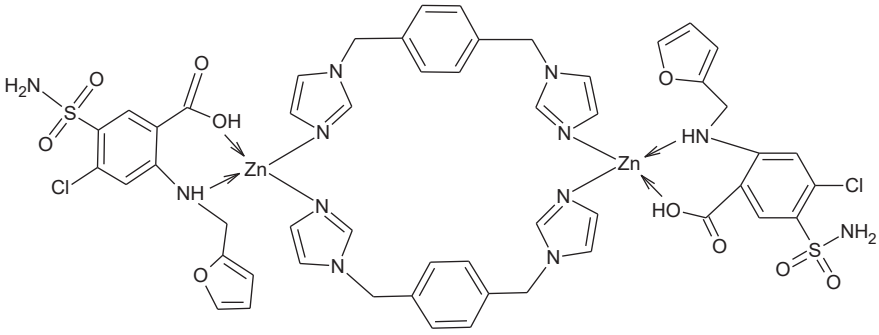

Figure 8. Chemical structure of Zn(II)–bix–FUR ternary complex.

Ksenofontov and co-workers describe the sensitivity of zinc(II) bis(dipyrromethenate) to the presence of furosemide in organic media. The instantaneous spectral response of the zinc complex was shown to be due to the fluorescent quenching effect by furosemide. This fluorescent quenching was ascribed to the formation of stable supramolecular system containing dipyrromethene and furosemide ligands of the zinc(II) complex, which is able to perform photoinduced electron transfer. The detection limit for furosemide with this dipyrromethene system was about 67-78 μg per liter. The authors describe potential use of this proposed sensor in areas like forensic medicine, clinical medicine, and sports medicine (Ksenofontov et al., 2019).

Furosemide was used as an extracting agent for mercury(II), from aqueous buffered solution, in benzyl alcohol. The method is economical, efficient, and simple. Various anions and cations and various parameters

on the extraction process were tested. In the presence of several transitions and rare earth metals at pH 3.5, the separation factor of mercury was quite high. Sodium thiosulfate was the most efficient stripping agent among others, and the recovery of mercury was 98%. M:L (1:2) stoichiometry was found as the composition of the extracted species (Abbasi et al., 2019).

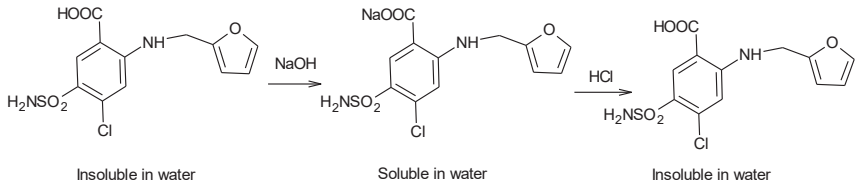

Figure 9. Purification of furosemide.

For poorly soluble drugs, nanosuspending technology is widely used and it increases the solubility of them. In this study, the aim was to develop and characterize nano-suspensions containing furosemide. Nanosuspending furosemide with Tween 80 was realized by high-pressure homogenization using ultrasonic probe or ultra turrax, ball milling, and a combination of them. According to FT-IR analyses, the characteristic peaks of furosemide were seen in every formulation. X-ray analysis revealed that the crystalline structure of furosemide was intact. Using nanosuspension method, the particle size of furosemide was decreased in a significant manner. Furosemide's solubility is dependent on pH value and the effect of nanosuspension on solubility was more pronounced at acidic area (for example, at pH 1.2). Furosemide's permeability is seemingly influenced by the nanosuspension method. Nanosuspension technology seems to be an excellent method to solubilize poorly water-soluble compounds and it increases the bioavailability of them (Gulsun et al., 2018).

Indipamide is another drug like furosemide and was subjected to computational studies as well. In this study, FT-IR and UV-Vis spectra were recorded and potential energy surface scans and molecular geometries, vibrational spectra, NBO analysis, UV spectral analysis, solvatochromism, and frontier HOMO-LUMO were covered. This article is recommended to readers who wish to gain more information about spectral studies of drugs (Bolukbasi et al., 2020).

BIOLOGICAL PROPERTIES OF FUROSEMIDE

Furosemide is a BCS (Biopharm. Class. System) class IV drug. Furosemide has a poor oral bioavailability owing to its low solubility and permeability. More soluble and permeable multi-component solid furosemide forms were sought to overcome and minimize the undesirable bio-pharmaceutical attributes. As a crystallization method, solvent evaporation was used, the authors prepared successfully the furosemide-imidazole and furosemide-5-fluorocytosine conformers as co-crystalline adducts. Imidazole and 5-fluorocytosine-containing furosemide adducts displayed superb solubility, intrinsic dissolution, and permeability properties as compared to the pure furosemide molecule. These new solid forms demonstrate the potential to increase furosemide's limited bioavailability (Diniz et al., 2020).

Another use of furosemide is to reduce pulmonary hemorrhage in racehorses. Furosemide is known to impair the calcium balance, therefore there are long-term implications for bone health. The horses were divided into two groups, the treatment group and control group. Both groups were assayed in terms of bone mineral content, bone metabolism biomarkers, and weight loss after administration. The horses in the treatment group were administered with furosemide weekly at 1 mg per kg of bodily weight weekly for seven weeks and blood was collected before and 24 hours after administration for biomarker analysis. Weight determinations were performed before and at 2^{nd}, 4^{th}, $8^{th,}$ 24^{th}, and 48^{th} hours after administration. The left third metacarpal was radiographed every 28 days of bone mineral content determination. Furosemide group lost more bodily weight than the control group even 2 hours after administration. These losses were greater than control group at 4 and 8 hours. Furosemide group lost more bodily weight at day 0 than the controls, but at 28^{th} day and 49^{th} day, furosemide bodily weight losses were not greater than the control group. Bone mineral content nor pyridinoline and osteocalcin concentrations did not tell about an effect of treatment. Reduced bodily weight changes, over time in furosemide (but not control) group needs additional exploration of frequent furosemide administration over long times (Pritchard et al., 2019).

Furosemide is a loop diuretic, helping the body not absorb too much salt and instead, pass it to the urine. It is used to treat edema in people having congestive cardiac failure, or a disease of the liver or kidney (like nephrotic syndrome). Furosemide is also a medicine for hypertension. Furosemide should not be used in the case of no urination. It is highly discouraged to take more than the dose recommended. High doses of furosemide may lead to hearing loss that might be irreversible.

Before use, the patients should consult to their doctor if they have problems of the kidney, prostate, difficulty of urination, problems about the liver, electrolytic imbalance, hypercholesterolemia, diabetes mellitus, gout, allergy to sulfa drugs (as the compound contains sulfa moiety), or lupus.

If the patients have recently had magnetic resonance imaging, before which a dyestuff was administered into their veins, or a radioactive dyestuff administered, they should immediately inform their doctors. Renal damage might occur when both the radioactive dye and furosemide are together. Taking more of furosemide than is recommended is discouraged.

High blood pressure patients should continue using furosemide (if they are prescribed) even if they feel fine. Often, high blood pressure does not have significant symptoms. It is generally unknown whether furosemide will harm a fetus or not. Patients should consult to their doctors if they are pregnant or planning to be. Breastfeeding, while using this medicine, may not be safe. For any risk, the patients should ask their doctors. Furosemide may make breast milk production slower.

Furosemide will make the takers urinate in a higher frequency and they may easily get dehydrated. Doctor's instructions should be followed about either potassium supplements should be used or enough salt and potassium should be placed their diet.

The medicine should be stored at room temperature and saved from heat, light, and moisture. Unused after 90 days, any oral liquid should be disposed of. If the patient has brought an reaction of allergic to furosemide (difficulty in breathing, appearance of hives, or if their face or throat is swollen up), or a severe dermal response (sore throat, fever, dermal pain, burning in the eyes, dermal rash red or purple in color, which causes peeling and blistering), an immediate consultation to the doctor is needed.

To make sure furosemide is safe for the patient, the doctor must be told to exercise the following conditions:

- passing out-like light-headed feeling;
- hearing loss and ring sounds in their ears;
- muscular spasms, contractions;
- easy bruising, pale skin, unusual bleeding;
- increased urination, fruity breath odor, hyperglycemia, featuring increased thirst and/or dry mouth;

• problems of the kidney- urination, either little or not at all, swelling on the feet or ankles, short of breath or feeling tired;
• Hepatic or pancreatic problems - upper stomach pain (it may affect the back too), loss of appetite, vomiting, nausea, dark appearance of urine, jaundice that is, yellowish color of the skin or eyes; or
• Electrolyte imbalance-showing findings, which are dryness of the mouth, being thirsty, general weakness, a sign of drowsiness, unsteady or jittery feel, heartbeats in an irregular shape, vomiting, fluttering sensation in the chest, tingling or numbness, muscular cramps or weakness or a feeling of limpness.

What other drugs will affect furosemide?

Using certain medicines simultaneously is sometimes not good and safe. Some medications might affect the blood levels, making the them less effective or increasing the side effects. For example, sucralfate users should take furosemide 2 hours before or 2 hours later when they took the former. The patients should inform all other medicines, especially the following:

- ethacrynic acid or other diuretics;
- chloral hydrate;
- lithium;
- phenytoin;
- an antibiotic that is administered by injection;
- cisplatin and other medicines that are used to treat cancer;
- cardiac medicines or those to treat high blood pressure,
- aspirin or other salicylates (Thornton, 2020).

Akbari and his colleagues investigated the drug loading of furosemide onto poly (glycidyl methacrylate-alt-maleic anlydride) P (GMA-alt-MA) by isopropylamine and ethylenediamine with different molar ratios of blending. Furosemide loading on the hydrogels and slow release in phosphate-buffered saline pH 7.41 at 37 °C were examined. The sample having the lowest amount of crosslinking agent was found to be the highest swollen one as compared with the others. When the rigidity of carrier increased, the crosslinker density increased too, and the amount of the released drug had a decrease. The release rate however for all samples were similar. A pH-dependent behavior was observed for all carriers and the maximum rate of release was seen in basic media. The release rate was dependent upon temperature and increasing it causes the release rate to be faster. Release data was compared with different mathematical models and Higuchi model, for all samples, proved to be the convenient one (Akbari et al., 2020).

REFERENCES

Abbasi, Y. A., Shahida, S., Ali, A., & Khan, M. H. (2019). Liquid–liquid extraction of mercury(II) from aqueous solution using furosemide in benzyl alcohol. *Journal of Radioanalytical and Nuclear Chemistry*, *319*(3), 1029–1036. https://doi.org/10.1007/s10967-018-6400-5

Agatonovic-Kustrin, S., Zivanovic, L., Radulovic, D., & Pecanac, D. (1990). Spectrophotometric determination its palladium(I1) complex. *Journal of Pharmaceutical & Biomedical Analysis*, *8*(8–12), 983–986.

Akbari, K., Moghadam, P. N., Behrouzi, M., & Fareghi, A. R. (2020). Synthesis of three-dimensional hydrogels based on poly (glycidyl methacrylate-alt-maleic anhydride): Characterization and study of furosemide drug release. *Arabian Journal of Chemistry*, *13*(12), 8723–8733. https://doi.org/10.1016/j.arabjc.2020.10.003

Bolukbasi, O., & Yilmaz, A. (2012). X-ray structure analysis and vibrational spectra of Furosemide. *Vibrational Spectroscopy*, *62*, 42–49. https://doi.org/10.1016/j.vibspec.2012.06.002

Bolukbasi, O., Yilmaz, A., & Ilhan-Ceylan, B. (2020). Solvent effects on UV–Vis and FT-IR spectra of indapamide combined with DFT calculations. Chemical Papers, 74(4), 1103–1111. https://doi.org/10.1007/s11696-019-00945-0

Diniz, L. F., Carvalho, P. S., Pena, S. A. C., Gonçalves, J. E., Souza, M. A. C., de Souza Filho, J. D., Bomfim Filho, L. F. O., Franco, C. H. J., Diniz, R., & Fernandes, C. (2020). Enhancing the solubility and permeability of the diuretic drug furosemide via multicomponent crystal forms. *International Journal of Pharmaceutics*, *587*, 119694. https://doi.org/10.1016/j.ijpharm.2020.119694

Gulsun, T., Borna, S. E., Vural, I., & Sahin, S. (2018). Preparation and characterization of furosemide nanosuspensions. *Journal of Drug Delivery Science and Technology*, *45*, 93–100. https://doi.org/10.1016/j.jddst.2018.03.005

Gölcü, A. (2006). Spectrophotometric determination of furosemide in pharmaceutical dosage forms using complex formation with Cu(II). *Journal of Analytical Chemistry*, *61*(8), 748–754. https://doi.org/10.1134/S1061934806080053

Hondrellis, V., Kabanos, T., Perlepes, S., & Tsangaris, J. (1988). Metal Complexes of the Diuretic Drug Furosemide. *Monatshefte fur Chemie*, *119*, 1091–1101.

Khade, B. (2015). Potentiometric studies on chromıum (III) metal complexes wıth high ceiling dıuretıc drug Furosemide and bıologıcal ımportant lıgand ın 80% ethanol-water mıxture. *World Journal of Pharmacy and Pharmaceutical Sciences*, *4*(4), 1694–1702.

Khade, B., Deore, P., & Ujagare, S. (2011). Equilibrium studies of calcium (II) complexes with drug Furosemide and some amino acids. *Journal of Chemical, Biological and Physical Sciences*, *1*(2), 179–187.

Ksenofontov, A. A., Stupikova, S. A., Bocharov, P. S., Lukanov, M. M., Ksenofontova, K. V., Khodov, I. A., & Antina, E. V. (2019). Novel fluorescent sensors based on zinc(II) bis(dipyrromethenate)s for furosemide detection in organic media. *Journal of Photochemistry and*

Photobiology A: Chemistry, *382*, 111899. https://doi.org/10.1016/j.jphotochem.2019.111899

Lamotte, J., Campsteyn, H., Dupont, L., & Vermeire, M. (1978). Structure cristalline et moléculaire de l'acide furfurylamino-2 chloro-4 sulfamoyl-5 benzoïque, la furosémide ($C_{12}H_{11}ClN_2O_5S$). Acta Crystallographica Section B Structural Crystallography and Crystal Chemistry, 34(5), 1657–1661. https://doi.org/10.1107/S0567740878006251

Latosińska, J. N., Latosińska, M., Medycki, W., & Osuchowicz, J. (2006). Molecular dynamics of solid furosemide (4-chloro-2-furfurylamino-5-sulfamoyl-benzoic acid) studied by NMR and DFT methods. Chemical Physics Letters, 430(1–3), 127–132. https://doi.org/10.1016/j.cplett.2006.08.080

Li, C., Liu, S., Liu, Z., & Hu, X. (2010). The interaction between furosemide-palladium (II) chelate and basic triphenylmethane dyes by resonance Rayleigh scattering spectra and resonance non-linear scattering spectra and their analytical applications. *Science China Chemistry*, *53*(8), 1767–1777. https://doi.org/10.1007/s11426-010-3176-z

Liu, Y., Wang, H., Wang, J., & Li, Y. (2013). A simple and sensitive spectrofluorimetric method for the determination of furosemide using zinc(II)-1,4-bis(imidazol-1-ylmethyl)benzene complexes: A spectrofluorometric method for the determination of furosemide. Luminescence, 28(6), 882–887. https://doi.org/10.1002/bio.2451

Lustri, W. R., Lazarini, S. C., Lustri, B. C., Corbi, P. P., Silva, M. A. C., Resende Nogueira, F. A., Aquino, R., Amaral, A. C., Treu Filho, O., Massabni, A. C., & da Silva Barud, H. (2017). Spectroscopic characterization and biological studies in vitro of a new silver complex with furosemide: Prospective of application as an antimicrobial agent. Journal of Molecular Structure, 1134, 386–394. https://doi.org/10.1016/j.molstruc.2016.12.056

Malik, S., & Wankhede, S. (2015). Synthesis, characterization and biologıcal actıvıty of Fe-III and Co-II complexes derived from 4-Chloro-2-[(2-Furanylmethyl-amino]-5 Sulfamoylbenzoıc acid. *International Journal of Applied Biology and Pharmaceutical Technology*, *6*(2), 205–210.

Mishra, P., Katrolia, D., & Agrawal, R. (1989). Simple Colorımetric estimation of Furosemide in dosage forms-Part I. *Current Science*, *58*(9), 503–505.

Pritchard, A., Spooner, H., & Hoffman, R. (2019). Influence of Long-Term Furosemide Use on Bone Mineral Content, Bone Metabolism Markers, and Water Weight Loss in Horses. Journal of Equine Veterinary Science, 82, 102800. https://doi.org/10.1016/j.jevs.2019.102800

Raymoni, G., & Abu Ali, H. (2019). Synthesis, Structures and Various Biological Applications of New Zn(II) Complexes Having Different Coordination Modes Controlled by the Drug Furosemide in Presence of Bioactive Nitrogen Based Ligands: Zinc(II) complexes, furosemide, hydrolysis, anti-bacterial activity. *Applied Organometallic Chemistry*, *33*(1), e4680. https://doi.org/10.1002/aoc.4680

Silva Semaan, F., & Cavalheiro, É. T. G. (2006). Spectrophotometric Determination of Furosemide Based on Its Complexation with Fe(III) in Ethanolic Medium Using a Flow Injection Procedure. *Analytical Letters*, *39*(13), 2557–2567. https://doi.org/10.1080/00032710600824698

Thornton, P. (2020). *Furosemide*. Drugs.com. https://www.drugs.com/furosemide.html#uses

Wang, Z., Wang, Y., Vilekar, P., Yang, S.-P., Gupta, M., Oh, M. I., Meek, A., Doyle, L., Villar, L., Brennecke, A., Liyanage, I., Reed, M., Barden, C., & Weaver, D. F. (2020). Small molecule therapeutics for COVID-19: Repurposing of inhaled furosemide. *PeerJ*, *8*, e9533. https://doi.org/10.7717/peerj.9533

Chapter 6

EXPERIMENTAL METHODS USED TO INVESTIGATE BSA BINDING ACTIVITIES OF METAL COMPLEXES

*Duygu İNCİ[1]**
Rahmiye AYDIN[2]

1 Assist. Prof. Dr., Department of Chemistry, Faculty of Arts and Sciences, Kocaeli University, 41380 Kocaeli, Turkey, duygu.inci@kocaeli.edu.tr, ORCID: 0000-0002-0483-9642

2 Prof. Dr., Department of Chemistry, Faculty of Arts and Sciences, Bursa Uludag University, 16059 Bursa, Turkey, rahmiye@uludag.edu.tr, , ORCID: 0000-0003-4944-0181

INTRODUCTION

Proteins are polypeptides containing carbon, hydrogen, oxygen, nitrogen atoms as well as sulfur atoms and whose structural units are amino acids. Proteins are structurally expressed in four different ways. These are primary, secondary, tertiary and quaternary structures. Straight chain structures formed by linking of amino acids to each other by forming peptide bonds form the primary structures of proteins. One end of the polypeptide chain in the protein structure has a free $-NH_3^+$ and the other end have a free $-COO^-$. These two free amino acid residues are defined the C-terminal and N-terminal end (Solomons and Fryhle, 2004). The $-NH_3^+$ and $-COO^-$ groups of all other amino acids, except the C-terminal and N-terminal end, are linked by covalent bonds to form peptides. Secondary structures are the structures formed by the bending and folding of the polypeptide chains in the structure of proteins. The structure defined as the three-dimensional state of the protein structure is the secondary structure of proteins (Geraldine and Takeuchi, 2011). It has been determined that the secondary structures of proteins whose three-dimensional structures are determined by X-ray diffraction method include α-helix, β-sheet and random rotation structures (Eckersall, 2008). Secondary structures are formed by the formation of H-bonds from amino acids in proteins. The α-helix structure is formed by the formation of H-bonds on the same polypeptide chain. The tertiary structures of proteins are formed by folding as a result of the interaction of the side chains of amino acids that make up the polypeptide chain in the protein structure. The tertiary structures of proteins are folding created by secondary structures. Thanks to these folds and twists, an amino acid in any region of the polypeptide chain can interact with an amino acid located in a distant region on the polypeptide chain.Intermolecular interactions are very important in the formation of the tertiary structure of proteins. There are covalent and non-covalent interactions that determine the structure and stability of proteins. Covalent interactions are peptide and disulfide bonds, while non-covalent interactions are ionic bond, H-bond, hydrophobic and van der Waals interactions. The covalently bonded C-N bonds formed between the carboxyl groups of another amino acid and the amino group of an amino acid by leaving 1 mole of water are peptide bonds. Peptide bonds formed by covalent bonds between amino acids enable the polymerization of amino acids to peptides and proteins. Another covalent bond observed in proteins is the disulfide bond formed between two sulfur atoms. Disulfide bonds are made up of cysteine monomers bearing the –SH (thiol) group in the amino acid side chain

that converges as a result of protein folding (Sewald, 2002). Hydrogen bonds are formed between α-helix and β-layered structures that form the secondary structures of proteins. Hydrophobic interactions are one of the factors that cause proteins to fold their structures to be stable in aqueous solution (Patthy, 1999). Proteins can be negatively charged (glutamic acid and aspartic acid) or positively charged (histidine, arginine and lysine) depending on the functional groups in amino acids. They also carry positive and negative charges due to the C-terminal and N-terminal ends of the polypeptide chains. Both situations allow electrostatic interactions to occur in the protein structure. These charged groups in the structure of proteins are located on the surface of the proteins in order to enable the protein to interact with water (Solomons and Fryhle, 2004). All these interactions are very important in the formation and stability of protein structure. The macromolecular structures formed by proteins with tertiary structures form the quaternary structure. The quaternary structures of proteins can be formed as a result of the interaction of the same or different polypeptide chains. An example of a quaternary protein is hemoglobin, which has 4 polypeptide side chains.

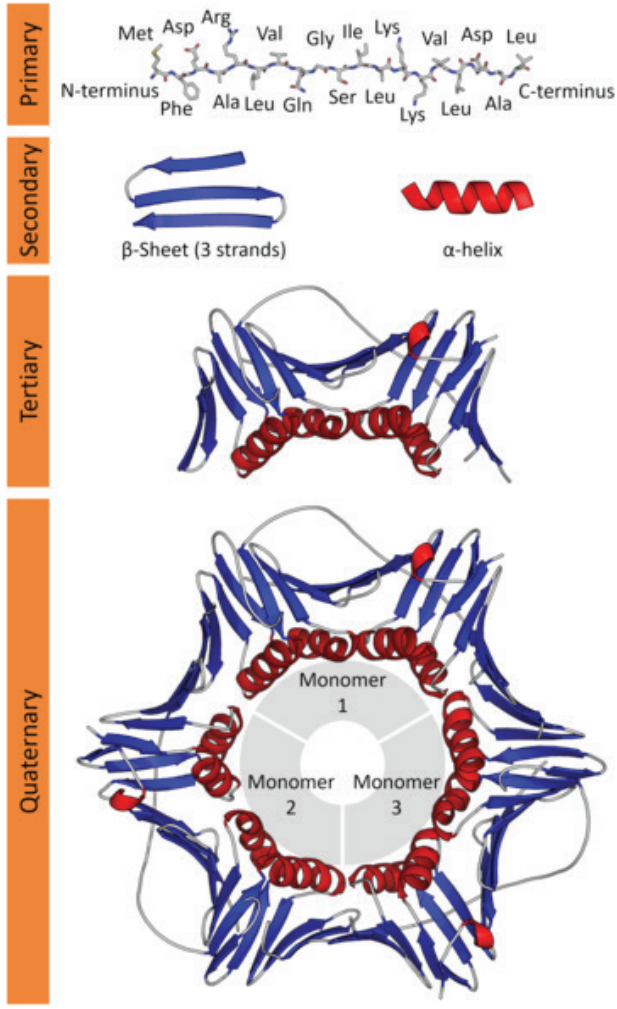

Figure 1. *Interactive diagram of protein structure (Gulbis et.al, 1996)*

Bovine Serum Albumin (BSA)

Serum albumin is one of the most studied proteins for many years. It is the most plentiful protein in blood plasma and functions as transport protein. It also plays a significant role in regulating the osmotic pressure of blood (Carter and Ho, 1994). Many researchers have examined functions, structures, and properties of serum albumin in order to research the interactions of proteins with biomolecules such as drugs, drug active substances and organic ligands. Serum albumin has been a model protein for physiological studies for many years. BSA (Brown, 1975) and HSA

(Behrens et al. 1975) are the first serum albumin structures. The primary structure of BSA was presented in the same year as HSA. The amino acid sequence proposed by Brown shows that BSA consists of three domains. Each domain can be divided into two subdomains, A, B and C. Each subdomain can be further subdivided into three helix structures, X, Y, and Z. The helices are interconnected by disulfide bridges. While almost all hydrophobic amino acid residues are found inside the cavity and between the helices, polar amino acid residues are mostly observed on the outer wall of the structure. Two subdomain grooves adhere towards each other, forming a field, and three such areas eventually form a serum albumin molecule (Kragh-Hansen 1981).

Tryptophan numbers of BSA and HSA are different. BSA has two tryptophan tips. One of the ends is in subdomain IA (Trp-134) and the other is in subdomain IIA (Trp-212). HSA has one tryptophan end and it is located in subdomain IIA (Trp-214). Trp-134 is located on the surface of BSA structure, while Trp-212 is located in the hydrophobic binding region inside BSA (Lu et al. 2007).

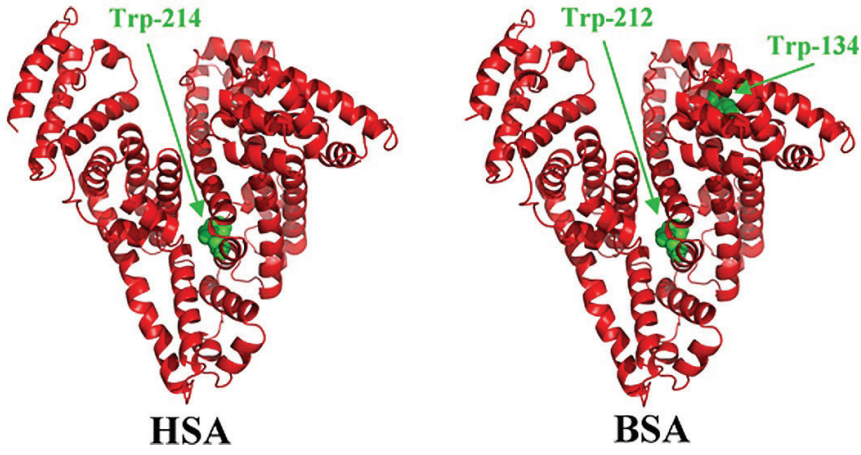

Figure 2. *Three-dimensional structures of HSA and BSA with tryptophan residues in green color (Belatik et al. 2015)*

The most interesting feature of serum albums is the high binding affinity of amino acid residues in different binding sites in serum albumin. The most striking feature of albumin-ligand interactions is the structural regions with high binding tendency and low binding tendency (Kragh-Hansen, 1981).

Investigation of BSA Binding Activities of Metal Complexes

Different spectroscopic techniques such as electronic absorption and fluorescence spectroscopy, X-ray crystallography, ESI-MS, NMR, electrophoresis and FT-IR can be used to investigate BSA-complex interactions. With the interaction of BSA and complexes, the microenvironments of the fluorescent amino acid residues in BSA structure and the secondary structure of BSA can change, causing a change in the conformation of BSA. The absorption and fluorescence properties of proteins are because of the amino acids phenylalanine, tryptophan and tyrosine.

Tryptophan, tyrosine and phenylalanine absorb UV rays in the wavelength range of 260-280 nm and give their unique peak. Tryptophan, an aromatic amino acid, gives fluorescence to proteins as it absorbs UV light at 280 nm. The amount of absorption and quantum yield of aromatic amino acids phenylalanine and tyrosine are less than the amino acid tryptophan. Emission of the amino acid tryptophan excited at 280 nm at 340 nm is obtained. The emission of the amino acid tryptophan is strongly dependent on its environment. Because the spectral changes in the emission of tryptophan amino acids occur as a result of their interaction with the complexes (İnci et al. 2017).

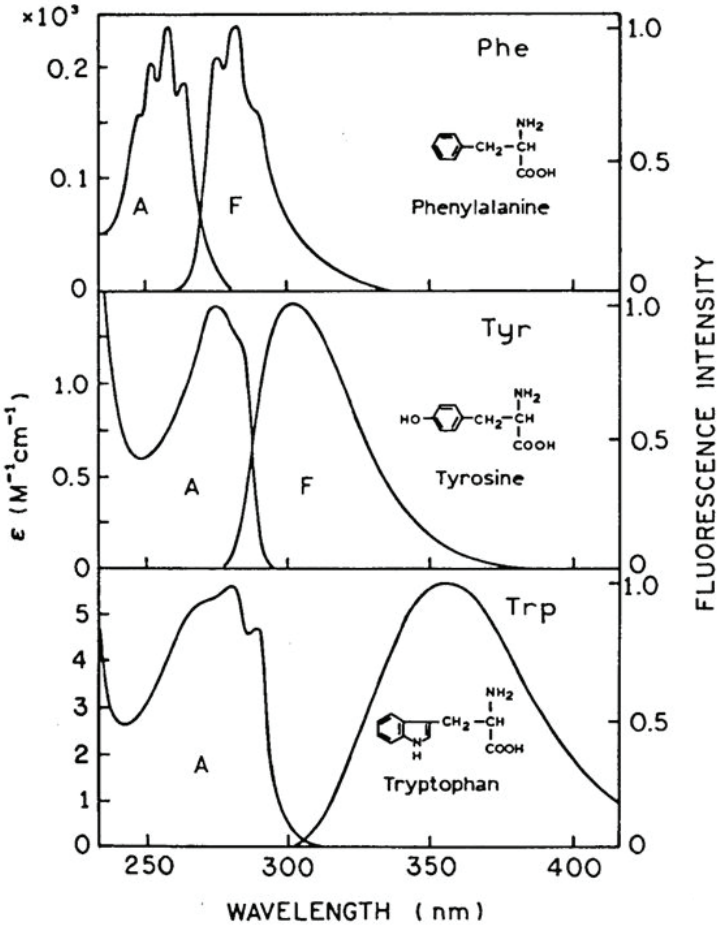

Figure 3. *Electronic absorption and fluorescence spectra of phenylalanine, tyrosine and tryptophan amino acids in protein structure (Wünsch et al.2015)*

The quenching in the fluorescence intensity as a result of interactions between BSA and the metal complexes provides information about the BSA. The reason for the quenching in the fluorescence intensity of BSA is molecular interactions. Fluorescence quenching takes place in two ways, dynamic and static. Dynamic quenching take places as a consequence of collisions between BSA and the metal complexes, while one of the molecules turns into an excited state, while the other turns into a non-radiative state. In static quenching, the BSA + metal complexes structure, which does not have fluorescence property, is formed between BSA and the metal complexes. Dynamic and static quenching; could be distinguished from each other by temperature, viscosity and lifetime measurements.

By using electronic absorption spectroscopy, the fluorescence quenching mechanism can be determined as a consequence of the interaction of metal complexes with BSA by making use of changes in absorbance and wavelength. The absorbance and wavelength of the BSA solution alone and the BSA+metal complexes containing solution are compared. If differences are observed in the absorbance and wavelength of the solution containing BSA+metal complexes, there is static quenching, if no difference is observed, dynamic quenching is in question. With fluorescence spectroscopy, the fluorescence quenching mechanism can be determined depending on the temperature and using the Stern-Volmer equation (Wang et al. 2006). In static quenching, as the temperature rises, the Stern-Volmer curves obtained for each temperature decline. In dynamic quenching, as the temperature rises, the Stern-Volmer curves rises. When static and dynamic quenching is observed at the same time, it is observed that it forms an upward concave curve (Lakowicz, 1983). To learn more about the BSA binding parameters of metal complexes, the modified Stern-Volmer binding constants of BSA+the metal complexes systems can be calculated (İnci et al. 2019). After determining that the fluorescence quenching mechanism is static quenching as a consequence of the interaction of BSA with the metal complexes, the binding constants of metal complexes to BSA and the number of binding sites are calculated (Guo et al. 2009).

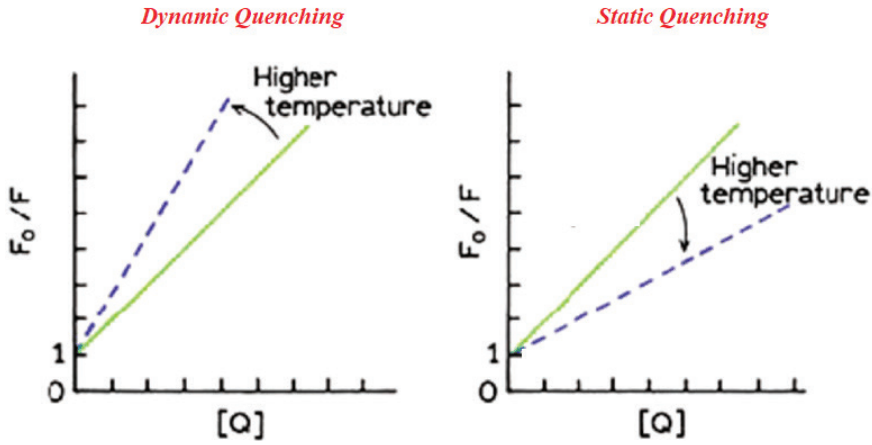

Figure 3. *Temperature dependent changes of static quenching and dynamic quenching graphics (Lakowicz, 2002)*

The type of interaction between BSA and metal complexes (hydrophobic, van der Waals, hydrogen bonds or electrostatics) and

thermodynamic parameters are calculated (Qin et al.2010). The determined ΔH and ΔS values provide information about the interaction type of BSA with the metal complexes. The following comments can be made:

(i) hydrophobic interaction; the positive values for both ΔH° and ΔS°

(ii) van der Waals and hydrogen bonding interactions; the negative values for both ΔH° and ΔS°

(iii) electrostatic interaction; the negative value of ΔH° and the positive value of ΔS°.

Ni(II) complex interacts with the Thr526, Lys523 and Ser109 residues by means of van der Waals interaction and is almost to hydrophobic residues in of IIe 525, Leu 112, Val 423 and Lys114. Additionally, there is an electrostatic interaction between the side chain carboxyl group of Glu424 residue and Ni(II) complex and is formed a hydrogen bonding interaction with Leu112 and a π-π interaction with Pro420. Consequently, these interactions play an important role in stabilizing of the Ni(II) complex intercalative mode (Yueqin et. al, 2017).

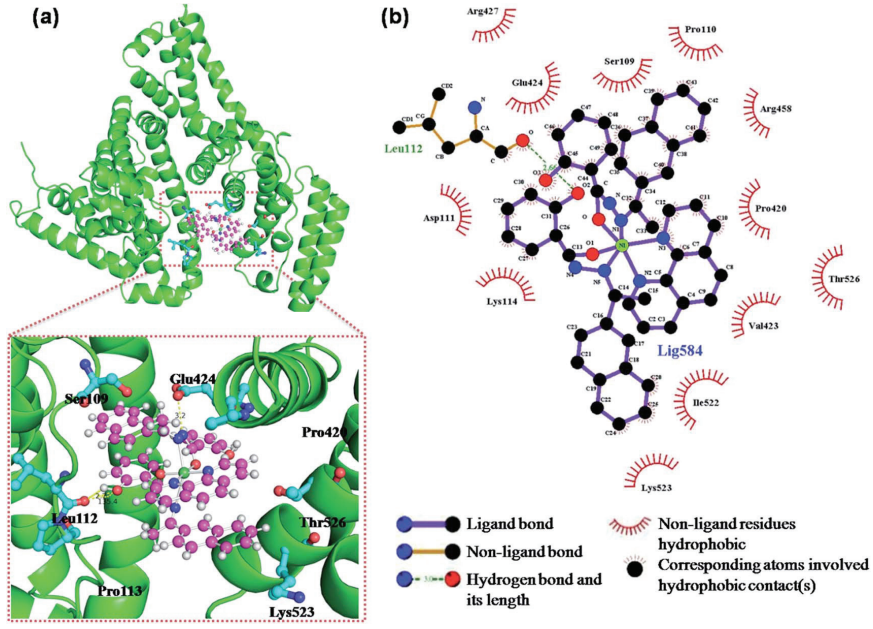

Figure 4. *((a) The Ni(2-acetonaphthone salicylylhydrazone)$_2$phen·CH$_3$CN complex was docked in the binding pocket of BSA (b) representation of 2D interactions (Yueqin et. al, 2017)*

BSA and the metal complexes must interact with each other in order to have an efficient energy transfer. Therefore, the distance between the metal complexes and BSA is very important. In order for energy transfer to occur between BSA and the metal complexes, the distance between them must be less than 8 nm. For an efficient energy transfer, the fluorescance spectrum of BSA and the electronic absorption spectrum of the metal complexes must partially overlap. The overlap area obtained as a result of overlapping the fluorescance spectrum of the BSA with the electronic absorption spectrum of the metal complexes could be determined (Lakowicz, 2002). The energy transfer efficiency between the metal complexes and BSA in fluorescence resonance energy transfer is important and transfer efficiency can be calculated (Lakowicz, 2002).

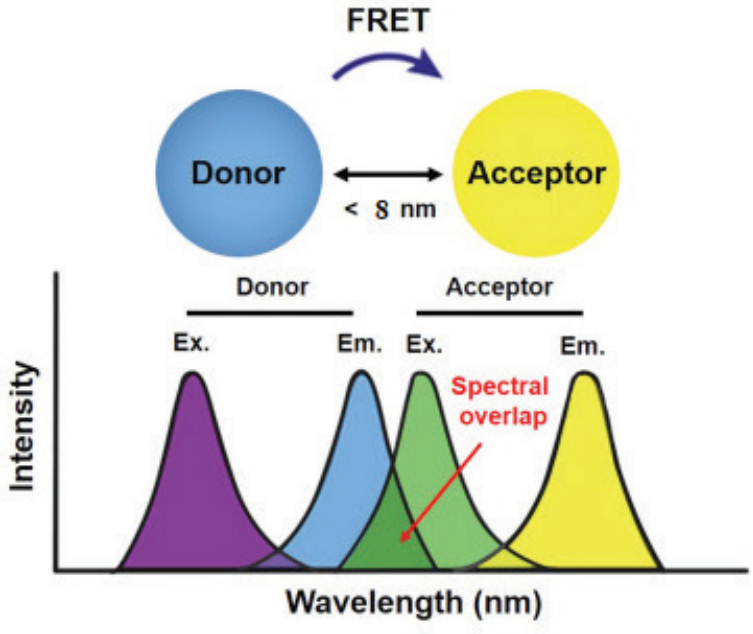

Figure 5. *Overlap between metal complexes and BSA where FRET takes place schematic representation of the area (overlap) (Broussard and Green, 2017)*

As a consequence of the interaction of BSA with the metal complexes, conformational changes caused by the metal complexes in tryptophan and tyrosine residues in BSA structure could be determined by synchronous fluorescence method. Synchronous fluorescence method is performed by applying the wavelength difference determined using emission and excitation wavelength of the BSA to fluorescence spectroscopy. When

the determined wavelength difference is Δλ = 15 nm, information about the microenvironment of the tyrosine amino acid residues in the BSA structure, and when Δλ = 60 nm, the microenvironment of the tryptophan amino acid residues can be obtained (Miller, 1979).

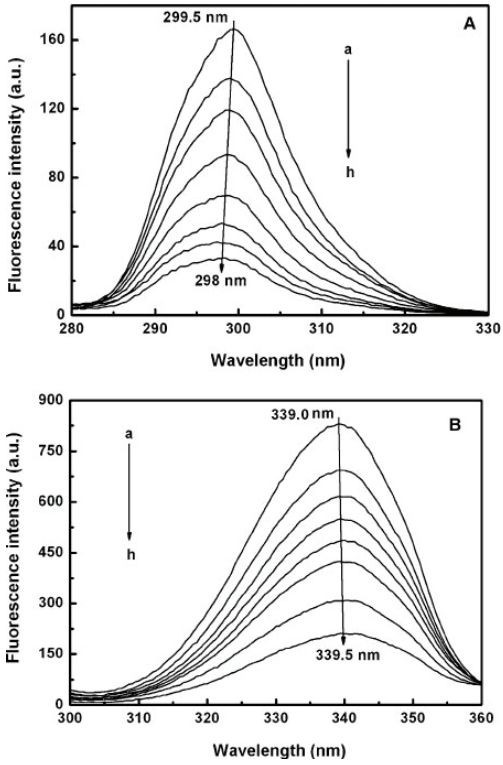

Figure 6. *Synchronous fluorescence spectra of trans-resveratrol–BSA mixture at*

a) λ = 15 nm b) λ = 60 nm (Cao et al, 2009)

In Figure 6 shows that a gradual decline of the fluorescence intensity of BSA is observed with rising concentration of trans-resveratrol at λ = 60 nm and λ = 15 nm (Cao et al, 2009).

Three-dimensional (3D) fluorescence spectroscopy is one of the analysis techniques that can provide a comprehensive and detailed analysis of conformational changes in the structure of the BSA. In this technique, the fluorescence properties of the metal complexes whose interactions with BSA are investigated are shown as a function of both excitation and emission wavelengths simultaneously. Two-dimensional

(2D) fluorescence spectroscopy ensures comprehensive knowledge about the environmental curve of the results obtained by three-dimensional (3D) fluorescence spectroscopy (Hantelmann et al. 2006).

FT-IR spectroscopy has been recognized as a powerful tool for analysising the interaction between the metal complexes and BSA. Because of the presence of characteristic functional groups of BSA, it has vibrational fingerprints at certain frequencies. Thus, the structure and composition of these groups can be estimated by evaluating the width of the spectral bands, intensity and position in FT-IR (Alhazmi, 2019).

CONCLUSIONS

In this study we have reviewed experimental methods used to investigate BSA binding activities of metal complexes. The structural characterization of the interaction between complexes and BSA is important and provides insight into what changes could be made to increase affinity and specificity for BSA. Structure-function relationships could also provide a significant information. It is clear that combinations of BSA interaction modes can be used to improve the binding affinity and selectivity of the metal complexes, but there are many more examples. What is clear is that the inherent physicochemical diversity of transition metals and the design flexibility provided by the virtually unlimited range of ligands for coordination makes metal complexes powerful biologically active agents that could be used to investigate the structural diversity of BSA.

REFERENCES

Alhazmi, H. A. 2019. FT-IR Spectroscopy for the Identification of Binding Sites and Measurements of the Binding Interactions of Important Metal Ions with Bovine Serum Albumin. *Scientia Pharmaceucita*, 87: 5.

Behrens, P. Q., Spiekerman, A. M., Brown, J. R. 1975. Structure of Human Serum Albumin. *Fedeartion Proceedings*, 34: 591.

Broussard, J. A., Green, K. J. 2017. Research Techniques Made Simple: Methodology and Applications of Förster Resonance Energy Transfer (FRET) Microscopy. *Journal of Investigative Dermatology*, 137: e185-e191.

Brown, J. R. 1975. Structure of Bovine Serum Albumin. *Federation Proceedings,* 34(3): 591.

Cao, S., Wang, D., Tan, X., Chen, J. 2009. Interaction Between Trans-resveratrol and Serum Albumin in Aqueous Solution. *Journal of Solution Chemistry*, 38: 1193-1202.

Carter, D. C., Ho, J. X. 1994. Structure of Serum Albumin. *Advances in Protein Chemistry*, 45: 153-203.

Eckersall, P. D. 2008. Proteins, Proteomics, and the Dysproteinemias. Clinical Biochemistry of Domestic Animals, Elsevier, UK, pp: 117-155.

Geraldine, S. M. J., Takeuchi, S. 2011. Understanding tools and techniques in protein structure prediction. Systems and Computational Biology-Bioinformatics and Computational Modeling, In Tech Publisher, Croatia, pp: 187-212.

Gulbis, J. M., Kelman, Z., Hurwitz, J., O'Donnell, M., Kuriyan, J. 1996. Structure of the C-terminal region of p21(WAF1/CIP1) complexed with human PCNA. *Cell*, **87**: 297-306.

Guo, X. J., Sun, X. D., Xu, S. K. 2009. Spectroscopic investigation of the interaction between riboflavin and bovine serum albumin. *Journal of Molecular Structure,* 931: 55-59.

Hantelmann, K., Kollecker, M., Hull, D., Hitzmann, B., Scheper, T. 2006. Two-dimensional fluorescence spectroscopy: A novel approach for controlling fed-batch cultivations. *Journal of Biotechnology*, 121: 410–417.

İnci, D., Aydin, R., Sevgi, T., Zorlu Y., Demirkan, E. 2017. Synthesis, crystal structure, stability studies, DNA/albumins interactions and antimicrobial activities of two novel Cu(II) complexes with amino acids and 5-nitro-1,10-phenanthroline, *Journal of Coordination Chemistry*, 70(3): 512-543.

İnci, D., Aydın, R., Huriyet, H., Vatan, Ö., Zorlu, Y., Çoşut, B., Çinkılıç, N. 2019. Cu (II) tyrosinate complexes containing methyl substituted phenanthrolines: Synthesis, X-ray crystal structures, biomolecular interactions, antioxidant

activity, ROS generation and cytotoxicity. *Applied Organometallic Chemistry*, Vol. 33(1), e4652.

Kragh-Hansen, U. 1981. Molecular Aspects of Ligand Binding to Serum Albumin. *Pharmocological Riviews*, 33(1): 17-53.

Lakowicz, J. R. 1983. Principle of flourescence spectroscopy. Plenium Pres, New York, pp: 248.

Lakowicz, J. R. 2002. Principles of Fluorescence Spectroscopy. Kluwer Academic publishers, New York, pp: 215.

Lu, J. Q., Jin, F., Sun, T. Q., Zhou, X. W. 2007. Multi-spectroscopic study on interaction of bovine serum albumin with lomefloxacin-copper(II) complex. *International Journal of Biological Macromolecules*, 40(4): 299-304.

Miller, J. N. 1979. Recent advances in molecular luminescence analysis. *Proceedings of the Analytical Division of the Chemical Society*, 16: 203-208.

Patthy, L. 1999. Protein Evolution: Published Blackwell Publishing, pp: 281.

Qin, Y., Zhang, Y., Yan, S.,Ye, L., 2010. A comparison study on the interaction of hyperoside and bovine serum albumin with Tachiya model and Stern-Volmer equation. *Spectrochimica Acta, Part A: Molecular and Biomolecular Spectroscopy,* 75: 1506-1510.

Sewald, N. J. H. 2002. Peptides: Chemistry and Biology, Wiley-VCH, pp: 147.

Solomons, G. T. W., Fryhle, C. B. 2004. Organic Chemistry, United States of America, John Wiley & Sons, pp: 325.

Wang, Y-Q., Zhang, H-M., Zhang, G-C. 2006. Studies of the interaction between palmatine hydrochloride and human serum albumin by fluorescence quenching method. *Journal of Pharmaceutical and Biomedical Analysis,* 41: 1041-1046.

Wünsch, U. J., Murphy, K. R., Stedmon, C. A. 2015. Fluorescence Quantum Yields of Natural Organic Matter and Organic Compounds: Implications for the Fluorescence-based Interpretation of Organic Matter Composition. *Frontiers in Marine Science,* 2(98): 1-15.

Yueqin, L., Zhiwei, Y., Minya, Z., Yun, L. 2017. Synthesis and crystal structure of new monometallic Ni(II) and Co(II) complexes with an asymmetrical aroylhydrazone: effects of the complexes on DNA/protein binding property, molecular docking, and in vitro anticancer activity. *RSC Advance*, 7: 49404-49422.